UNIVERSIDAD COMPLUTENSE DE MADRID
FACULTAD DE MEDICINA

TESIS DOCTORAL

Impact of HIV and Schistosoma co-exposure on pulmonary vascular pathophysiology

Impacto de la co-exposición a VIH y Schistosoma en la fisiopatología vascular pulmonar

MEMORIA PARA OPTAR AL GRADO DE DOCTOR

PRESENTADA POR

Sandra Medrano García

Director

Edgar Fernández Malavé

Madrid

UNIVERSIDAD COMPLUTENSE DE MADRID

FACULTAD DE MEDICINA

TESIS DOCTORAL

Impact of HIV and Schistosoma co-exposure on pulmonary vascular pathophysiology

Impacto de la co-exposición a VIH y Schistosoma en la fisiopatología vascular pulmonar

MEMORIA PARA OPTAR AL GRADO DE DOCTOR
PRESENTADA POR:

SANDRA MEDRANO GARCIA

DIRECTOR:

Dr. EDGAR FERNÁNDEZ MALAVÉ

Universidad Complutense de Madrid

Facultad de Medicina

Impact of HIV and Schistosoma co-exposure on pulmonary vascular pathophysiology

Impacto de la co-exposición a VIH y Schistosoma en la fisiopatología vascular pulmonar

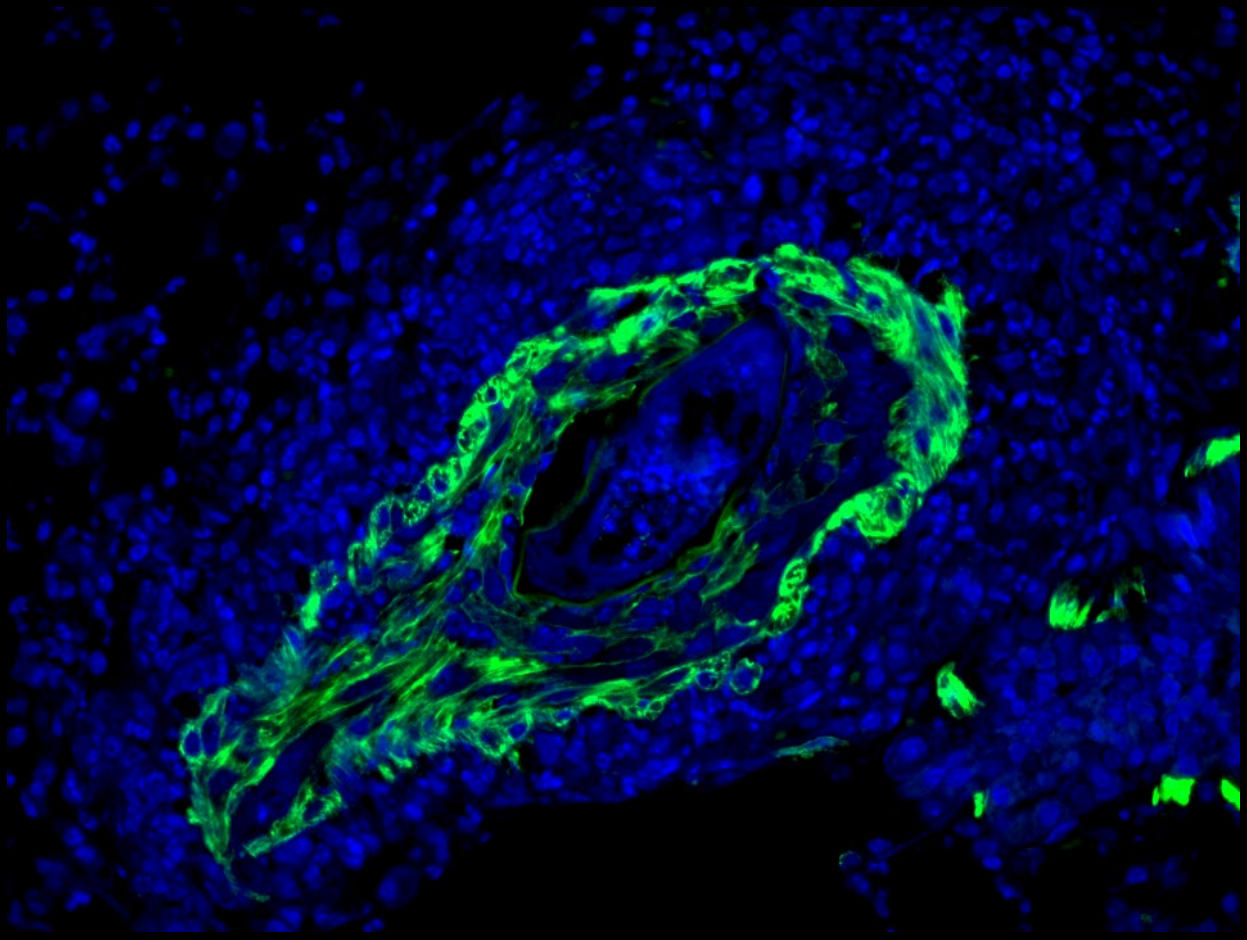

TESIS DOCTORAL

Sandra Medrano Garcia

DIRECTOR

Dr. Edgar Fernández Malavé

Madrid, 2021

MENCIÓN DE DOCTORADO INTERNACIONAL

La presente tesis doctoral de Dña. Sandra Medrano Garcia titulada "Impact of HIV and Schistosoma co-exposure on pulmonary vascular pathophysiology", realizada en el Departamento de Inmunología, Oftalmología y ORL, de la Facultad de Medicina de la Universidad Complutense de Madrid, cumple los requisitos exigidos por la Universidad Complutense de Madrid para obtener la mención de Doctor Internacional (R.D. 99/2011):

1. Haber realizado una estancia **mínima de 3 meses** fuera de España en un centro de investigación de prestigio, realizando trabajos de investigación, durante el periodo de realización del programa de doctorado:
   - Institution: **Vienna University of Technology & General Hospital of Vienna**. Vienna, Austria.
     Supervisor: **Prof. Dr. Eugenijus Kaniusas**. Duración: 1mes (Enero-Febrero 2015).
   - Institution: **Max Planck Institute for Heart and Lung Research**, Bad Nauheim, Alemania.
     Supervisor: **Prof. Dr. Soni Savai Pullamsetti**. Duración: 4 meses (Enero-Mayo 2021).

2. La tesis doctoral ha sido evaluada por **dos expertos doctores pertenecientes a instituciones internacionales**:
   - **Prof. Dr. Vinicio de Jesus Perez**, Medicine School, Stanford University, EEUU.
   - **Prof. Dr. Ghazwan Butrous**, Medway Pharmacy School, University of Kent, Inglaterra.

3. Un **miembro del tribunal evaluador** de la tesis doctoral pertenece a un centro de investigación **extranjero**.
   - **Prof. Dr. Rajkumar Savai**, Max Planck Institute for Heart and Lung Research, Bad Nauheim, Alemania.

4. La tesis doctoral **ha sido redactada en inglés** y, al menos, una parte de la defensa será presentada en una de las lenguas habituales para la comunicación científica en su campo de conocimiento, distinta a cualquiera de las lenguas oficiales en España.

The work described in this Doctoral Thesis has been carried out in the "T cell physiopathology laboratory" in the Department of Immunology, Ophthalmology and ENT of the School of Medicine and has been funded by the following research projects and foundations:

- "Surface and intracellular T lymphocyte activation physiopathology". MINECO 2014. Principal Investigator: José R. Regueiro & Edgar Fernández-Malavé. Immunology department, School of Medicine, Complutense University of Madrid
- "Lymphocyte integration of TCR and complement cues" (RTI2018-095673-B-I00). MICINN 2018. Principal Investigator: José R. Regueiro & Edgar Fernández-Malavé. Immunology department, School of Medicine, Complutense University of Madrid
- "The effect of coinfection with HIV and schistosomiasis on the pulmonary vascular bed" (FIBHGM-CCA028-2017). Principal Investigator: Angel L. Cogolludo Torralba. Department of Pharmacology and Toxicology, School of Medicine, Complutense University of Madrid
- The Cardiovascular Medical Research and Education Fund

This thesis work was supported by a predoctoral fellowship from Complutense University, a research contract associated to project RTI-2018-095673-B-I00 from the Spanish Ministry of Science and Innovation, and by the Cardiovascular Medical Research and Education Fund.

A todos los animales que han dado su vida por la ciencia
(To all the animals that have given their lives for science)

“Nunca dejes que nadie te diga que no puedes hacer algo. Ni siquiera yo. Si tienes un sueño, tienes que protegerlo. Las personas que no son capaces de hacer algo por ellos mismos, te dirán que tú tampoco puedes hacerlo. ¿Quieres algo? Ve a por ello y punto”.

En busca de la felicidad (2006)

“Hey. Don’t ever let somebody tell you… You can’t do something. Not even me. Alright? You got a dream… You gotta protect it. People can’t do something’ themselves, they wanna tell you you can’t do it. If you want something’, go get it. Period.”

The pursuit of happiness (2006)

Agradecimientos / Acknowledgements

Gracias a todos los que os habéis cruzado en mi camino de vida a lo largo de esta tesis doctoral, pero también a los que ya estabais antes, por forjar la personalidad que me ha llevado a poder terminarla.

A pesar de ser de las primeras páginas de esta tesis doctoral, es lo último que estoy escribiendo. Llevo meses evitando esta sección porque nunca he sido buena expresando por escrito lo que llevo dentro y tengo demasiada gente a la que estar agradecida, de manera que, si me dejo algo o a alguien, o si es muy largo, pido disculpas de antemano, pasad directamente a introducción.

A mi director de tesis, Edgar Fernández Malavé, y al destino, porque aunque haya sido un camino difícil, quiso que acabásemos trabajando juntos. Muchas gracias por su experiencia, por su conocimiento y por ser compañero de bancada (de pocos jefes se puede decir haber tenido la suerte de haber aprendido todo de él, codo con codo en el laboratorio). Me llevo de él no solo los experimentos, sino algo mucho más importante: haber aprendido a pensar mejor (como él dice: "usar bien esa cabecita que tengo"). Gracias por estar siempre presente en mi vida, no solo en lo profesional, sino por preocuparte por mí y estar siempre a mi lado en lo personal. Muchas gracias también por entender mi personalidad, tan loca siempre, tan hiperactiva y permitirme organizar miles de actividades divulgativas, a las que incluso he conseguido liarte. Me llevo muchos buenos momentos discutiendo datos, pero también muchas risas, congresos, canciones y tardes tomando algo. También dar las gracias **a Maripaz**, que ha sido cómplice de esta tesis y de las "células con mucha miga", por todos los momentos que le he robado a Edgar en estos últimos meses de tesis.

A Ángel Cogolludo, por brindarme la oportunidad de entrar en este proyecto que se ha convertido en mi tesis doctoral, pero sobre todo por darme su experiencia, recursos, tiempo y alegría. Los experimentos infinitos no hubiesen sido iguales si no hubiese estado siempre aportando su experiencia, pero también su alegría. Muchas gracias por estar presente en lo personal, por los consejos sabios y los cafés en la terraza de su casa.

A José R. Regueiro, por su infinito apoyo a la ciencia, su dedicación, su perseverancia y por siempre escuchar las voces de los doctorandos y el sector joven del Departamento. Por

ayudarme siempre con las locuras de la Semana de la Ciencia y muchas otras actividades de divulgación de conocimiento.

To Ghazwan. Thank you for the opportunity of participate in this project, which has become my thesis. You have been the engine of the whole project, you have always been available to comment actively the results and help in anything needed for me. In addition, you have gave me the opportunity to learn and participating on the dissemination of the project by inviting us to attend all the meetings, which have been a very nice experience not only scientifically, but a very nice personal experience.

A Daniel Morales Cano. Gracias por convencernos ese día en la cafetería a tomar un café, hablar de inmunología y hacer unas "pruebas" de experimentos, la que lió… He aprendido muchísimo de ti, horas de experimentos juntos, reflexiones, muchas "brainstorming", pint of science… y muchos otros momentos, que han hecho que al final, te hayas convertido en uno de mis pilares del laboratorio, pero también en un gran amigo. Gracias por ser tan activo y estar siempre dispuesto a todo.

A la Fundación "Cardiovascular Medical Research and Education Fund", a la que pertenece la financiación de este proyecto, por hacer posible la investigación básica en temas no *trending topic* de la ciencia y permitir que ésta avance en todas direcciones.

I am particularly grateful **to Professor Soni Pullamsetti and Professor Rajkumar Savai** for opening the doors of their laboratory to me in Germany, to give me the chance to participate in fascinating projects, for their wise advice and experience.

Thanks to **Professor Eugenijus Kaniusas** for considering me a one more member of the group, making me feel at home during my stay in Vienna, for encouraging me at all times, for transmitting me his passion for science.

Al Departamento, por apoyar mi doctorado, mis proyectos y escuchar nuestras sugerencias en la labor que he realizado de representante de estudiantes de postgrado. En especial, gracias **a Pedro Roda Navarro**, por ser mi tutor y tener siempre tan sabios consejos. Gracias **a Manolo Martín Villa**, por todos los buenos ratos que hemos pasado y ser tan activo tanto a nivel científico como personal. **A Javier Cubero**, por los experimentos de los proyectos que hemos trabajado juntos, pero también por sus buenos consejos y apoyo para mi contrato. **A Javier Redondo**, por siempre estar disponible en lo científico, pero también ser un buen compañero y amigo. **A Elena Goicoechea**, por ser para mí un modelo a seguir de mujer IP, ojalá algún día pueda llegar a ser algo parecido a ella científicamente hablando.

A todos mis compañeros del Departamento de Inmunología, los que continúan y los que ya no están, por todos los buenos momentos vividos, pero también por hacer piña en los malos momentos. **A Rebeca, Irene, Arantza, Laura, Marta, José Luis, Bea, Bea, Nacho, Oscar, Sergio, Alex, Anaïs, Patricia, Rocío, Marina, Olga, Raquel**. **A Ana**: por tantos buenos consejos científicos, protocolos, cotilleos, tardes de experimentos, risas y por ser como es, porque sin gente como ella, los laboratorios serían a veces, sitios muy oscuros y egoístas. Sin olvidarme de darle las gracias por ser la tía favorita de Unut, cuidarle y mimarle mientras yo tenía que estar haciendo experimentos de miles de horas. **A Dani**, por todo: las mañanas, tardes, noches, brunch, paseos, lloros, risas, lágrimas, consejos…y lo que nos queda, ahora empieza lo mejor.

A Agus, por haber podido disfrutar con él tanto de la ciencia en todas nuestras visitas a los colegios enseñando inmunología (¡la de cosas que nos han pasado juntos!), por las comidas y cafés, pero también por sus locuras y días mágicos.

A todos los compañeros de farmacología. En especial: **A Bianca**, por ser la mejor técnica de laboratorio que he tenido el placer de conocer en mi vida, su trabajo constante, facilitar lo difícil, y los cafés a primera hora después de acabar los experimentos. **A Maria Callejo**, compañera de laboratorio, pero también de "tesis en 3 minutos", pint of science y muchos otros momentos fuera del laboratorio que han sido tan especiales.

Thanks to the Max Plack people. Thanks **to Edibe and Golnaz**, for helping me whenever you could. **To Anoop**, for teaching me so many things, for being my friend and making me feel at home. **To Utta, Jana, Jeanette and Yanina** for being such good lab technicians and facilitating my stay in the lab. **To Monika,** for organising my stay and her availability to solve all problems with a smile. **To David, Tessa, Solmaz, Despina** and all the nice moments and coffees. **To Fran and Misa**, to be my family in Germany, for all these amazing dinners, nights taking about everything and nothing, for all your love and happiness. The best thing I take away from my stay is you guys.

A Ignacio Lisoazaín, por ser Vicerrector de Investigación, pero preocuparse de escuchar las voces de los doctorandos, por atender nuestras sugerencias y mejorar el sistema de contratos predoctorales. Gracias por ayudarme a organizar el primer evento de "Ciencia y Cine". Donde todo eran problemas… él consiguió soluciones. Y por último… gracias por autorizarme a usar el citómetro de su laboratorio cada vez que se rompía el nuestro.

A **María Ángeles Vicente**, coordinadora del programa de doctorado, por siempre estar tan atenta a todas las necesidades que tenemos, por aguantarnos (que no debe de ser fácil, jeje). Por haberme apoyado y dado siempre soluciones en todas las complicaciones de papeleos de esta tesis. **A Carmen**, de secretaría de alumnos de doctorado, por todo el trabajo que hace y ser tan eficiente. **A Alfonso**, de la Facultad de Medicina, por ser tan amable siempre y estar dispuesto siempre a ayudar en cualquier actividad de la Facultad. **A tod@s los bedel@s** de la facultad, por siempre echar un cable en lo necesario y ser tan colaborativos. **A Luis, Quique, Paco y Sanae** de la cafetería, por ser siempre tan amables y profesionales, por poner los cafés con mucho cariño y una sonrisa.

Al Departamento de Matemática Aplicada de la Facultad de Biología. Por mis primeros dos años allí, con gente tan maravillosa. **A Abel**, gracias por haberme apoyado en la etapa más oscura de mi doctorado, por no haber permitido que abandonara, pero sobre todo por tus buenos consejos y los buenos momentos, cafés y comidas que hemos disfrutado todos juntos. **A Anabel**, por ser la mejor Directora de Departamento que he tenido el placer de conocer. Por poder estar al lado de una mujer tan inteligente, con tanto coraje y con ganas de luchar por los derechos y responsabilidades de las personas que trabajan en la Universidad pública, pero también por ser siempre tan amable y traernos pastelitos tan ricos. **A Antonio**, por todo el cariño mostrado y por su profesionalidad.

Gracias a los que confiaron en mí, contratándome en otros trabajos que me permitieron trabajar mientras no tenía contrato predoctoral y a mis compañeros del Corte Inglés y de la farmacia por ser fantásticos amigos. **A Ana Landa**, mi jefa en Grupo Puig. Gracias por ser una de las mejores jefas que he tenido. Por escuchar a tus empleados y ser tan justa siempre. **A Noe**, por ser tan divertida, ser buena amiga y hacer las tardes de trabajo mucho más amenas. **A Gema**, por todos

los domingos de trabajo infinitos deseando que llegase la hora de comer para vernos y contarnos los nuevos cotilleos de la semana, ¡que hubiese sido de todos esos festivos ahí metidas sin ti!. A mis chicas Dior, pero **a Oksana** en especial, por ser tan dulce, divertida y simpática, por tener siempre un momento para alegrarme el día cuando más cansada estaba. **A Rous**, un ejemplo de perseverancia, pero también de buena amiga y ¡estilazo!. De la farmacia dar las gracias **a Carlos**, por ser tan buen compañero y amigo, pero sobre todo por elevar la profesión de farmacia a un nivel casi inalcanzable. Muy pocas personas en mi vida he visto tan profesionales y guiadas por su motivación en el día a día. Siempre formándose, pero también formándonos y siendo el mejor guía en nuestro día a día. Por siempre estar ahí cuando más lo he necesitado, ser mi alma gemela de pensamiento y por con su consejo farmacéutico (soy una pupas muy grande).

A todas mis amigas del cole: **Diana, Tubi, Sonia, Arlan y Bego**, por todos los buenos momentos vividos juntas y por haber tenido la suerte de seguir contando con ellas en mi vida, porque a pesar de estar siempre todas separadas, siempre encontramos muchos momentos para estar juntas. Muchas gracias también a sus parejas, por ser tan buenos compañeros y haber pasado a formar parte de nuestra "familia". **A Edu y Silvia**, por haber aparecido para quedarse y proporcionarme tantas alegrías y buenos momentos.

A todos mis compañeros de "bio-cracks", vaya grupo de gente "especial" que nos juntamos en la carrera, ¿se puede ser más friki y a la vez tan cracks todos?". **A Alberto**, mi "bicho", te admiro desde el día en que nos conocimos y que casi me matas del susto con la serpiente, el tiempo ha demostrado que eres el mejor herpetólogo que ha conocido este planeta, pero también de los mejores amigos que se pueden tener. **A Arlo y David** por ser una alegría constante en mi vida, cuantas salidas de campo, estudio en la biblioteca, viajes y discotecas han sido geniales gracias a vosotros. **A Nacho,** por transmitirme siempre tu fuerza, tu cariño y tu amistad incondicional. **A Marta**, por ser una amiga en la que confiar, por siempre tener tiempo para quedar, para hablar y disfrutar a pesar de la distancia. **A Alicia**, compañera de pupitre de la facultad, por tener un corazón enorme y haber tenido la suerte de pasar tanto juntas. **A Manu**, por haberse convertido desde el principio en mi amigo y seguir ahí, por las noches de estrellas, por los paseos por Madrid, por el cine y por la pizza. Por tener el placer de poder aprender siempre tanto de él. A **Javi, Jessi, Concha, Felipe y Loreto** por formar parte de esta gran etapa.

A la familia de Pint of Science. A Patricia, por ser tan activa, tan resolutiva, tan dispuesta siempre. **A Antonio,** por ser buen amigo, pero también por siempre estar dispuesto a comunicar ciencia de una manera tan sencilla, por su compromiso con la y su gran sabiduría. **A Nuria** por toda su alegría y optimismo, por siempre saber sacar lo bueno de todas las malas situaciones. **A Rafa**, el "gran jefe", porque sin su entrega, ofrecimiento y gran trabajo sería muy difícil haber llegado que *Pint of Science Spain* sea lo que es hoy en día. Por siempre tener tiempo para un café, una barbacoa, o una buena charla en los momentos más estresantes. También gracias por las paellas con bogavante y las catas de queso que tanto disfrutamos todos gracias a su buena mano en la cocina. **A Belén**, por ser amiga, confesora, tutora, compañera…por todos los buenos momentos juntas en su casa, las tardes hablando de ciencia y de la vida, por saber sacar de mí siempre lo mejor, no solo en los buenos momentos sino cuando más estrés he tenido. **A José**, por aguantar siempre todas las chapas que le damos de ciencia con una sonrisa y preparar esas maravillosas barbacoas y cocidos mientras nosotras "cocinamos ciencia".

A Gonzalo, por todas las tardes de cocina, de paseos por Madrid, de pelis y de series juntos, por hacer que el tiempo vuele, por siempre saber escuchar. **A Gerardo** por los millones de horas juntos, incontables, por ser tan buen amigo, por haber incluso dedicado tu tiempo libre a construir una cámara anecoica para la tesis. Haber vuelto a recuperarte ha sido una de mis mayores alegrías.

A Andrés, ¿qué sería yo sin ti? Mi tutor no oficial de tesis, mi consejero, mi compañero de *Ciencia y Cine,* mi más mejor amigo. No tengo palabras para expresar en todo lo que te has convertido para mí en los últimos años. Muchas gracias por tus sabios consejos, por enseñarme tantas cosas, por siempre tener un hueco para mí, por escucharme, y por dedicar tu tiempo libre al proyecto que tenemos juntos y que tantas alegrías me proporciona.

A Marta, por haber encontrado una amiga que se ha convertido en una hermana. Por estar ahí siempre, por todo lo bueno y malo que hemos vivido juntas y por todo lo que nos queda por vivir. Por haberme dado en estos últimos meses un regalo de sobrina, **Eva**.

Gracias a mi familia. A mi madre, porque gracias a ella soy como soy. Gracias por su perseverancia, por ser tan inteligente, por dar tan buenos consejos y por educarme como me ha educado. Por apoyarme siempre, por dejarme que estudiase e hiciese lo me que guiase el corazón, por hacerme entender que es mucho más importante la felicidad que el dinero, porque sin ella jamás estaría donde estoy. **A mis abuelos, Conchi y Cholo,** por haberme criado como a una hija, por estar siempre ahí, por siempre confiar en mí y en mis capacidades. Por siempre regalarme su tiempo y una sonrisa. Gracias por ser siempre mis mecenas cuando lo he necesitado. A mi **tio Gonzi**, por ser mi tío favorito, por protegerme y estar siempre a mi lado, por siempre poder contar con él y siempre preocuparse por mí. **A Carlos**, por proporcionarme siempre todas las herramientas necesarias para estudiar y apoyarme en lo que he necesitado. **A Jose Mari**, por inculcarme el valor de la naturaleza, la curiosidad por la historia y el amor por los animales, que es lo que me ha movido siempre a estudiar Biología.

Gracias a mi otra familia. Gracias **a José y a Carmen** por siempre estar disponibles, por preocuparse tanto, por siempre estar tan pendientes de mis avances y progresos con la tesis. Gracias por todas las vacaciones en familia, por las comidas de los domingos y por haberos convertido en alguien tan importante en mi vida. Gracias a **Raquel, Pablo, Blanca y Jaime**, por ser los mejores hermanos postizos que se puede tener. Gracias a **Ángel Manuel**, por todas las súper conversaciones de ciencia, por sus buenos consejos laborales, pero también personales. Gracias a él y **a Sara** por hacer que el confinamiento de mi estancia fuese tan guay y por todos los buenos momentos que pasamos juntos.

A Unut, por todas las alegrías que me ha dado, por hacerme tan sumamente feliz, y por todas las alegrías que actualmente proporciona a **Toño y Ana,** gracias a ellos también por cuidarle tan bien y seguir haciéndome partícipe de su día a día.

Por último, agradecer todo a Álvaro, por ser mi compañero de vida. Mi tesis comenzó casi a la vez que le conocí, así que es la persona que más presente ha estado en todo el trabajo (aunque creo que sigue sin saber de qué va todo esto, jaja). Porque la vida sin él está bien, pero con él es mucho mejor. Todo a su lado es más intenso y más divertido. Gracias por estar ahí en todo momento, en lo bueno y en lo malo. No hay paso que dé en el que él no vaya a mi lado, y el que no soy capaz de dar, me lleva en brazos.

Abbreviations

5-HT	serotonine
+Schisto	exposed to Schistosoma eggs
Ach	acetylcholine
AM	alveolar macrophage
ART	antiretroviral therapy
α-sma	alfa smooth muscle actin
BAL	bronchoalveolar lavage
BW	body weight
CAP	community acquired pneumonia
cART	combined antiretroviral therapy
CCR5	C-C chemokine receptor-5
COPD	obstructive pulmonary disease
CXCR4	C-X-C chemokine receptor-4
DC	dendritic cell
dPAP	diastolic Pulmonary arterial pressure
Eos	eosinophils
FSC	forward scatter
GEO-MFI	geometric mean fluorescence intensity
HIV	human immunodeficiency virus
HIV mice	HIV-1 (Tg26) transgenic mice
HPAH	hereditary pulmonary arterial hypertension
IFM	immunofluoresce microscopy
IFN-γ	interferon-γ
IL-1	interleukin-1
IL-13	interleukin-13
IL-17	interleukin-17
IL-4	interleukin-4

IM	interstitial macrophage
iMonocyte	inflammatory monocyte
IRIS	immune reconstitution inflammatory syndrome
i.p.	intraperitoneal
IPAH	idiopathic pulmonary arterial hypertension
i.v.	intravenous
LV+S	left ventricle plus septum
mPAP	mean pulmonary arterial pressure
NHP	nonhuman primate
NK	natural Killer
NKT	natural killer T cell
NPs	neutrophils
PA	pulmonary arteries
PAH	pulmonary arterial hypertension
PAP	pulmonary arterial pressure
PCNA	proliferating cell nuclear antigen
pMonocyte	patrolling monocyte
PVD	pulmonary vascular disease
PVR	pulmonary vascular resistance
RV	right ventricle
RV/(LV+S)	Fulton index
RVSP	right ventricular systolic pressure
SHIV	chimeric viruses harbouring fragments of SIV and HIV genomes
SNP	sodium nitroprusside
sPAP	systolic pulmonary arterial pressure
SSC	side scatter
TGF-β	transforming growth factor β
Th1	T helper type 1
Th2	T helper type 2
TNF	tumor necrosis factor
UNAIDS	Joint United Nations Programme on HIV/AIDS
VSMC	vascular smooth muscle cells
vWF	Von Willebrand factor
WHO	World Health Organization
Wt	wild-type

Contents

Figure content

Table content

1

Abstract

Abstract

HIV and Schistosoma infections have been individually associated with pulmonary vascular disease. Co-infection with these pathogens is very common in tropical areas, with an estimate of more than six million people co-infected only in Africa. However, the effects of HIV and Schistosoma co-exposure on the pulmonary vasculature and its impact on the development of pulmonary vascular disease are largely unknown, due partly to the scarcity of experimental models. Since HIV proteins and Schistosoma eggs are the primary triggers of vascular pathology, it could be hypothesized that co-exposure to HIV and Schistosoma would allow for severe and rapidly pulmonary vascular disease progression, such as pulmonary arterial hypertension (PAH).

HIV-associated PAH is characterized by proliferative vasculopathy with intimal fibrosis and development of plexiform lesions. This vascular damage is associated with a narrowing of the pulmonary vessel lumen, which over time, increases pulmonary pressure. The mechanisms involved in HIV-associated PAH are not yet well understood. Still, viral proteins have been postulated to play a role in the endothelial dysfunction observed. On the other hand, schistosomiasis-associated lung pathology is thought to be triggered by embolization of schistosome eggs into the lungs, leading to inflammation and pulmonary vascular remodelling. Thus, peri-egg granulomas formation and vascular remodelling with perivascular infiltrates and vessel wall thickening are considered critical events in the schistosomiasis-associated pulmonary pathology.

Here, we have approached the analysis of the impact of HIV and Schistosoma co-exposure on the development of pulmonary vascular pathology by using a non-infectious animal model based on lung embolization of *Schistosoma mansoni* eggs in egg-sensitized HIV-1 transgenic (HIV) mice. This HIV transgenic line harbours a replication-deficient non-infectious HIV-1

pro-viral genome, which encodes seven of the nine HIV-1 proteins and allows their expression in different tissues, including the lung.

Compared to wild-type (Wt) animals, HIV mice displayed an impaired granulomatous immune response to parasite eggs in the lung, as suggested by the smaller size and increased fibrosis of granulomas and augmented residual egg burden; with the latter further suggesting impaired capability of granulomas for clearing parasites eggs. The lung vasculature demonstrated a higher degree of perivascular fibrosis in egg-treated HIV than in Wt mice, while medial wall muscularization was similarly increased in both types of mice. Notably, schistosome-exposed HIV mice but not Wt counterparts showed exacerbated endothelial remodelling, including intimal proliferation, increased vessel obliterations and formation of plexiform-like lesions, with markedly suppressed endothelial-dependent vasodilation and associated augmentation of the pulmonary arterial pressure. These structural and functional changes in the pulmonary vasculature correlated with an altered pulmonary immune landscape in co-exposed mice, characterized by increased abundance of γδ T cells with intermediate-to-high levels of surface TCR and upregulated CD27, patrolling-type monocytes and interstitial and alveolar macrophages, and heightened expression of IFN-γ/IL-17A by $TCR^{int\text{-}hi}$ γδ T cells and CD4 T cells, and IL-4/IL-13 in myeloid cells; which globally suggest a shift in T cells from a type 2 to a type 1/17 pro-inflammatory phenotype and enhanced local inflammation with relevance to development of vascular pathology.

Our study shows for the first time that combined exposure to HIV and Schistosoma, as it may occur in co-infected people, targets the pulmonary vascular endothelium and results in aggravated endothelial remodelling and dysfunction. Thus, persistent expression of HIV proteins in the lung, as occurs in HIV-infected people under antiretroviral therapy, may cause an initial endothelial insult that may be exacerbated in a subsequent Schistosoma infection; and foster ultimately the development of pulmonary vascular pathology. Furthermore, the mouse model of HIV and Schistosoma co-exposure may provide a valuable experimental tool for a deeper understanding of pulmonary vascular disease associated to the HIV and Schistosoma co-morbidity; and for designing and testing of novel or improved therapeutic strategies for the treatment of co-infected people.

2

Resumen

Resumen

Las infecciones por VIH y Schistosoma están asociadas de forma independiente con el desarrollo de enfermedad vascular pulmonar. La co-infección con estos patógenos es muy común en zonas tropicales. A nivel mundial, se estima que existen seis millones de personas co-infectadas. Sin embargo, se desconocen los efectos de la co-exposición a estos agentes infecciosos en los vasos sanguíneos del pulmón y su impacto en el desarrollo de enfermedad vascular pulmonar; esto debido en parte a la escasez de modelos experimentales. Ya que tanto VIH como Schistosoma pueden inducir patología vascular en el pulmón, se podría hipotetizar que la co-exposición a estos patógenos podría acelerar la progresión a formas graves de enfermedad vascular pulmonar, como es el caso de la hipertensión arterial pulmonar (HAP).

La HAP asociada a la infección por VIH se caracteriza por una vasculopatía proliferativa con fibrosis de la capa íntima y aparición de lesiones plexiformes. El daño vascular se asocia con una reducción de la luz de los vasos pulmonares, que con el tiempo, aumenta la presión pulmonar. Los mecanismos subyacentes a este tipo de patología se desconocen casi totalmente. Se ha postulado, sin embargo, que las proteínas virales pueden estar implicadas en la disfunción endotelial observada. Por otra parte, en el caso de la esquistosomiasis, se piensa que la patología vascular es causada por los huevos del parásito embolizados en los vasos pulmonares, lo que daría lugar a inflamación y remodelado vascular. Así, la formación de granulomas alrededor de los huevos, el remodelado vascular, la presencia de infiltrados perivasculares y el engrosamiento de la pared vascular se consideran eventos críticos en la patología pulmonar asociada a la esquistosomiasis.

En el presente trabajo de Tesis Doctoral se ha abordado el análisis del impacto de la co-exposición a VIH y Schistosoma en el desarrollo de patología vascular pulmonar empleando un modelo animal de tipo no infeccioso, basado en la embolización en el pulmón de huevos

de Schistosoma mansoni en ratones VIH-1 transgénicos (ratones "HIV"). Esta línea de ratones transgénicos porta un genoma pro-viral no-replicativo de VIH-1 que codifica siete de las nueve proteínas virales, permitiendo su expresión en diferentes tejidos, incluido el pulmón.

En comparación con ratones controles ("Wt"), los ratones HIV mostraron una deficiencia en la respuesta inmunitaria a los huevos del parasito, como lo sugiere la formación de granulomas más pequeños, fibróticos y con una capacidad reducida de eliminación de los huevos. En los vasos pulmonares de los ratones HIV tratados con huevos se observó un mayor grado de fibrosis perivascular, en comparación con los ratones Wt tratados, pero un engrosamiento similar de la pared vascular media. Notablemente, los ratones HIV tratados con huevos, pero no sus correspondientes controles Wt, mostraron un remodelado endotelial exacerbado, incluyendo proliferación de la capa íntima, aumento del número de vasos ocluidos y formación de lesiones plexiformes, con una supresión marcada de la vasodilatación dependiente de endotelio y un aumento asociado de la presión arterial pulmonar. Estos cambios estructurales y funcionales en los vasos del pulmón se correlacionaron con una alteración de las células inmunitarias pulmonares, caracterizada por un incremento en la abundancia de linfocitos Tγδ expresando niveles aumentados de TCR y CD27, monocitos de tipo "patrullero" y macrófagos intersticiales y alveolares; y un aumento en la expresión en el pulmón de las citocinas IFN-γ/IL-17A en células Tγδ ($TCR^{int\text{-}alto}$) y en linfocitos T CD4, y de IL-4/IL-3 en células mieloides; lo que sugiere una transición en los linfocitos T de una respuesta de tipo 2 a una pro-inflamatoria de tipo 1/17 y un aumento en la inflamación local que puede ser relevante en el desarrollo de patología vascular.

Nuestro estudio muestra, por primera vez, que la exposición combinada a VIH y Schistosoma, como puede ocurrir en personas co-infectadas, afecta particularmente al endotelio vascular pulmonar y causa un agravamiento del remodelado y la disfunción endotelial. Así, la expresión persistente de proteínas de VIH en el pulmón, tal y como se ha observado en individuos infectados con VIH bajo tratamiento anti-retroviral, podría provocar un daño inicial en el endotelio vascular susceptible de ser exacerbado por una infección subsecuente con Schistosoma, lo que promovería el desarrollo último de patología vascular pulmonar. Además, nuestro modelo de co-exposición a VIH y Schistosoma puede constituir una valiosa herramienta experimental para profundizar en la compresión de la enfermedad vascular pulmonar generada por la co-morbilidad asociada a estos agentes infecciosos, y también para el diseño y prueba de nuevas o mejoradas estrategias terapéuticas para el tratamiento de las personas co-infectadas.

3

Introduction

Introduction

3.1. PULMONARY VASCULAR DISEASE

The pulmonary circulation plays the crucial role of ensuring a continuous supply of oxygenated blood to the body. Compared to the systemic circulation, the pulmonary circulation is a low-pressure, high-flow system characterised by a low pulmonary vascular resistance, about 1/10 of systemic vascular resistance. In addition, pulmonary arteries (PA) show high distensibility and may increase their size to accommodate for increased blood flow. All these features allow the pulmonary circulation to carry out fundamental functions such as ventilation and gas exchange, which may be affected under pathological conditions such as pulmonary vascular diseases. Inasmuch, the increase in pulmonary arterial pressure leads to impaired gas exchange and commonly manifests as dyspnoea. If prolonged, it can lead to right ventricular failure.

Pulmonary vascular diseases (PVD) constitute a global health concern. Aside from the idiopathic or heritable forms, in many cases, PVD are secondary to other pathological processes affecting the pulmonary vasculature. In particular, infectious diseases such as those caused by Human Immunodeficiency Virus (HIV) and Schistosoma are leading causes of PVD (Barnett & Hsue, 2013; Butrous & Mathie, 2019; Cribbs et al., 2020a; Crothers et al., 2011; Knafl et al., 2020) especially of pulmonary arterial hypertension (PAH) (Butrous et al., 2008; Butrous & Mathie, 2019).

PAH is defined as a sustained mean pulmonary arterial pressure (PAP) over 20 mmHg together with pulmonary vascular resistance (PVR) ≥3 Wood units (WU) during right heart catheterization. PAH is a rare disease affecting 15 to 50 individuals per million within the United States and Europe (Beshay et al., 2020). The persistent elevation of PAP in PAH may progress

into right ventricular failure and premature death. There are several types of PAH according to the 6th World Symposium in Pulmonary Hypertension **(Figure 1)**.

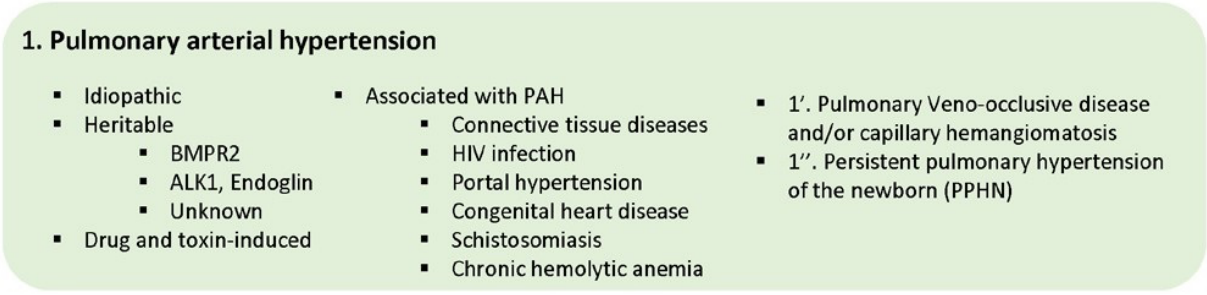

Figure 1. Causes of PAH according to the 6th World Symposium in Pulmonary Hypertension. Source: 6th World Symposium in Pulmonary Hypertension.

Idiopathic PAH (IPAH) include forms of the disease without a clear cause. Hereditary PAH (HPAH) is linked to genes that are inherited from family members. PAH may even be associated with past or current drug use, such as methamphetamine use or certain diet pills. PAH can also develop in association with other medical conditions such as congenital heart disease, liver disease, HIV or Schistosomiasis. Thus, infectious diseases such as HIV and Schistosomiasis are leading causes of PVD, especially PAH, globally. Unfortunately, although there are treatment options for PAH, there is no known cure, apart from lung transplantation.

The elevated PAP in PAH is attributed to persistent vasoconstriction and pulmonary vascular remodelling characterized by smooth muscle cell hypertrophy and progressive neointimal proliferation of endothelial cells, leading to occlusive vascular lesions of the smallest pulmonary arteries (PA) (Abe et al., 2010; Humbert et al., 2019; Tuder et al., 2013).

Therefore pulmonary vascular structure and composition may be altered during PAH development. Pulmonary arteries consist of the intima layer: the innermost layer of the blood vessel is a non-fenestrated monolayer of endothelial cells lining the vessel lumen; the media layer: the interlayer of the vessel which it is comprised by vascular smooth muscle cells (VSMC) and connective tissue; and finally the adventitia: the outermost layer, in general, it is loosely organized, comprised by extracellular matrix of collagen and elastin fibers, fibroblast or other interstitial cells, and a neural network **(Figure 2,A)**. When PAH develops, thickening and stiffening of the arteries limit blood flow and increase blood flow resistance **(Figure 2,B)**. At moderate PAH the flow through the artery is severely restricted **(Figure 2,C)**. Finally, severe PAH leads to vascular leaks with abnormal growth of endothelial cells, called plexiform lesions, and where blood flow is so poor that blood clots are produced **(Figure 2,D)**.

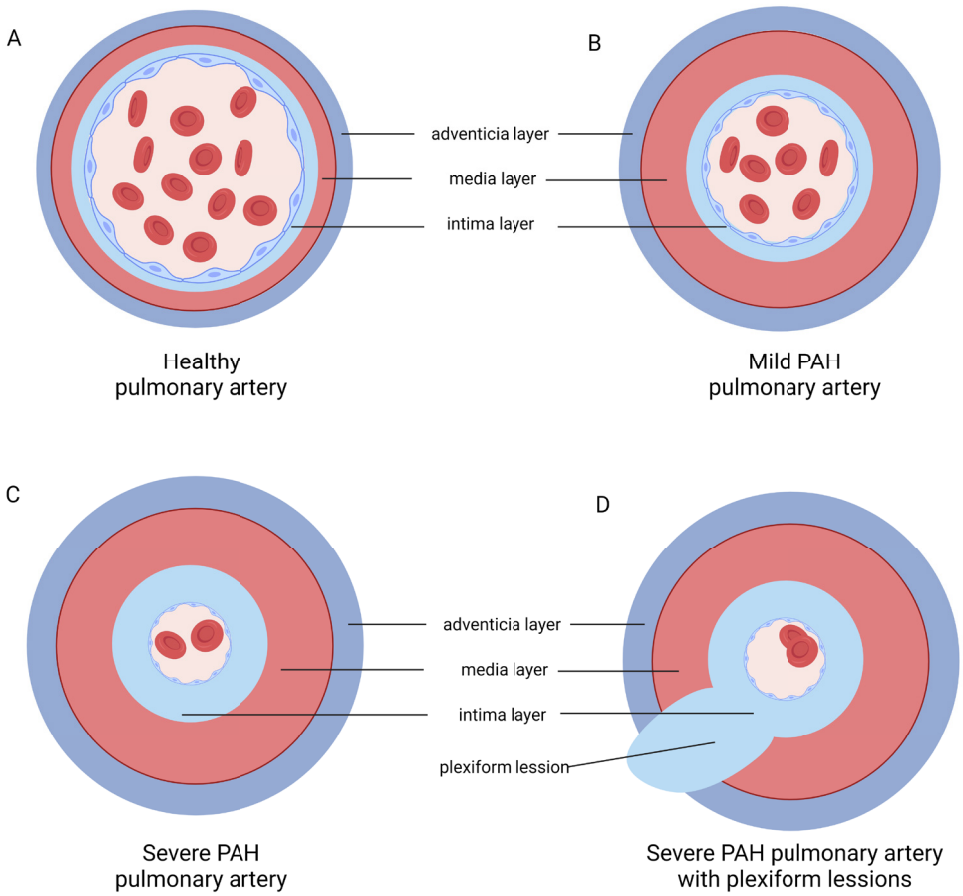

Figure 2. Vascular remodelling in pulmonary arterial hypertension. Adapted from Pulmonary Hypertension Association (https://phassociation.org/).

3.2. PULMONARY PATHOLOGY ASSOCIATED WITH HIV INFECTION

3.2.1. HIV INFECTION AND DISEASE

According to the World Health Organization (WHO), since the beginning of the epidemic, 76 million people have been infected with the HIV virus and about 33 million people have died of HIV. In 2020, 38 million worlwide were living with HIV, 73% of all the people living infected had access to antiretroviral therapy (ART), 16% of all the people living with HIV did not know that they have HIV and 1.7 [1.4–2.2] million people were newly infected worldwide in 2020 **(Figure 3)**.

An estimated 0.7% [0.6-0.9%] of adults aged 15–49 years worldwide are living with HIV, although the burden of the epidemic continues to vary considerably between countries and regions. HIV infection is not exclusive to developing countries, but is quite prevalent in developed countries as well. The WHO African region remains most severely affected, with

nearly 1 in every 25 adults (3.7%) living with HIV and accounting for more than two-thirds of the people living with HIV worldwide **(Figure 4)**.

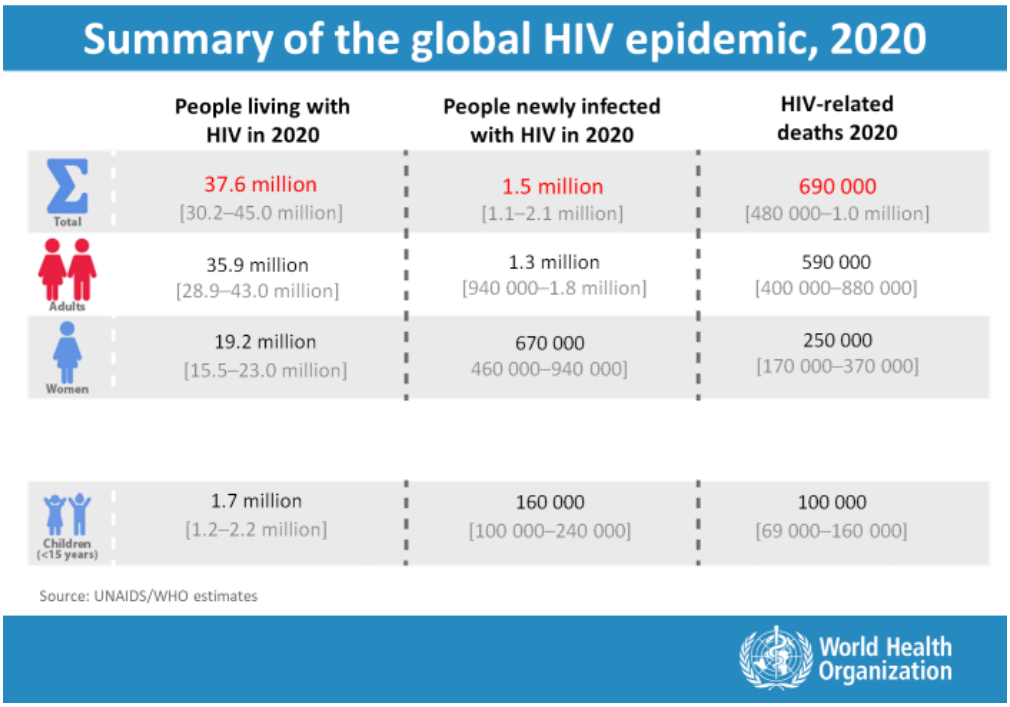

Figure 3. Summary of the global HIV epidemic. Source: World Health Organization 2020.

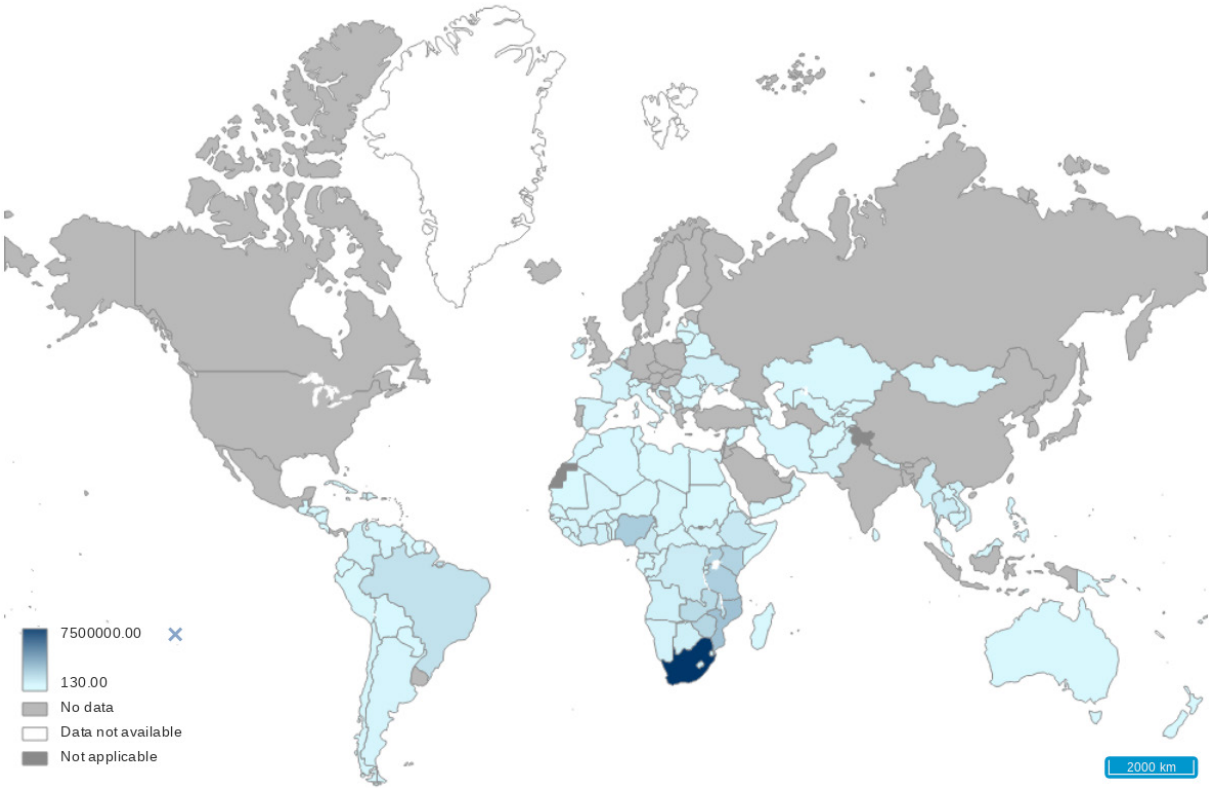

Figure 4. Estimated number of people (all ages) living with HIV. Source: World Health Organization 2020.

HIV are part of the genus *Lentivirus*. They are a group within the family *Retroviridae*. HIV was discovered in 1983 by Barre-*Sinoussi et al.* and *Gallo et al.* (Barre-Sinoussi et al., 1983; Gallo et al., 1983). The HIV virus causes an infection that primarily attacks the human immune system, which is key to survival in a world surrounded by pathogens. Specifically, the HIV virus infects CD4 T lymphocytes via C-C chemokine receptor-5 (CCR5) and C-X-C chemokine receptor-4 (CXCR4), although it is also capable of infecting other cell types such as macrophages or dendritic cells that also express these receptors on their membranes, including microglial cells (Feng et al., 1996).

As mentioned above, most of HIV infected people is being treated with ART, but still represents a lifelong treatment with no definitive cure. HIV-infected individuals who are compliant to ART show an apparent clearance of the virus in the peripheral blood shortly after initiating therapy (Almodovar, 2014). However, viral particles can be detected after stopping antiretrovirals suggesting that there is still some viral re-transcription even with treatment (Costiniuk et al., 2012; Goujard et al., 2012; Zugna et al., 2012). To identify the properties of these reservoirs, four SIV239-infected Rhesus macaques were treated with combined antiretroviral therapy (cART) for 1 year, while plasma viral RNA (vRNA) was effectively suppressed, a systemic analysis revealed that the highest vRNA prevalence was found firstly in the lymphatic tissues and secondly in the lungs and intestine much more than in the other tissues. (Horiike et al., 2012). Cryptic replication of HIV in the lung might contribute to immune disturbances leading to pulmonary complications, and hence, deserves close attention (Almodovar, 2014).

3.2.2. PULMONARY COMPLICATIONS OF HIV INFECTION

Since HIV was first discovered, pulmonary complications have been a frequent cause of morbidity and mortality (Wallace et al., 1997). ART treatment has increased the life expectancy of patients and has also changed the associated pulmonary complications. For example, the incidence of opportunistic infections such as Pneumocystis pneumonia (PCP) has declined significantly while the incidence of community acquired pneumonia (CAP) has not decreased proportionately. In addition, non-infectious complications such as chronic obstructive pulmonary disease (COPD), asthma, lung cancer, and PAH have emerged as significant comorbidities (Cribbs et al., 2020b). While PAH is a rare disease in the general population, it occurs significantly more frequently in the HIV-infected population reported to be 1 in 200 (0.5%) individuals.

The pathogenesis of HIV-associated PAH is very complex and results from genetic and environmental interaction. The possible mechanisms are unclear although numerous studies

have attempted to clarify part of the pathophysiological process of HIV-related PAH. Three main mechanisms are responsible for the HIV PAH: the HIV viral proteins found in the pulmonary vascular endothelium, immune system and cytokine release alteration due to the presence of HIV and increase the genetic predisposition due to HIV (Bigna et al., 2015).

3.2.3. PATHOLOGICAL EFFECTS OF HIV PROTEINS IN THE LUNG

Numerous mechanisms exist as to how HIV-1 proteins damage the endothelium. The HIV-1 genome contains 9 main genes: *gag*, *pol*, *env*, *tat*, *rev*, *vpu*, *vpr*, *vif*, and *nef*. Proteolytic cleavage of the Gag-Pol precursor protein yields the major structural components of the viral core, Env produces the important envelope glycoproteins gp120 and gp41 and the remaining genes encode for the regulatory proteins Tat and Rev, and the accessory proteins Vpu, Vpr, Vif, and Nef (Kline & Sutliff, 2008). These proteins have been probed to induce vascular oxidative stress, smooth muscle cells proliferation and migration, and endothelial injury leading to HIV related PAH.

Complex plexiform-like lesions characterized by luminal obliteration, intimal disruption, medial hypertrophy, thrombosis, and recanalized luminal were found exclusively in animals infected with SHIV-Nef (a chimeric viral construct containing the HIV Nef gene in an SIV backbone), but not in animals infected with SIV, demonstrating that Nef induces directly complex plexiform lesion in the pulmonary vasculature (Marecki et al., 2006). Nef was present in endothelial cells of HIV patients with PAH and infected porcine pulmonary arteries (Duffy et al., 2009). Two studies found that Nef can enter into the pulmonary endothelial cells via the CXCR4 receptor and thus induce proliferation and apoptosis of endothelial cells in the lung (Briggs et al., 2001; James et al., 2004).

Tat down-regulates bone morphogenetic protein type II receptor (BMPR2) expression and signaling by ~50% (Caldwell et al., 2006). BMPR2 participate in many physiological and pathological processes including inhibition of vascular smooth muscle proliferation and promoting the survival of pulmonary arterial endothelial cells, therefore preventing arterial damage and adverse inflammatory responses (Ehrlich et al., 2012). Reports on hereditary PAH have suggested that this level of decreased BMPR2 expression can lead to altered lung physiology and PAH (Machado et al., 2001).

GP120 induces apoptosis and endothelin-1 secretion in primary human lung endothelial cells (Kanmogne et al., 2005) and it is a potent stimulator of monocytic endothelin-1 production (Ehrenreich et al., 1993).

3.2.4. EFFECTS OF HIV INFECTION ON THE PULMONARY IMMUNE SYSTEM

The pulmonary immune function during HIV infection is impaired and have direct implications on the associated pathophysiology. In fact, HIV can affect both innate and acquired immune function.

Innate immunity and lung cell compartments can be affected by HIV infection **(Figure 5)**. Surfactant proteins D and A can modulate HIV, inhibiting infectivity of $CD4^+$ T cells, but also stimulating HIV transfer from dendritic cells (DCs) to CD4 T cells (Madsen et al., 2013). HIV can also infect alveolar macrophages (AMs) (Kanmogne et al., 2005). AMs perform a variety of important functions as phagocytosis, superoxide burst, proteolysis, killing and remove senescent cells, repair tissue, and intimately coordinate with T cells in adaptive immune function. Infection of AMs can cause impaired phagocytosis, killing, and dysfunctional immune responses to pathogens. HIV infection of AMs can lead to HIV persistence in the lung and can result in altered cytokine release by AMs (Tachado et al., 2005).

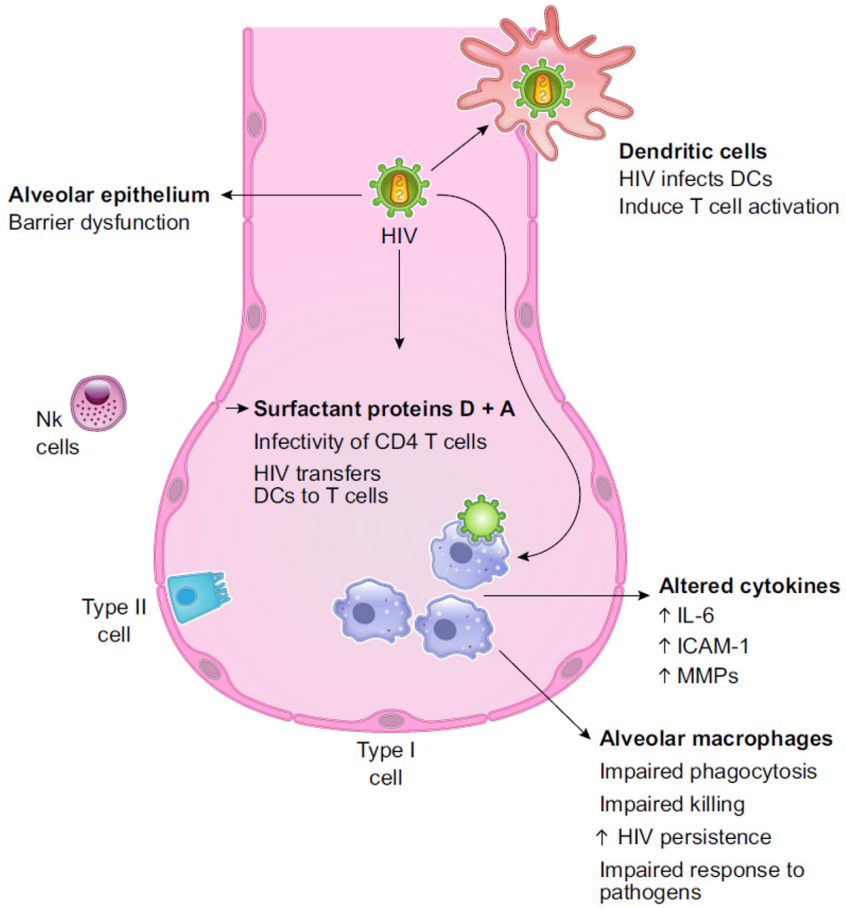

Figure 5. Pulmonary innate immunity can be affected by HIV infection. Source: Pathogenesis of HIV-Related Lung Disease: Immunity, Infection, and Inflammation. Cribbs *et al,* 2020.

Similar to AMs, DCs are key cells of innate immunity and can be primarily infected by HIV. Studies show direct interactions between NK cells and HIV peptides (Mavilio et al., 2003). NK cells are additionally known to have an important role in controlling HIV infection through production of interferon-γ (IFN-γ) (Terunuma et al., 2008).

HIV affects many aspects of adaptive immune system in the lung **(Figure 6)**. HIV can infect DCs, primary antigen-presenting cells located in the airway epithelium, resulting in T cell activation. Chronic immune activation in the lung causes an influx of HIV-specific CD8 T cells, resulting in a decreased CD4/CD8 T cell ratio, impaired proliferative responses, and T cell exhaustion (Neff et al., 2014). HIV can also affect the differentiation of CD4 T cells, which is mediated by cytokines and transcription factors. HIV-induced chronic immune activation can also shift T cell immune responses, inhibiting the production of Th1 cytokines to favour a more Th2 response. In addition to alterations in cell-mediated immunity and chronic T cell activation, HIV also increases B cell activation impairing serologic response, resulting in impaired antibody responses.

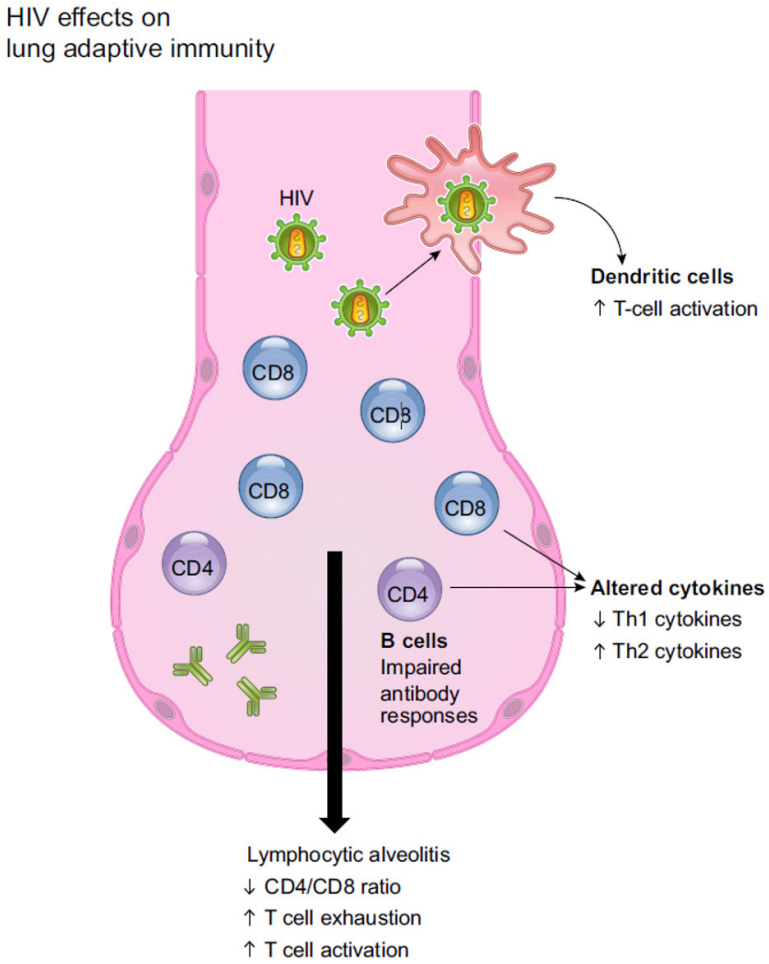

Figure 6. Pulmonary adaptative immunity can be affected by HIV infection. Source: Pathogenesis of HIV-Related Lung Disease: Immunity, Infection, and Inflammation. Cribbs *et al,* 2020.

3.2.5. THE PULMONARY IMMUNE SYSTEM OF HIV-INFECTED PEOPLE UNDER ART

ART can reconstitute some of the immune function lost with HIV replication. BAL CD4+ T cells thru proliferation of memory T cells result in an improved functionality of the T cell function (Knox et al., 2010). Also, HIV suppression restores the lung mucosal CD4+ T-cell viral immune response and resolves CD8+ T-Cell alveolitis in patients at risk for HIV-associated chronic obstructive pulmonary disease (Popescu et al., 2016). In addition, ART-induced decrease in HIV viremia was associated with a significant increase in B cell counts, similar to increases in $CD4^+$ T cell counts yet distinct from the lack of increase in $CD8^+$ T cells. The increase in B cell counts was accompanied by a significant decrease in the frequency of apoptosis-prone B cell subpopulations, namely mature activated and immature transitional B cells, which are overrepresented in untreated HIV disease. The increase in B cell counts was reflected by a significant increase in naive and resting memory B cells, both of which represent populations that are essential for generating adequate humoral immunity. This data explain the improvement in humoral immunity reported to occur after an ART-induced decrease in HIV viremia (Moir et al., 2008). Although HIV infection of tissue macrophages is rapidly suppressed by ART, as reflected by decreases in cell-associated virus, delayed viral rebound in tissue macrophages occurs in about one-third of animals studied reinforcing the notion of established persistence of HIV infection within macrophages (Honeycutt et al., 2017).

ART can also impact the lung by causing immune reconstitution inflammatory syndrome (IRIS). Reconstitution of CD4+ T cells with ART results in AM activation in the setting of mycobacterial infections (Lawn et al., 2009) and increased pro-inflammatory mediators (Barber et al., 2012).

3.2.6. ANIMAL MODELS OF HIV INFECTION

Animal models for HIV pathophysiology include rhesus, pigtail and cynomolgus macaques that can be infected with a simian immunodeficiency virus (SIV) or chimeric viruses harbouring fragments of SIV and HIV genomes (SHIV). These models recapitulate many aspects of the human HIV-induced immunopathology in the context of simian AIDS and have largely contributed to a better knowledge of HIV physiology in particular in the field of vaccine and drug testing. Nevertheless, studies using nonhuman primate (NHP) models are limited by several factors, including high cost, small experimental groups and an ever-increasing reticence secondary to ethical concerns (Masse-Ranson et al., 2018).

Of note, murine cells are refractory to HIV-1 infection, even when genetically engineered to express the CD4 receptor molecule, but they do express HIV-1 genes when the virus is introduced by non-infectious processes (Maddon et al., 1986). Subsequently, the development of humanized mice and rat models have been useful in studying HIV. There are several types of humanized rodents including those that are immunodeficient and transplanted with human cells or tissue, $CD34^+$ hematopoietic cells, or some combination of these (Masse-Ranson et al., 2018).

Also transgenic mice have been created for the HIV virus expression. Transgenic models in mice and rats that express HIV proteins such as Nef, Tat, and gp120 are useful to investigate the deleterious effects of these proteins, but cannot replicate active HIV infection. Each model has unique strengths and weaknesses, and use of particular models is dictated by the scientific question to be examined.

3.2.6.1. THE TG26(HIV) TRANSGENIC MOUSE MODEL

The non-replicative proviral transgene (Fetser et al., 1989) *TgN(pNL43d14)* transgene was designed with 7.4-kb proviral human immunodeficiency virus (HIV) DNA construct carrying a deletion, encompassing most of the gag and pol genes, to render it non-infectious. The transgene was microinjected into fertilized FVB/NJ oocytes and mice from founder line 26, containing 10-20 copies of the transgene, were bred to FVB/NJ mice to establish a colony of *Tg26(HIV)* mice (Dickie et al., 1991). These mice have been bred to FVB/NJ mice for at least 10 generations. The inframe deletion of gag and pol sequences encompasses the coding sequences for protease, reverse transcriptase, and the amino-terminus of p34 endonuclease. This construct, encodes the regulatory gene products Nef and Rev, as well as Vpu, Vpr, Vif, and a pl7/p34 fusion gene product (Dickie et al., 1991).

3.3. PULMONARY PATHOLOGY ASSOCIATED WITH SCHISTOSOMA INFECTION

3.3.1. SCHISTOSOMA INFECTION AND DISEASE

Schistosomiasis (bilharziasis) is a disease caused by infection of a parasite of the genus *Schistosoma* of the class of *Trematoda* of the phylum of *Platyhelminthes* (flatworms). The disease is transmitted to human by contact with infested water with special fresh water snails, which act as intermediary for the life cycle of the parasite.

According to the World Health Organization estimates (WHO, 2020) at least 236.6 million people required preventive treatment in 2019 **(Figure 7)**.

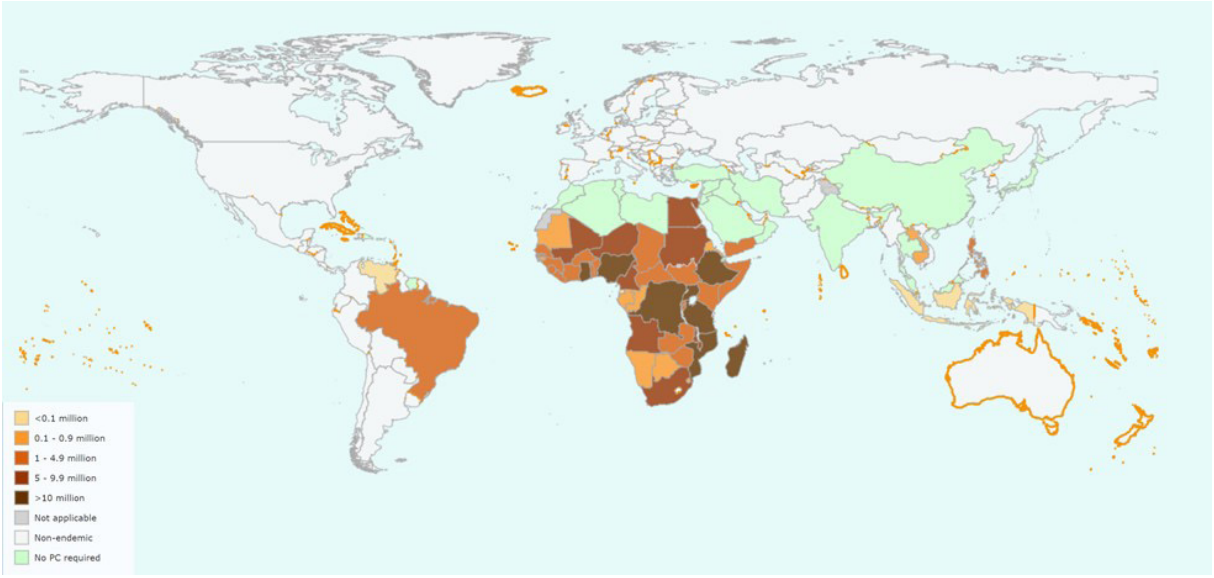

Figure 7. Estimated number of people (all ages) living with Schistosomiasis. Source: World Health Organization 2019.

Preventive treatment, which needs to be repeated over a number of years, reduces and prevents morbidity. Highly active Schistosomiasis transmission has been reported from 78 countries. However, preventive chemotherapy for schistosomiasis, where people and communities are targeted for large-scale treatment, is required in 51 endemic countries with moderate-to-high transmission. (WHO 2021) As such, along with malaria, schistosomiasis is one of the most important of all human parasitic diseases which high rates of disability, which continues to be a global public health concern in the developing world.

Although five species can infect humans, the three most important human schistosomes are *S. mansoni*, *S. japonicum*, and *S. haematobium* (Nelwan, 2019). They live within either the perivascular (*S. haematobium*) or mesenteric (*S. mansoni, S. japonicum*, and others) venules. Ones arrives in the mesenteric venules, the female starts to release eggs. Schistosomes are remarkably fecund: *S. mansoni* worm pairs can lay >300 eggs per day (Cheever et al., 1994)

Schistosomes have a complex life cycle involving both a snail intermediary and a vertebrate definitive host **(Figure 8)**.

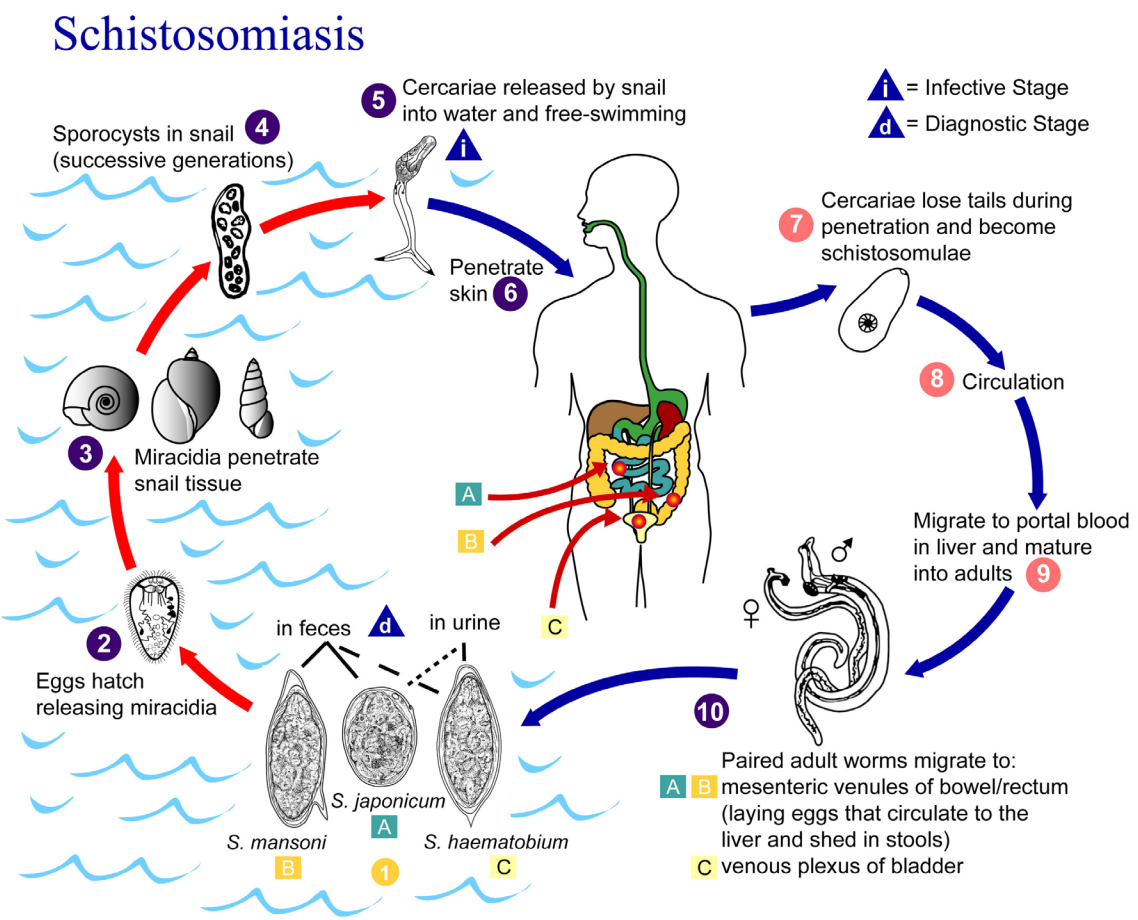

Figure 8. Schistosoma life cycle. Eggs are eliminated with feces or urine (1). Under optimal conditions the eggs hatch and release miracidia (2), which swim and penetrate specific snail intermediate hosts (3). The stages in the snail include 2 generations of sporocysts (4) and the production of cercariae (5). Upon release from the snail, the infective cercariae swim, penetrate the skin of the human host (6), and shed their forked tail, becoming schistosomulae (7). The schistosomulae migrate through several tissues and stages to their residence in the veins (8,9). Adult worms in humans reside in the mesenteric venules in various locations, which at times seem to be specific for each species (10). For instance, S. japonicum is more frequently found in the superior mesenteric veins draining the small intestine [A], and S. mansoni occurs more often in the superior mesenteric veins draining the large intestine [B]. However, both species can occupy either location, and they are capable of moving between sites, so it is not possible to state unequivocally that one species only occurs in one location. S. haematobium most often occurs in the venous plexus of bladder [C], but it can also be found in the rectal venules. The females (size 7 to 20 mm; males slightly smaller) deposit eggs in the small venules of the portal and perivesical systems. The eggs are moved progressively toward the lumen of the intestine (S. mansoni and S. japonicum) and of the bladder and ureters (S. haematobium), and are eliminated with feces or urine, respectively (1). Source: United States Department of Health and Human Services.

The cardinal feature of schistosomiasis is not the mature worm, which has evolved immune evasion mechanisms that allow them to remain incognito within the bloodstream (Pearce, 2005), but the highly antigenic egg-associated pathology that is central to the morbidity and mortality. Eggs that distribute into systemic blood circulation can get trapped, for instance, in the capillary beds of the lungs (Cheever et al., 1994). During chronic stages of infection, half to two thirds of the eggs deposited in mesenteric venules are swept away in the circulation to multiple organs, with the majority ending up in the liver and in the lungs (Cheever et al., 1994). In one histological

autopsy study, 59% of 108 cases had eggs in the lungs, 94% of these being *S. haematobium* (and the remainder mixed *S. haematobium* and *S. mansoni*) (Gelfand, 1948). Actually, schistosomiasis is the most common parasitic disease associated with PAH. It induces remodelling via complex inflammatory processes, which eventually produce clinical signs and symptoms of PAH that are not distinguishable from other forms of the disease (Butrous, 2019).

3.3.2. PULMONARY PATHOLOGY ASSOCIATED WITH SCHISTOSOMIASIS

The aetiology of pulmonary pathology in acute schistosomiasis is not well understood (Gobbi et al., 2020). Although lung symptoms can occur in both acute and chronic schistosomiasis, as shown in **Figure 9**.

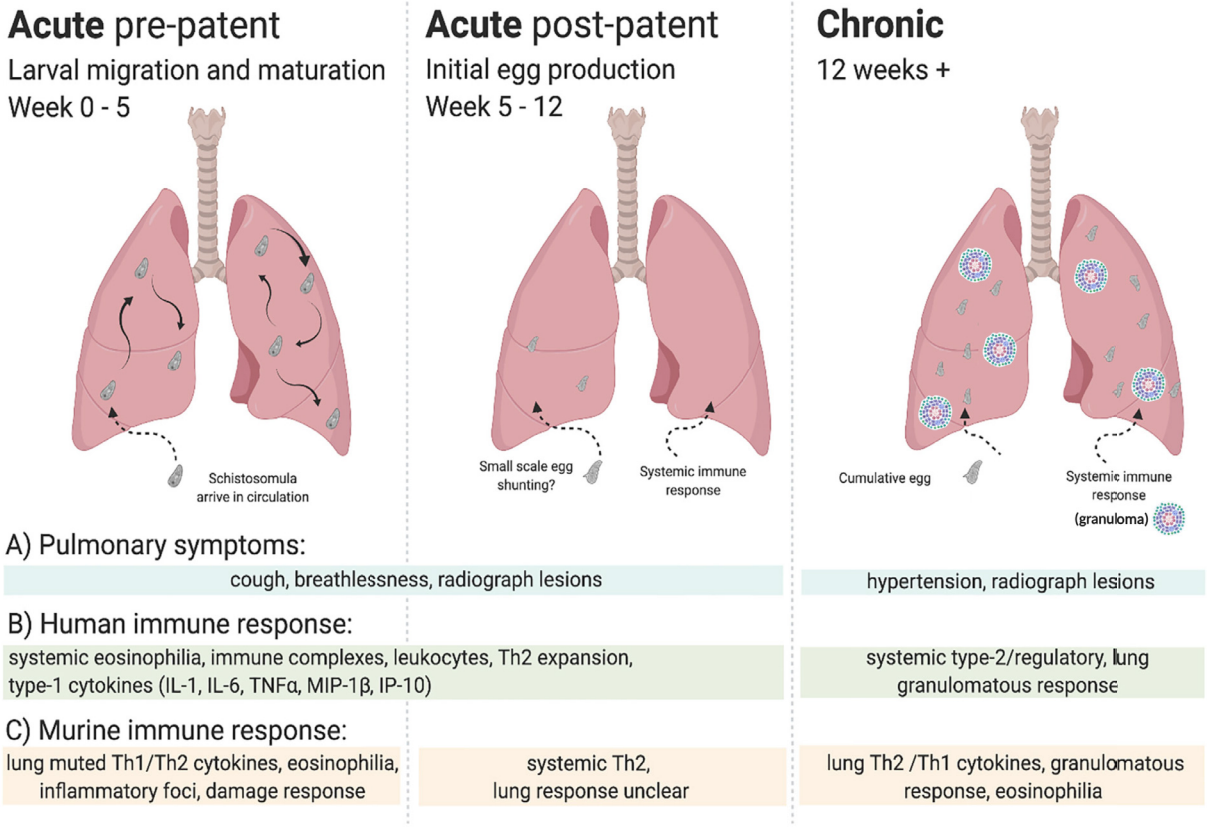

Figure 9. Pulmonary clinical signs in acute and chronic schistosomiasis. Source: Adapted from Front. Immunol., 19 April 2021 https://doi.org/10.3389/fimmu.2021.635513.

One of the main responses to the egg in the lungs is the granulomas formation. Granuloma due to chronic schistosoma infection in the lung may cause nearby vascular changes. After granuloma formation severe intimal, medial, and adventitial hypertrophy and proliferation of a plethora of inflammatory cells occurs in the pulmonary vasculature, which contributes to the development of PAH (Knafl et al., 2020; Shaw & Ghareeb, 1938). Indeed endothelial cell

dysfunction, loss of endothelial barrier integrity, aberrant proliferation of endothelial cells and fibroblasts, thrombi and intimal fibrosis (Basile et al., 2011) are some similarities to the pulmonary vascular remodelling reported in idiopathic PAH (Good et al., 2015).

3.3.3. GRANULOMA FORMATION IN SCHISTOSOMIASIS

What distinguishes granuloma formation from a chronic inflammatory aggregate is the characteristic organization of mature macrophages into a compact structure. A granuloma is defined as a compact (organized) collection of mature mononuclear phagocytes, the specialized differentiation of macrophages into epithelioid cells and giant cells, and the presence of other immune cells like lymphocytes and plasma cells (Pagán & Ramakrishnan, 2018).

Depending on the stimulus and/or disease process, the granuloma macrophages then evolve to undergo various changes. In schistosomiasis they undergo epithelioid transformation in which adjacent cells are linked to each other by tightly interdigitated cell membranes in zipper-like arrays (Schwartz & Fallon, 2018). They fuse their membranes entirely to form multinucleated giant cells (Helming & Gordon, 2008). In schistosomiasis, the granuloma environment is dominated by the T helper type 2 (Th2) cytokines IL-4 and IL-13, which are thought to induce E-cadherin via STAT6 signalling (Moreno et al., 2007; Van Den Bossche et al., 2009). Granuloma macrophages resemble alternatively activated macrophages like those found in schistosome granulomas and had a propensity to aggregate in vitro in response to IL-4 (Linke et al., 2017). However, it is not clear if this pathway is involved in epithelioid transformation in the tuberculous granuloma, which does not have a strong Th2 bias (Cooper, 2009). As granulomas mature, they may undergo structural changes, such as becoming fibrotic, which contributes to morbidity by causing tissue damage. Fibroblasts synthesize extracellular matrix components primarily in response to the cytokines TGF-β1 or IL-4/IL-13, with other cytokines feeding into the TGF-β1 pathway: IL-1β, IL-17A, IFN-γ, and possibly TNF (Mi et al., 2011; Wilson et al., 2010; Wynn & Vannella, 2016). Each of these cytokines can be produced by individual constituent cells of granulomas: monocytes; resident macrophages; atypical monocytes morphologically resembling granulocytes; CD4+, CD8+, and γδ T cells; innate lymphocytes; and eosinophils (Satoh et al., 2017; Wilson et al., 2010). Fibrosis can be beneficial, e.g., by sequestering parasite eggs and larvae. But in many granulomas, fibrosis is pathological, often leading to severe morbidity and fibrosis resulting from dysregulated inflammation leading to fatal organ failure (Eming et al., 2017) **(Figure 10)**.

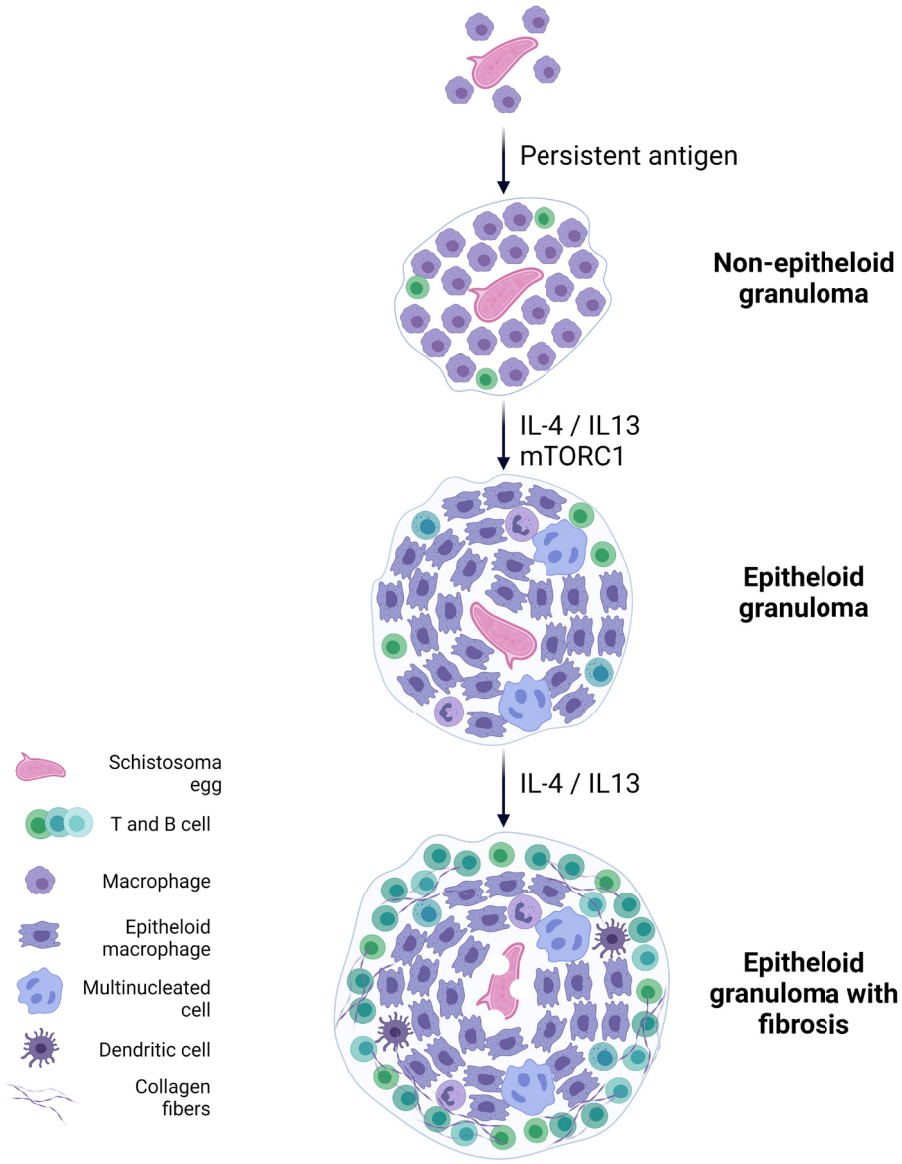

Figure 10. Granuloma formation induced by schistosome eggs. Source: adapted from Pagán, AJ and Ramakrishnan, L. *Annual Review of Immunology* 2018.

3.3.4. PULMONARY IMMUNE FUNCTION IN SCHISTOSOMIASIS

Most of the lung pathology that occurs in Schistosoma infection is associated with granuloma formation and the inflammation that ensues, eventually leading to fibrosis induced by the parasite eggs in the tissue.

The inflammatory response that occurs in schistosomiasis is caused first by the recognition of the parasites in the lung and systemically, and then by the inflammatory response associated with the eggs and their antigenic recognition. During the initial stages of infection, mice display a balanced or Th1-type immune response to parasite antigens. However, once egg

deposition begins around 6 weeks of infection, a dramatic shift to a Th2-type response ensues (Colley & Secor, 2014).

First, occurs the parasite-associated inflammatory response, which is characterised as a Type I response. This Type I response it is characterize by increase of IL-1, IFN-γ and IL-12. The IFN-γ level is elevated after Schistosoma infection in Schistosoma-infected patients at early stages (Mutapi et al., 2007) which is also correlated in acute mice models of Schistosome infection (R. A. Wilson & Coulson, 2009). IL-1, a profibrotic cytokine secreted by monocytes and macrophages, it is also released in the early stages of Schistosoma infection (El Ridi et al., 2006). After, specific schistosome egg antigens interacting with dendritic cells are responsible for this immunologic shift to Type 2 response, partially through the action of certain carbohydrate epitopes (Everts et al., 2012). Transition to the Th2 response occurs approximately 8 weeks post-transfection, and is characterized by secretion of IL-4, IL-13 (Dessein et al., 2004; Fallon et al., 2000; Pearce et al., 1996; Wilson et al., 2007). Finally, fibrosis and granuloma formation cause the ultimate lung damage.

3.4. HIV AND SCHISTOSOMA CO-INFECTION

HIV and schistosomiasis are two of the most widespread infections worldwide; nonetheless, their combined effect has not been fully delineated (Bustinduy et al., 2014). Actually, schistosomiasis appears to be a cofactor in the spread and progression of HIV/AIDS in areas wherein both diseases are endemic (Secor, 2012).

There are approximately 200 million schistosome-infected individuals living in African countries with generalized HIV-1 epidemics, and HIV and Schistosoma co-infection is estimated in 6 million individuals only in Africa with no global estimates ~~worldwide~~ (Joint United Nations Programme on HIV/AIDS (UNAIDS), 2019; Ndeffo Mbah et al., 2016). Therefore, Butrous in 2015 mentioned for the first time that the coinfection by Schistosoma and HIV is a plausible circumstance that would allow for severe and rapidly progressive pulmonary hypertension (Butrous, 2015). In line with this, the requirement for a "second hit" (hypoxia, cocaine or morphine) for HIV-associated PAH has been demonstrated in previous experimental studies (Agarwal et al., 2020; Dhillon et al., 2011; Porter et al., 2013). In addition, schistosomiasis is associated with incident HIV transmission and death in Zambia (Wall et al., 2018) and more death associated with vascular disease is found in patients co-infected in Uganda (Dam et al.,2016); although generalized ART treatment and parasite praziquantel are widely distributed

in those populations. Therefore, the present study was designed to define the effects of HIV and Schistosoma co-exposure on the development of vascular pathology that have not been studied to our knowledge yet.

In fact, climate change, the current mobility of people around the world and the evolution of nature itself is leading to the emergence of new types of infections, caused by viruses, parasites and other previously unknown pathogens. In the coronavirus pandemic that occurred during the development of this doctoral thesis, previous knowledge in techniques and basic science have been key to its mitigation. The study of basic science and of the mechanisms that lead to some of the known diseases, may be key in the future for the study of new infections and pandemics, that could save many lives and be important health drivers. The basic science study of this work on HIV and Schistosoma co-infection and pulmonary involvement can hopefully contribute to improving the quality of life of millions of people affected by it, or in the future, be a small grain of knowledge for the development of science.

4

Rationale & Hypothesis

Rationale & Hypothesis

HIV and Schistosoma infections have been individually associated with pulmonary vascular disease. However, to date, no clinical or experimental studies have assessed the effect of co-exposure to HIV and Schistosoma on the pulmonary vasculature. Since both Schistosoma and HIV are main triggers of vascular pathology, it could be hypothesized that combined exposure to HIV and Schistosoma would allow for severe and rapidly pulmonary vascular disease progression; and that such exacerbation of pathology might be revealed in a non-infectious mouse model for HIV and Schistosoma co-exposure.

5

Objectives

Objectives

GENERAL AIM

To determine the impact of combined exposure to HIV and Schistosoma in pulmonary vascular pathophysiology by using a novel mouse model of co-exposure.

SPECIFIC AIMS

Comparative analysis of the effects of individual or combined exposure to HIV and Schistosoma on the pulmonary vasculature, with regard to vascular remodelling and dysfunction and their association with pulmonary hypertension; and characterization of the pulmonary immune landscape and its involvement in the development of vascular disease.

6

Materials & Methods

Materials & Methods

6.1. ANIMALS

All experimental procedures utilizing animals were carried out according to the Spanish Royal Decree 1201/2005 and 53/2013 on the Care and Use of Laboratory Animals and approved by the institutional Ethical Committees of the Universidad Complutense de Madrid (Madrid, Spain) and the regional Committee for Laboratory Animals Welfare (Comunidad de Madrid, Ref. number PROEXO-003/18). Animal studies are reported in compliance with the ARRIVE guidelines (Kilkenny et al., 2010). Age matched (9-10 weeks) male FVB/NJ (Wt) and HIV-1 (HIV) transgenic mice on the FVB/NJ background (FVB/N-Tg(HIV)26Aln/PkltJ; Tg26) from the Jackson Laboratory (USA) were provided by Charles River (France). This HIV-1 Tg26 mice model express a transgene containing a portion of the HIV genome, including Env and Tat, Nef, Rev, Vif, Vpr, and Vpu accessory genes but lacking part of the Gag-Pol region, rendering the virus non-infectious (Dickie et al., 1991). Animals were kept under standard conditions of temperature 22±1°C and 12:12 hour dark/light cycle with free access to food and water.

6.2. TREATMENT WITH SCHISTOSOMA EGGS

Mice were randomly assigned to four groups: Wt, parasite egg-treated Wt (Wt+Schisto), HIV and egg-treated HIV (HIV+Schisto). *Schistosoma mansoni* eggs were isolated from homogenized and purified livers of Swiss-Webster mice infected with cercariae, provided by the Biomedical Research Institute (Rockville, MD). Eggs were then inactivated by freezing (-60 to -80°C) and stored at -80°C until used. To induce pulmonary vascular disease, we used an experimental model previously reported (Graham et al., 2013; Joyce et al., 2012; Kumar et al., 2015, 2019). In brief, mice were intraperitoneally sensitized to 240 *Schistosoma mansoni* eggs/gram body

weight, and then intravenously challenged two weeks later with 175 *Schistosoma mansoni* eggs/gram body weight. Animals were analyzed seven days after intravenous egg administration (Figure 16). Control mice were unexposed to *S. mansoni* eggs but received the same volume of 1.2% sodium chloride used as vehicle. Experiments were performed in a coded format, with the investigators lacking knowledge of the specific experimental group.

6.3. SCHISTOSOME OVA TISSUE COUNTING

The number of *S. mansoni* eggs present in the mouse lung tissue was determined after digestion of a piece of right lung lobe with shaking in 4% potassium hydroxide for 18 hours at 33°C. The number of eggs present in aliquots of the digest was counted three times, as previously described (Graham et al., 2010).

The protocol had been optimized for mouse lung frozen tissue (stored at -80°C): Addition of approx. 10-15mg of tissue sample to 4% KOH (diluted in ddH2O) was performed. An amount of 25µL KOH/mg tissue was placed in 1.5ml Eppendorf tube and later incubated with shaking (speed 120rpm) for 18 hours at 33°C. After the samples were moved to a 4 degree chamber to slow further digestion, or -80 degrees for longer term storage. The samples were vortex and placed in 25µL aliquots onto slides and count directly using microscope. The number of eggs were counted 3-5 times per sample and mean was calculated. If individual count variated by >10% from the mean, additional aliquots were taken. The mean was multiplied by the volume ratio (total KOH volume / 25µL) to get the total number of eggs. Finally, total number of eggs was divided by total mg tissue.

6.4. ASSESSMENT OF COLLAGEN DEPOSITION

Collagen deposition in the lung was measured by Sirius red staining. Paraffin-embedded lung sections were preheated at 63°C for 30 min. Paraffin was removed with xylene followed by serial rehydration with decreasing percentages of ethanol and washed for 2 minutes in distilled water. The sections were placed in picrosirius red (Sigma) solution for 60 minutes and in acidified water (acetic acid in distilled water) for 4 minutes, followed by two washes first in ethanol and then in xylene. Finally, the slides were mounted with ProLong™ Gold Antifade Mountant (Life Technologies). Quantification of the percent vascular area fraction positive for Sirius red staining was performed with ImageJ.

6.5. LUNG HISTOLOGY

The right lung was washed with saline solution followed by 4% paraformaldehyde infusion through the right bronchus and embedded in paraffin. All sections were cut at 5 μm and were stained with hematoxylin and eosin and examined by light microscopy. For quantification of pulmonary vascular remodeling, PA (25–250 μm outer diameter; OD) were analyzed in a blinded fashion and categorized as muscular, partially muscular or non-muscular. The medial wall thickness was examined by light microscopy, and elastin was visualized by its green autofluorescence. For vessel occlusion analysis all small pulmonary vessels per cross section of the right lobe were evaluated and classified according the evidence of luminal occlusion. Around 500 representative vessels within a range of diameters from 20 to 70 μm were measured per sample. Peri-egg granulomas size were determined in histological sections stained with hematoxylin and eosin containing a single visible egg using NDP view2 software.

6.6. IMMUNOHISTOCHEMICAL ANALYSIS

Paraffin sections of 3-μm thickness were stained with antibodies to α smooth muscle actin (α-SMA) (dilution 1:900, clone 1A4, Sigma, St. Louis, MO, USA), von Willebrand factor (vWF) (dilution 1:900, Dako, Hamburg, Germany) and proliferating cell nuclear antigen (PCNA) (dilution 1:200, sc-56, Santa Cruz Biotechnology, Inc.). Automated quantification of PCNA immunopositive labelling was performed using QuPath (Bankhead et al., 2017). The software was trained to recognize PCNA-stained nuclei and positive labelled cells using positive cell and subcellular detection modules. The number of cells with PCNA-positively labelling per μm^2, and the percentage of cells detected with PCNA immunolabeling were recorded and compared between all groups.

6.7. CLASSIFICATION OF OCCLUDING LESIONS

Small arteries with an outer diameter (OD) < 100μm were analyzed and the type of vessel occlusion were determined according to the pattern of von-Willebrand Factor (vWF) staining. Briefly, non-plexiform-like lesions presented vWF-positive (endothelial) cells as a concentric rim of cells in the inner layer, while plexiform-like lesions showed a complex/disorganized luminal occlusion (Toba et al., 2014).

6.8. RECORDING OF PULMONARY ARTERIAL VASODILATION

Resistance PA were carefully dissected free of surrounding tissue, cut into rings (1.8-2 mm length) and placed in a sterile plate containing serum-free DMEM for 20 h. After that, PA rings were mounted in a wire myograph with Krebs buffer solution maintained at 37 °C and bubbled with 21% O_2, 74% N_2 and 5% CO_2 (Mondejar-Parreño et al., 2018). Vessels were stretched to give an equivalent transmural pressure of 20 mmHg. Preparations were firstly stimulated by raising the K^+ concentration of the buffer (to $80x10^{-3}$ M) in exchange for Na^+. Vessels were washed three times and allowed to recover before a new stimulation. The relaxant effects induced by acetylcholine (ACh, 10^{-9}-10^{-5} M, and endothelial-dependent vasodilator) or sodium nitroprusside (SNP, 10^{-11}-10^{-5} M, an endothelial independent vasodilator) were examined in arteries stimulated with serotonin (5-HT, 10^{-5} M).

6.9. HEMODYNAMIC MEASUREMENTS

One week after intravenous administration of *S. mansoni* eggs, mice were anesthetized i.p. with a mixture of 80 mg/kg ketamine (Mearial Lyon, France) plus 8 mg/kg xylazine (KVP Pharma und Veteriär-Produkte GmbH, Kiel, Germany). Before initiation of surgical procedure, general anesthesia was confirmed by assessing the absence of response to any stimulus. Then, animals were placed in a supine position on a thermostatically controlled electric heating blanket (Homeothemic Blanket Control Unit, Harvard Apparatus, March-Hugstetten, Germany) to maintain body temperature at 38°C. The tracheostomy was performed by a ventral neck incision followed by insertion of a 1.3-mm outer diameter tracheotomy cannula in the trachea. Animals were ventilated with room air (tidal volume 9 mL/Kg, 100 breaths/min, and a positive end-expiratory pressure of 2 cm H_2O) with a rodent ventilator (MiniVent Type 845, Harvard Apparatus, USA). After sternotomy, right ventricular systolic pressure (RVSP), and systolic, diastolic and mean PAP (sPAP, dPAP and mPAP) were measured in open-chest mice as previously reported (Mondejar-Parreño et al., 2018). Measurements were recorded with a pressure transducer via a 0.7-mm internal diameter catheter (24 GA, BD Insyte, USA) introduced in the right ventricle and then advanced to the main PA. Thereafter, animals were sacrificed by exsanguination in the continuous presence of anesthesia and organs were harvested for analysis.

6.10. CARDIAC REMODELING

At the end of the recordings, hearts were excised and the right ventricle (RV) and the left ventricle plus septum (LV+S) were carefully dissected and weighed. The Fulton index [RV/

(LV+S)] and the ratio RV/body weight (BW) were calculated to assess right ventricular hypertrophy (Mondejar-Parreño et al., 2018).

6.11. IMMUNOFLUORESCENCE IN TISSUE SECTIONS

Immunostaining was performed on paraffin-embedded tissue. The paraffin blocks were sliced into 3-µM thick sections, deparaffinized with xylene (Fisher Scientific) for 10 minutes three times, and rehydrated with decreasing concentrations of ethanol in water 100% to 70% 5 minutes each. Antigen retrieval was performed incubating the slides for 20 minutes in the hot (95 ^{0}C) citrate buffer pH 6.0 (Thermofisher, Ref 005000) in a cooker, and 10 minutes of cooling at room temperature. The sections were then washed with phosphate-buffered saline (PBS) (Fisher Scientific) for 10 min. Blocking solution of BSA 5% was incubated in the sections 1 hour at RT. Primary antibodies were applied for overnight at 4ºC temperature in a humidified chamber. The day after, the slides were raised in PBS, and incubated with the right secondary antibody for 1 hour at room temperature. For triple and quadruple staining, the same protocol was repeated for primary and secondary antibody on consecutive days. After washing with PBS for 10 minutes, the slides were incubated with DAPI (Thermo Scientific, Ref 62248) for 10 minutes. After washing with PBS for five minutes the sections were mounted by cover-slipped using a water-based mounting medium (Fisher Scientific). See **Table 1&2** for primary and secondary antibodies.

Table 1. Primary antibodies for immunofluorescence assays.

Antibody	Reactivity	Host	Source	Reference
α-sma FITC	mouse	mouse	Sigma-Aldrich	F3777
CD19	mouse	rabbit	Abcam	ab245235
CD3(17A2)	mouse	goat	Abcam	ab16669
CD3(17A2)	mouse	rat	RD Systems	MAB4841
CD45	mouse	rabbit	Sigma	SAB4502541-100U6
CD45	mouse	rat	Novus	NB10077417SS
F4/80	mouse	rabbit	Cell Signalling	70076s
IFNg	mouse	goat	RD Systems	AF585NA
IL13	mouse	goat	RD Systems	AF413NA
IL17	mouse	rabbit	Abcam	ab79056
IL4	mouse	rat	Novus	NB10064798
IL6	mouse	rabbit	Abcam	ab208113
NEF (HIV)	HIV	mouse	Abcam	ab42358
TCRδ(GL7)	mouse	hamster	Invitrogen	14571182

Table 2. Secondary antibodies for immunofluorescence assays.

Antibody	Conjugation	Source
Donkey Anti-Goat	Alexa Fluor 594	Invitrogen
Goat Anti-Rabbit	Alexa Fluor 555	Invitrogen
Goat Anti-Hamster	Alexa Fluor 647	Abcam
Goat Anti-Mouse	Alexa Fluor 555	Abcam
Goat Anti-Rat	Alexa Fluor 594	Invitrogen

6.12. ISOLATION OF LUNG LEUKOCYTES

After measuring PAP, mouse lungs were perfused by right ventricle administration of PBS and digested for flow cytometry analysis. Left lobes were finely chopped into small pieces and placed in 1mg/ml of Liberase TM (Sigma) dissolved in RPMI. The digested samples were incubated at 37ºC for 30 minutes. Subsequently 100µl of EDTA was added to stop the reaction. After 2 minutes 1 ml of RPMI was added and the tissue was disrupted by vigorous pipetting using a 1ml pasture pipet. The cell suspension was filtered using a 40 µm cell strainer (Corning®), followed by centrifugation for 10 minutes at 300g. The supernatant was removed and the cells were resuspended into 1 ml red blood cell lysis buffer (ACK lysing bufferGibco®/Life technologies®) 10 minutes for red blood cells lysis followed by adding 14ml of RPMI. Next, the suspension was centrifuged again at 300g for 10 minutes and the pellet resuspended in RPMI. Cell counting was performed using a Neubauer chamber after staining with trypan blue to exclude dead cells **(Figure 11)**.

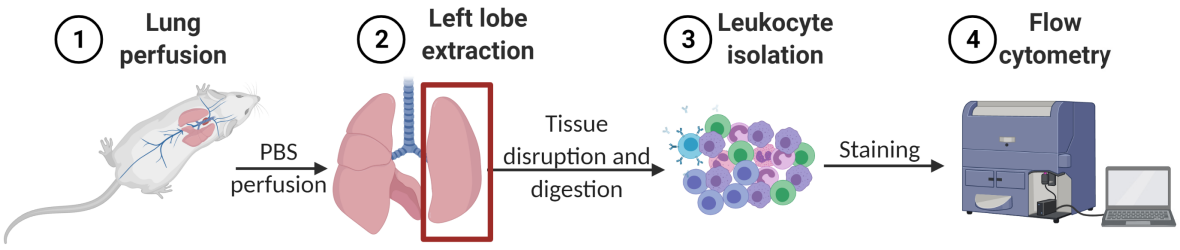

Figure 11. Isolation of lung leukocytes.

6.13. CELL STAINING FOR FLOW CYTOMETRY

For flow cytometry analysis, cells were resuspended in FACS buffer (PBS containing 5% bovine serum albumin, 0.1 % sodium azide). The samples were distributed into 5^5 cells/100µl of flow wash buffer. Following blocking of Fc receptors with anti-CD16/CD32 antibodies (BD

Pharmingen), and the cells were initially stained extracellularly for extracellular leukocyte markers using fluorochrome conjugated antibodies in a concentration of 1µg/ml. The samples were incubated at 4°C in the dark for 30 minutes. The cells were then centrifuged, the supernatant discarded and the cells were fixed using a 1% BD Cell Fix (BD Biosciences). For intracellular staining, cells were treated with a final concentration of 0.5% cytofix/cytoperm and stained intracellularly for intracellular markers using fluorochrome conjugated antibodies at a concentration of 2µg/ml and incubated at 4°C in the dark for 30 minutes. The cells were then washed and ready for analysis. See **table 3** for antibody details. Data were acquired with a BD FACSCalibur flow cytometer and analyzed using FlowJo software (BD Biosciences).

Table 3. Primary antibodies for cytometry.

Antibody	Clone	Source
CCR6	29-2L17	BioLegend
CD11b	M1/70	E-BioScience
CD11c	HL3	BD Pharmingen
CD19	ID3	E-BioScience
CD25	2A3	BD Pharmingen
CD27	L67F9	E-BioScience
CD3e	145-2C11	BD Pharmingen
CD4	GK1.5	E-BioScience
CD45	30-F11	E-BioScience
CD64	X54.5/7.1	BD Pharmingen
CD8	H35-17.2	E-BioScience
F4/80	T452342	BD Pharmingen
FOXP3	NRRF30	E-BioScience
IFN-γ	XMG1.2	BD Pharmingen
IL-13	Ebio13A	E-BioScience
IL-17	Ebio17B7	E-BioScience
IL-4	BVD4-1D11	BD Pharmingen
Ly6C/Ly6G	RB68C5	BD Pharmingen
MHCII	M5/114.15.2	BD Pharmingen
NK1.1	PK136	BD Pharmingen
TCRβ	H57597	BD Pharmingen
TCRδ	GL3	BD Pharmingen

6.14. IMMUNOPHENOTYPING OF PULMONARY LEUKOCYTE SUBSETS

The immunophenotype of pulmonary leukocyte subsets was analyzed by flow cytometry using the gating strategies depicted in **Figure 12** and **Figure 13** (adapted from Yu et al, 2016).

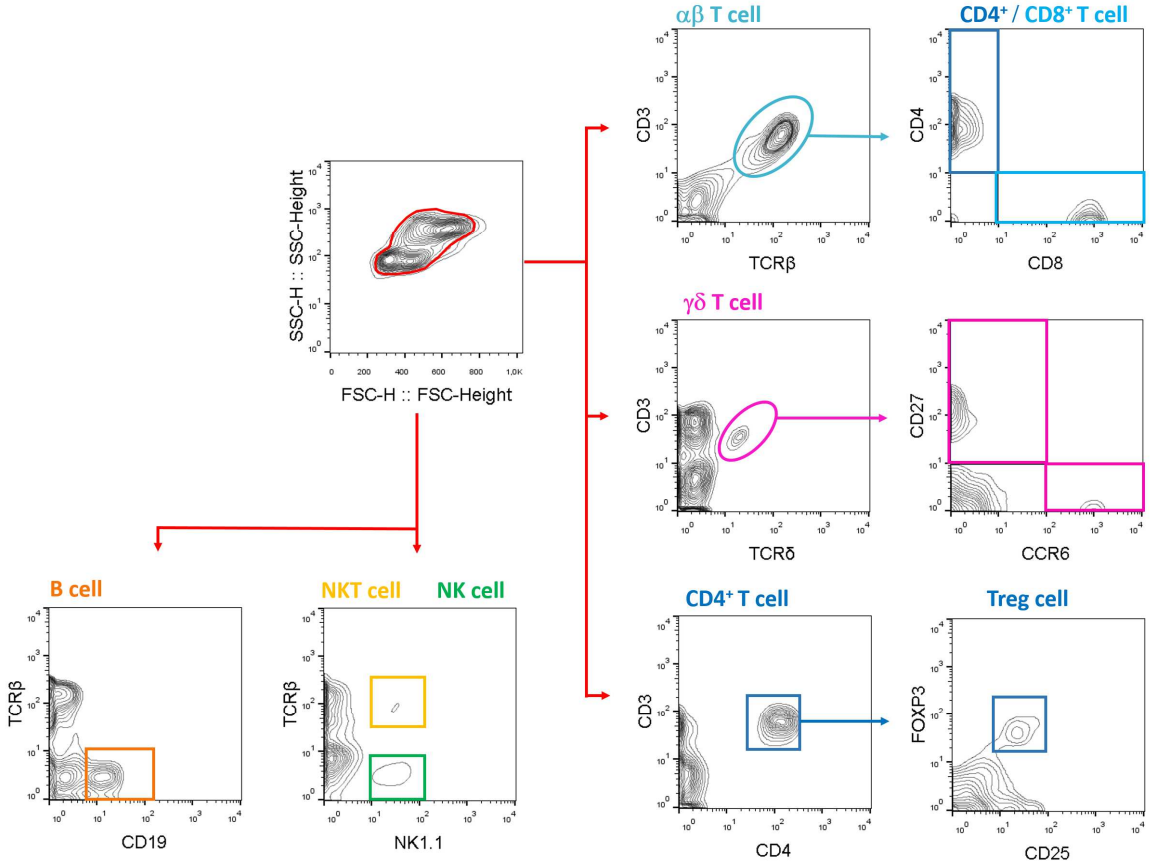

Figure 12. Flow cytometry gating strategy for identification of pulmonary lymphoid cells. The starting population in the FSC (forward scatter) versus SSC (side scatter) plot were viable leukocytes, as determined in independent 7-AAD/CD45 staining.

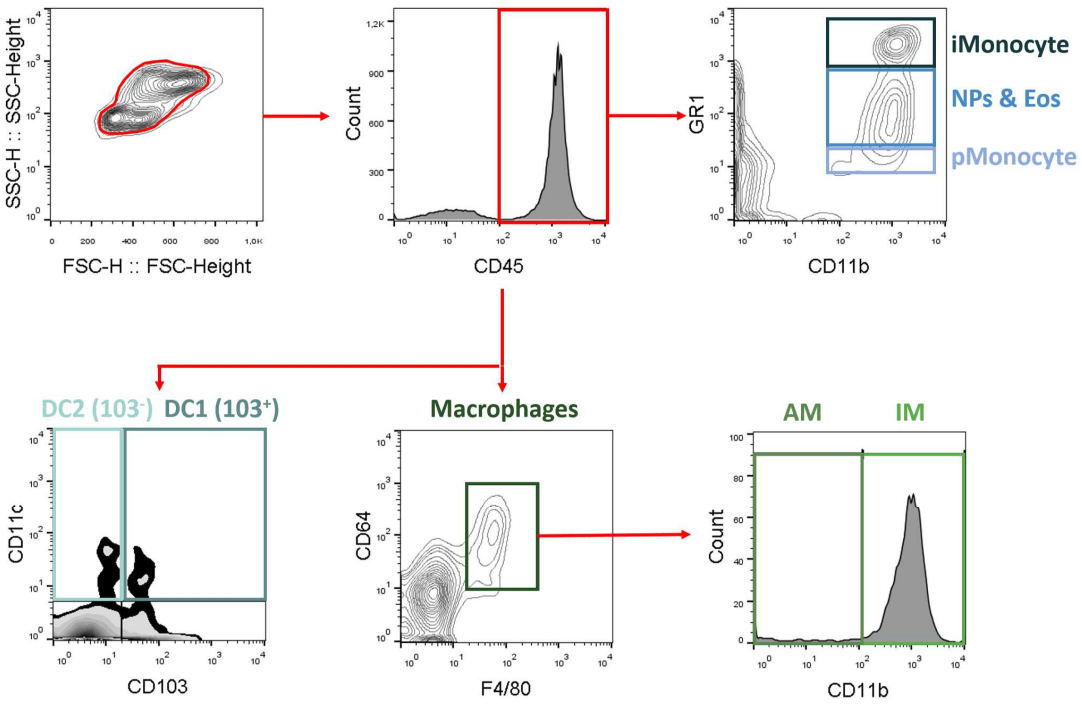

Figure 13. Flow cytometry gating strategy for identification of pulmonary myeloid cells. iMonocyte: inflammatory monocyte; pMonocyte: patrolling monocyte; NPs: neutrophil; Eos: eosinophil; DC: dendritic cell; AM: alveolar macrophage; IM: interstitial macrophage. The starting population in the FSC (forward scatter) versus SSC (side scatter) plot were viable leukocytes, as determined in independent 7-AAD/CD45 staining.

6.15. ANALYSIS OF CYTOKINE EXPRESSION IN PULMONARY LEUKOCYTES

Cytokine expression in distinct subsets of pulmonary leukocytes was analyzed by flow cytometry according to the gating strategy depicted in **Figure 14** and **Figure 15** for T cells and myeloid cells, respectively.

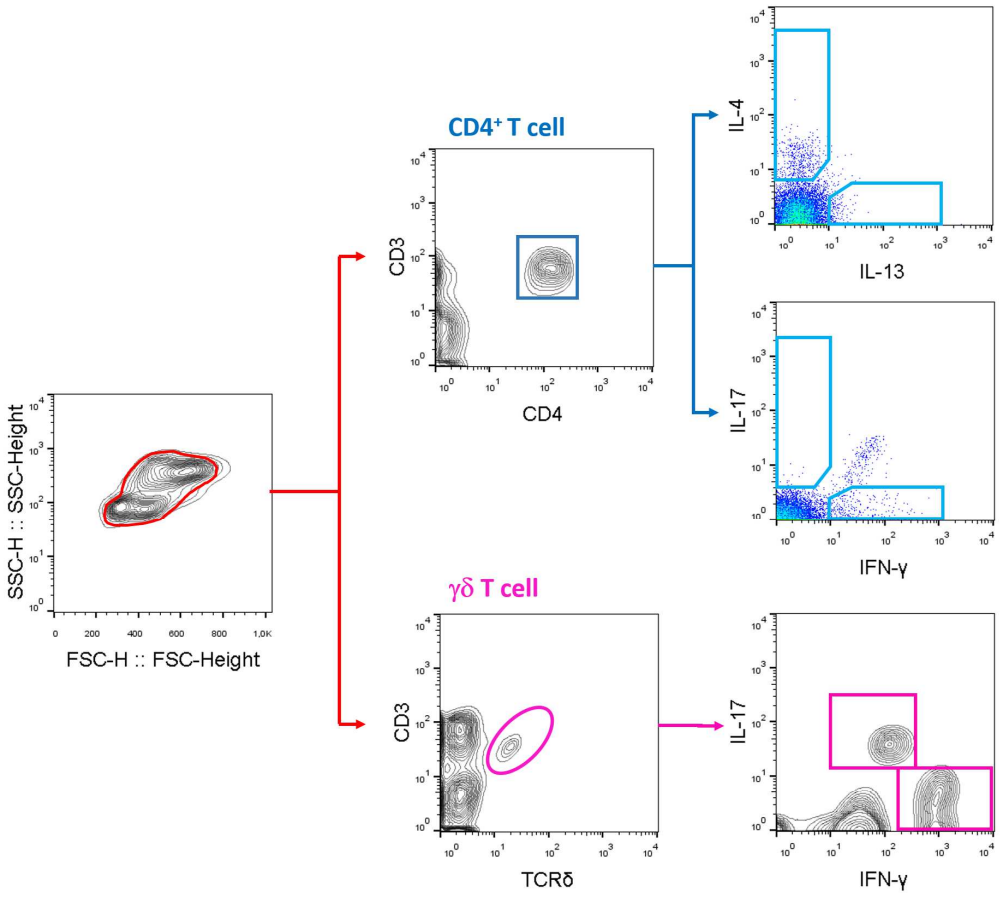

Figure 14. Flow cytometry gating strategy for identification of cytokine-expressing T cells in the lung.

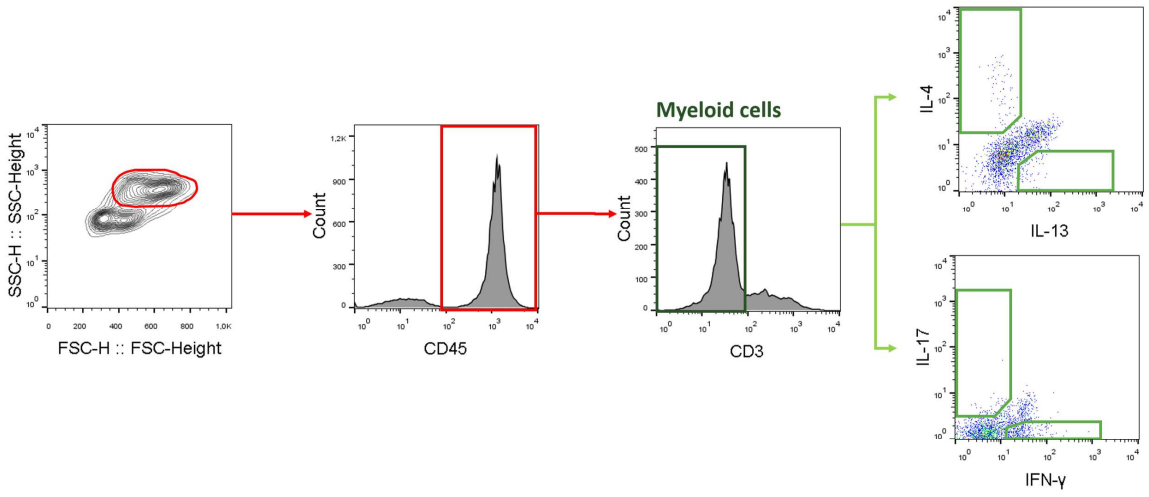

Figure 15. Flow cytometry gating strategy for identification of cytokine-expressing myeloid cells in the lung.

6.16. REAGENTS

Drugs and reagents were obtained from Sigma-Aldrich Quimica (Spain). Drugs were dissolved in distilled water.

6.17. STATISTICAL ANALYSIS

Data are expressed as mean ± SEM.; n indicates the number of experiments from different animals unless otherwise stated. Statistical analysis was performed using a Student's t test and one-way ANOVA (for normally distributed data) followed by Tukey post hoc test. Two-way ANOVA and the Bonferroni multiple comparison test was used to compare dose–response curves. When more than one sample came from the same animal, the nested ANOVA was applied. Differences were considered statistically significant when *P* value was less than 0.05.

7

Results

Results

7.1. A MOUSE MODEL OF HIV AND SCHISTOSOMA CO-EXPOSURE AND ITS IMPACT ON PULMONARY VASCULAR PATHOPHYSIOLOGY

The effects of HIV and Schistosoma co-exposure on the pulmonary vasculature and its impact on the development of pulmonary vascular disease are largely unknown. We have approached these questions in a novel non-infectious model of combined exposure to HIV and Schistosoma.

To model exposure to Schistosoma, inactivated *S. mansoni* eggs were used for lung embolization in previously sensitized HIV mice or Wt counterparts as controls, according to the experimental design depicted in **Figure 16**.

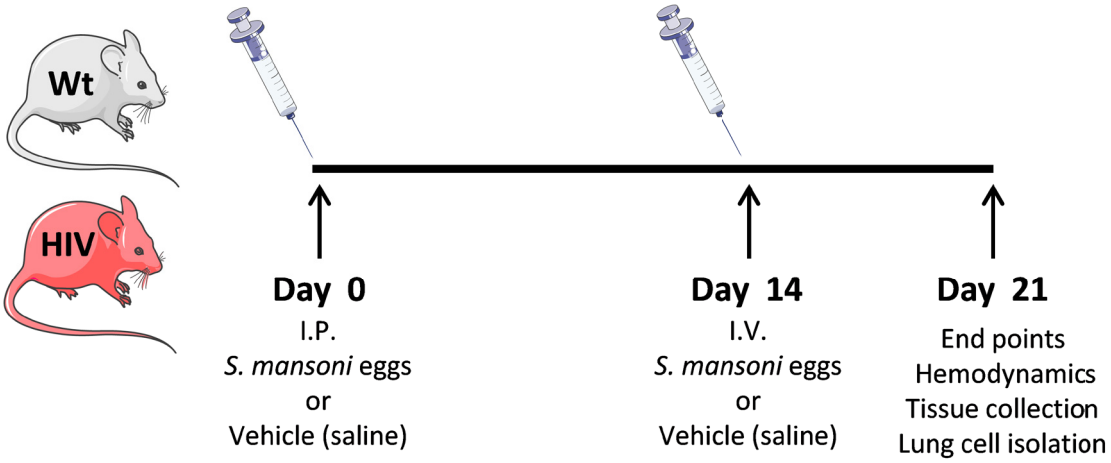

Figure 16. Outline of administration of *S. mansoni* eggs and mouse analysis.

To model HIV exposure, HIV-1 (Tg26) transgenic mice (hereafter referred to as "HIV mice") were used. This transgenic line harbours a replication-deficient HIV-1 pro-viral genome encoding

Env and Tat, Nef, Rev, Vif, Vpr, and Vpu accessory genes but lacking part of the Gag-Pol region, rendering the virus non-infectious. Viral transcripts are expressed at low levels in immune cells such as monocytes, macrophages and lymphocytes. HIV-1 transgene expression is detectable in different tissues, including the lung, as shown for the viral protein Nef in **Figure 17, A**.

To our knowledge, this is the first time that such a model of HIV-1 and Schistosoma co-exposure is used for the specific analysis of pulmonary vascular pathology.

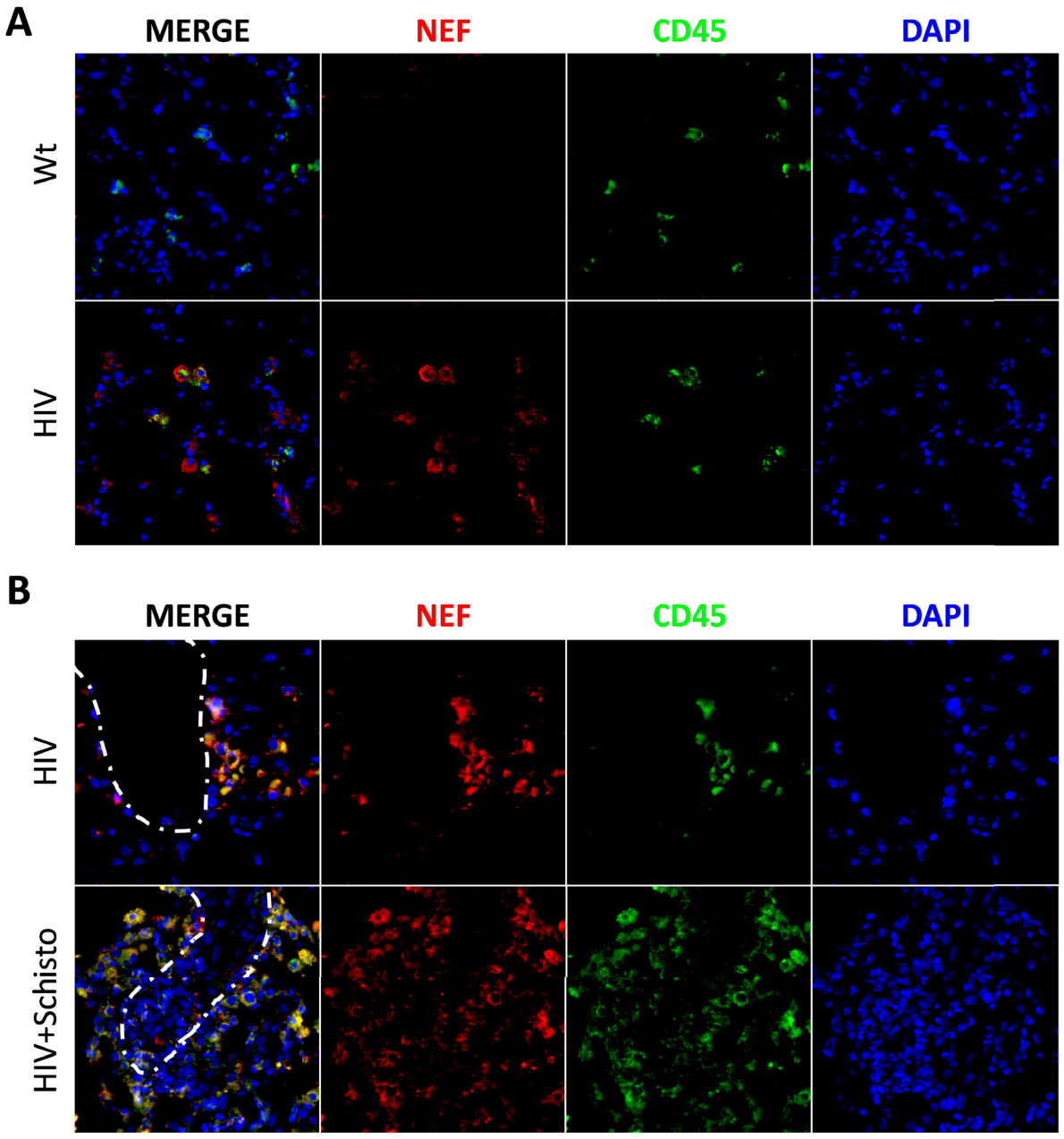

Figure 17. Expression of the HIV-1 NEF protein in the lung of HIV mice. (A) Representative examples of IFM analysis of NEF expression in the pulmonary parenchyma of Wt and HIV mice. **(B)** NEF expression around pulmonary vessels in HIV mice untreated or treated with schistosome eggs. Vessels are marked with a dotted line. CD45 staining was used to identify leukocytes and DAPI to stain cell nuclei.

7.2. LETHALITY ASSOCIATED TO THE HIV/SCHISTOSOMA CO-EXPOSURE MODEL

Wt and HIV mice were randomly assigned to either saline or *S. mansoni* egg administration. As shown in **Figure 18**, all Wt mice treated with saline survived until the end of the study. One egg-treated Wt mouse died between IP and IV egg administration, and thus total survival rate was 97%. With regard to HIV mice, in the saline group, one animal died after IP administration and another three after IV administration, so that total survival rate was 85%. In the egg-treated group, from 50 animals that started the assay, eight died after IP injection and another nine after IV administration; so that total survival rate was 66%. These data show that schistosome egg administration neither in Wt nor in HIV mice (with 3% and 15% mortality rates, respectively) produces a mortality rate beyond 15%. In contrast, egg-treated HIV mice displayed a very high mortality rate, which reached almost 40% of the animals. The causes of this heightened mortality in co-exposed mice are unknown.

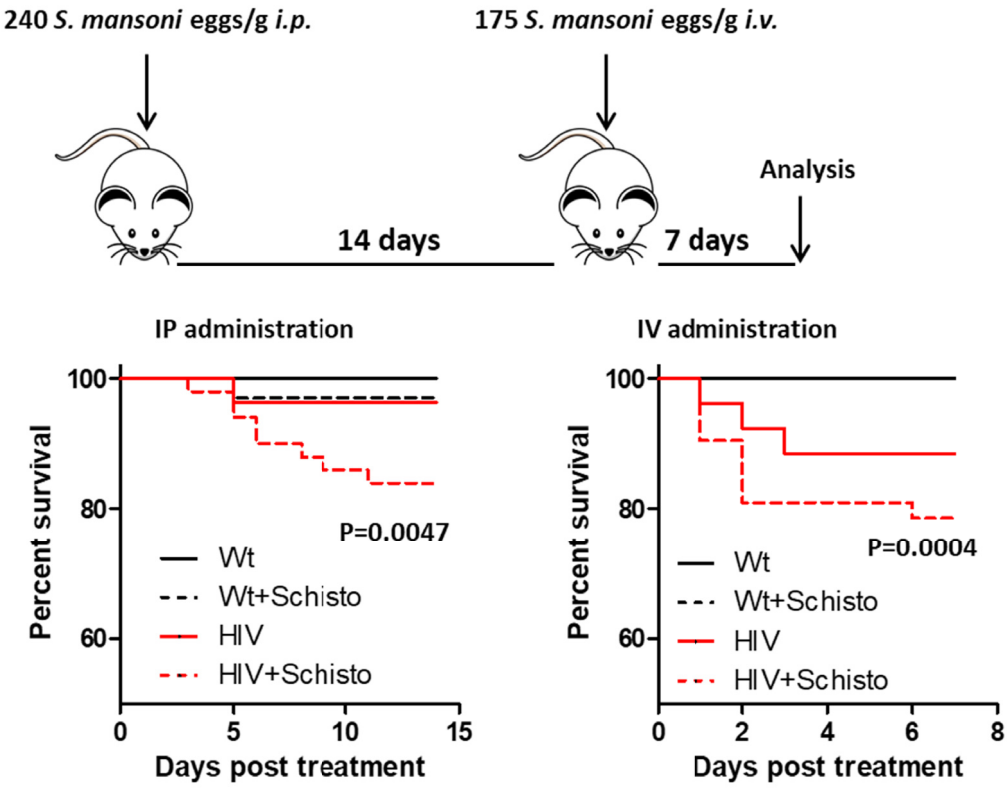

Group	n day 0	day 14	% survival
Wt	30	30	100
Wt+Schisto	34	33	97
HIV	27	26	96
HIV+Schisto	50	42	84

Group	n day 0	day 7	% survival
Wt	30	30	100
Wt+Schisto	33	33	100
HIV	26	23	88
HIV+Schisto	42	33	78

Figure 18. Mortality rate and Kaplan-Meier analysis of survival in Wt and HIV mice exposed or not to schistosoma eggs.

7.3. GRANULOMA: FORMATION AND FIBROSIS

Formation of peri-egg granulomas is typical feature of the immune response induced by Schistosoma eggs trapped in the pulmonary vasculature (Graham et al., 2010; Joyce et al., 2012).

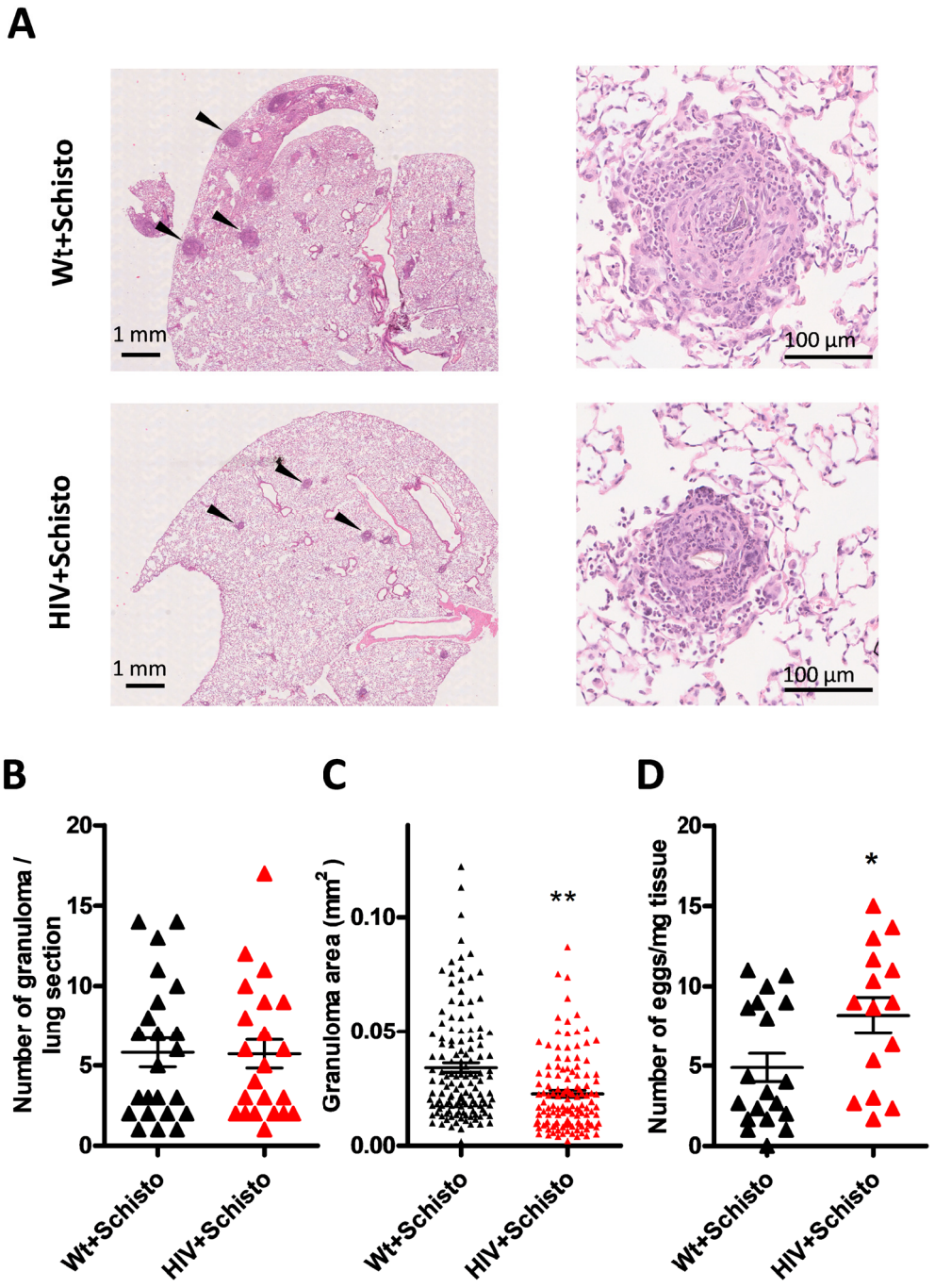

Figure 19. Reduced granuloma size and increased egg burden in HIV mice after Schistosoma egg exposure. **(A)** Left: representative images showing lung granulomas (solid arrowheads) in hematoxylin-and-eosin-stained lung sections from Wt and HIV mice exposed to Schistosoma eggs. Right: magnification of representative images of an intraparenchyma peri-egg granuloma. **(B)** Number of granulomas per lung section (n=22-23 mice), **(C)** granuloma area (126 and 134 granulomas analyzed from n=22-23 mice, respectively) and **(D)** number of eggs recovered from lung digests in Wt (n=15) and HIV (n=19) mice exposed to Schistosoma eggs. Results are shown as mean ± SEM. **P*<0.05 and ***P*<0.01 (Student's unpaired *t*-test).

Embolization of Schistosoma eggs led to the formation of peri-egg granulomas in the lung of Wt and HIV mice, which displayed a similar gross appearance in both mice **(Figure 19, A)**. The number of granulomas was also comparable between Wt and HIV mice **(Figure 19, B)** but, interestingly, granuloma size was significantly smaller in the latter **(Figure 19, C)**. Moreover, granulomas in HIV mice showed an impaired capability for egg clearance, as indicated by significantly higher residual egg burden observed in these mice compared to Wt counterparts **(Figure 19, D)**.

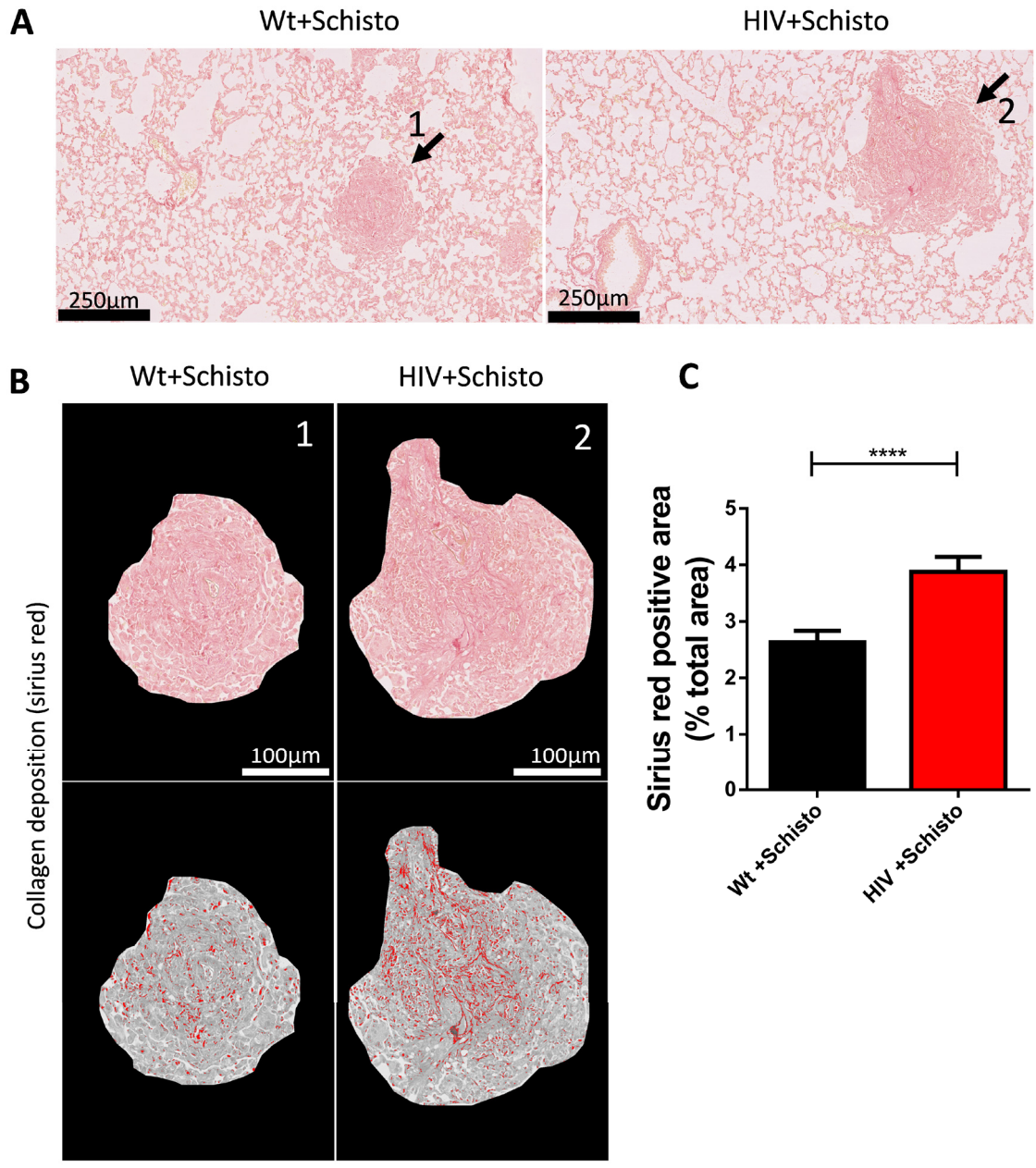

Figure 20. Exacerbated fibrosis in lung granuloma from HIV mice exposed to Schistosoma eggs. (A) Representative pulmonary granulomas of Wt (1) and HIV (2) mice exposed to Schistosoma eggs. **(B)** Collagen deposition assessed by Sirius Red staining in the granulomas indicated in A. **(C)** Quantification of Sirius Red staining. Mice and granulomas analyzed per group were: Wt+Schisto (5; 46) and HIV+Schisto (5; 51). Results are expressed as mean ± SEM. ****P<0.0001 as determined by Student's t-test.

To analyse the impact of Schistosoma exposure on granuloma fibrosis in Wt and HIV mice, collagen deposition was assessed by Sirius red (SR) staining **(Figure 20, A&B)**. Quantification of SR staining revealed that granulomas in HIV mice had a significantly higher degree of fibrosis compared to Wt animals **(Figure 20, C)**. Also, collagen fibres appeared much more disorganized and located in the middle of the granuloma in egg-treated HIV mice. These data suggest that a more rapid and intense fibrosis occurs in co-exposed mice.

Collectively, these results suggest that maturation of schistosoma-induced granulomas is affected in HIV mice.

7.4. PULMONARY VASCULAR REMODELLING

7.4.1. VASCULAR MUSCULARIZATION

To determine the effect of individual or combined exposure to HIV and Schistosoma eggs on pulmonary vascular remodelling, we analysed hematoxylin/eosin stained lung sections from untreated and egg-treated Wt and HIV mice **(Figure 21, A)**.

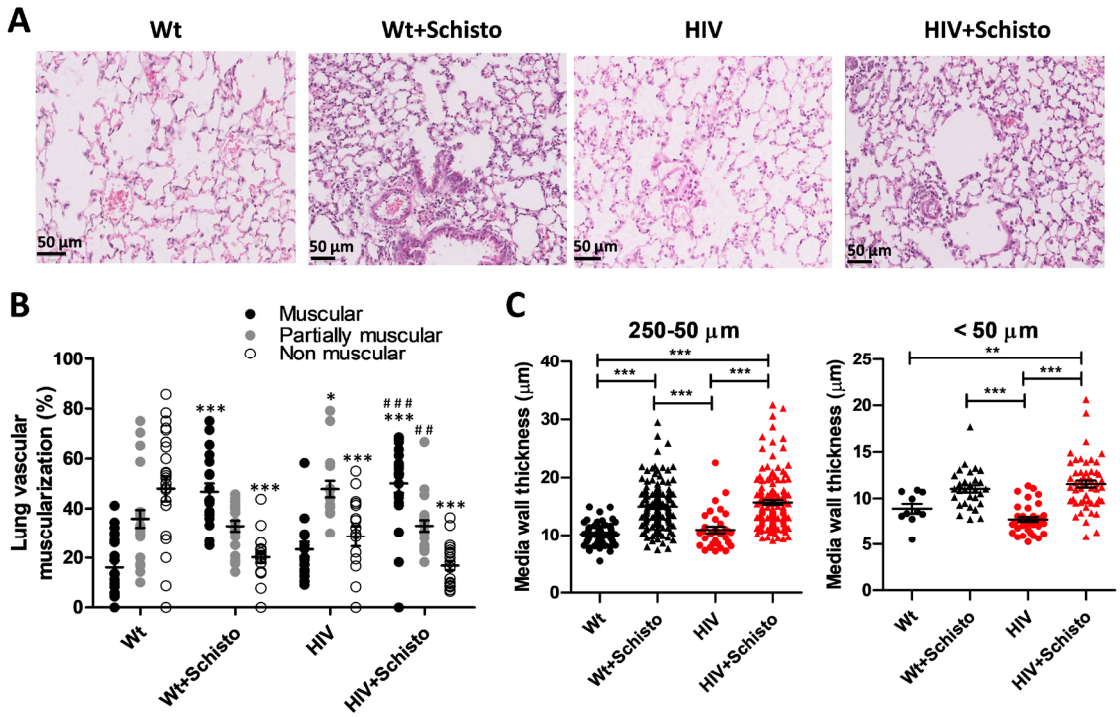

Figure 21. Schistosoma egg exposure induces a similar degree of vascular medial wall remodeling in Wt and HIV mice. (A) Representative hematoxylin-eosin staining of paraffin-embedded lung sections from Wt and HIV mice exposed or unexposed to Schistosoma (Solid arrowheads mark pulmonary arteries) **(B)** Percentage of muscular (black), partially muscular (grey), and non-muscular (white) vessels (n=16-23 mice per group). * and *** indicate P<0.05 and P<0.001, respectively vs Wt; ## and ### indicate P<0.01 and P<0.001 vs HIV, respectively. **(C)** Medial wall thickness of PA between 250 and 50 µm (left panel) and < 50 µm (n=8-13 mice). **P<0.01 and ***P<0.001. Results are shown as mean ± SEM. One-way ANOVA analysis followed by Tukey post hoc test was applied.

Small PA were classified in a blinded fashion as muscular, partially muscular and non-muscular arteries. We found a modest vascular remodelling in HIV respect to Wt mice suggested by an increased percentage of partially muscular PA and a decreased percentage of non-muscular PA **(Figure 21, B)**.

These observations are in line with a previous study comparing Wt and HIV mice (Mondejar-Parreño et al., 2018). Administration of Schistosoma eggs in Wt mice led to a clear vascular remodelling indicated by a much higher percentage of muscular PA and a lower percentage of non-muscular PA. A similar pattern of PA muscularization was observed in egg-exposed HIV mice. Quantification of the vascular remodelling in PA (250-50 μm) showed a comparable increase in the medial wall thickness in egg-exposed Wt and HIV mice, compared respectively to untreated counterparts **(Figure 21, C, left panel)**, with this enhancement being not significantly different between egg-treated mice. A similar finding was observed in smaller (<50 μm) PA **(Figure 21, C, right panel)**.

7.4.2. ENDOTHELIAL CELL PROLIFERATION

Next, we assessed the cellular proliferation in the lung by immunohistochemical staining for the proliferating cell nuclear antigen (PCNA) marker **(Figure 22)**. Histological examination of lung sections demonstrated enhanced PCNA staining in egg-treated compared to untreated mice **(Figure 22, A)**. Specific quantification of PCNA positive cells within the vessels area showed a significant increase in animals exposed to Schistosoma eggs **(Figure 22, B)**. Of note, egg-exposed HIV mice exhibited significantly higher frequencies of proliferating cells compared to all other groups. Moreover, in stained lung sections from egg-treated animals, occluded vessels were strongly positive not only for PCNA expression **(Figure 22, C)** but also for the endothelial cell marker von Willebrand Factor (vWF) **(Figure 22, D)**. Noticeably, these endothelial cells did not form a monolayer, as expected in healthy vessels, but piled up to fill the vascular lumen, suggesting the involvement of endothelial cell proliferation in vessel obliteration.

7.4.3. VESSEL OCCLUSION: PLEXIFORM-LIKE LESSIONS

Analysis of fully closed vessels revealed that none of the untreated Wt or HIV mice showed lumen occlusion of pulmonary vessels. In contrast, occluded vessels were observed in mice exposed to Schistosoma eggs **(Figure 23A, left images)**. Notably, 9 out of the 19 egg-exposed Wt animals (47%) displayed at least one occluded vessel, while this was observed in 14 out of 20 (70%) in the egg-exposed HIV group **(Figure 23A, middle panel)**. Indeed, the percentage of occluded vessels was double in egg-treated HIV mice compared to Wt counterparts **(Figure 23, right panel)**.

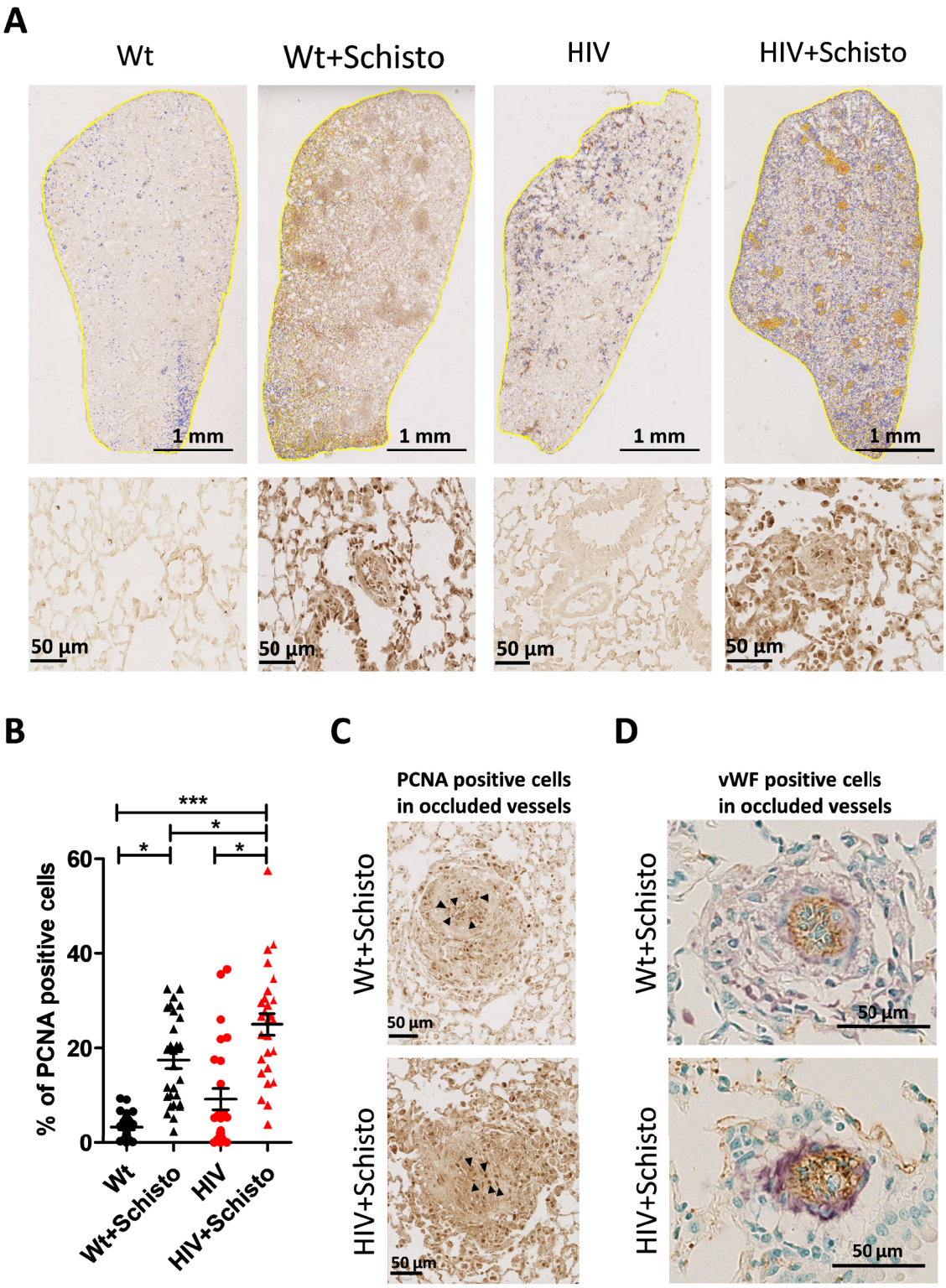

Figure 22. Enhanced pulmonary endothelial proliferation in HIV mice exposed to Schistosoma eggs. (A) Representative images of proliferating cell nuclear antigen (PCNA) in lung sections and amplified vessels from Wt and HIV mice exposed and unexposed to Schistosoma eggs. **(B)** Quantification of the PCNA positive cells within the vessels area (n=25-28 from 5 mice in each group). **(C)** Representative images of PCNA staining in occluded lesions (solid arrowheads point to representative PCNA+ cells). **(D)** Representative images of occluded lesions where cellular identity was visualized by antibodies against α-smooth muscle actin (purple/violet color) and von-Willebrand factor (vWF, brown color) in Wt (upper panel) and HIV (lower panel) mice exposed to Schistosoma eggs. Results are expressed as mean ± SEM. *P<0.05 and ***P<0.001 (one-way ANOVA analysis followed by Tukey post hoc test).

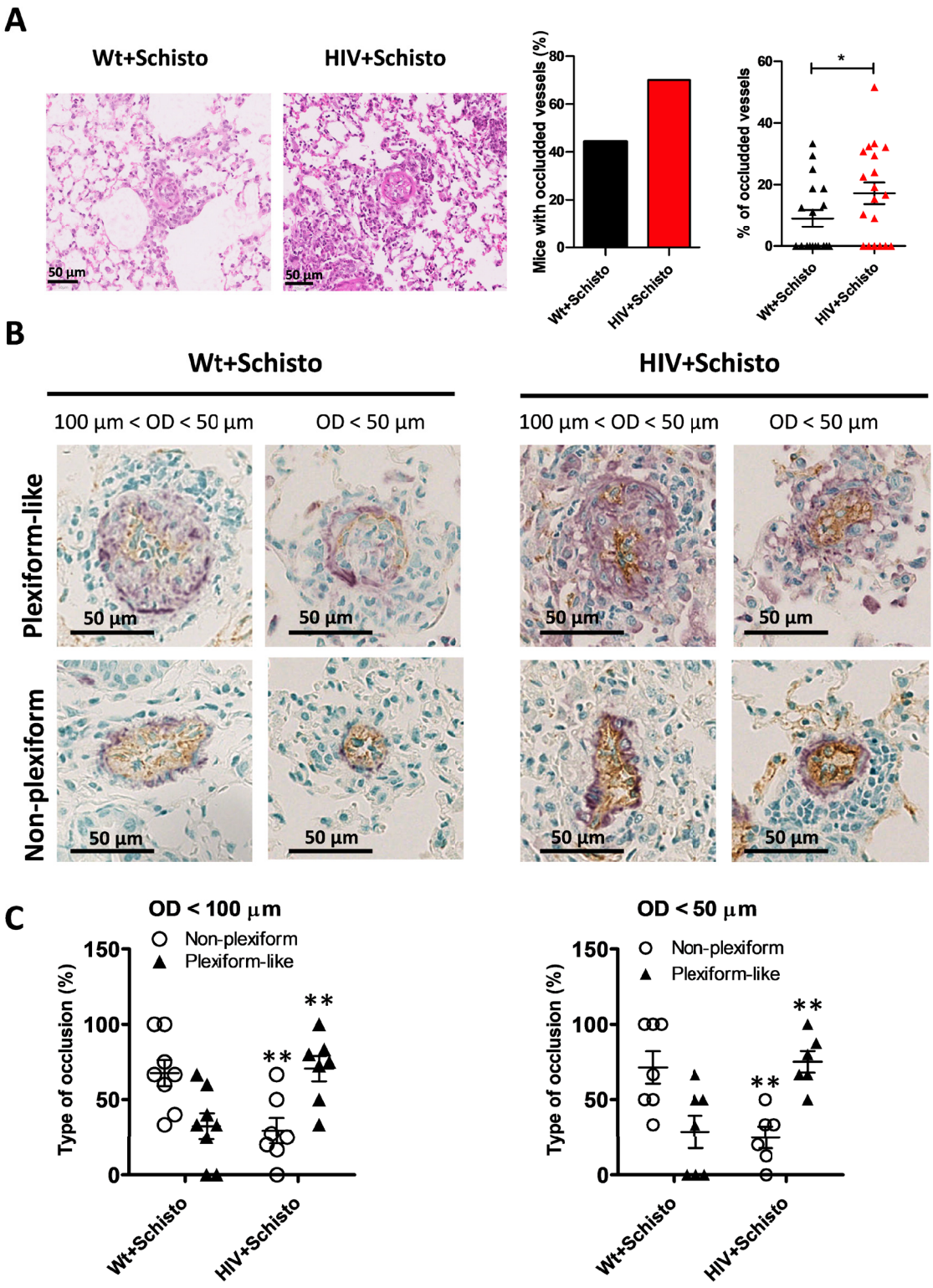

Figure 23. Increased vessel obliteration and plexiform-like lesions in HIV mice exposed to parasite eggs. **(A)** Representative photomicrographs of hematoxylin and eosin stained occluded vessels (Solid arrowheads) (left panels). Frequencies of animals with occluded vessels (middle panel) and percentage of occluded vessels (right panel) (n= 19 mice per group). **(B)** Representative cross-sectional views of α-smooth muscle actin (purple/violet color) and von-Willebrand factor (vWF, brown color) staining of plexiform-like (upper panels) and non-plexiform-like type (bottom panels) of occluded vessels of size between 50 and 100 µm and < 50 µm (magnification 40x; scale bar 50 µm). **(C)** Percentage of severe occluded vessels of outer diameter (OD) < 100 µm (left panel) and < 50 µm (right panel). Results are expressed as mean ± SEM. *P<0.05 and **P<0.01 versus Wt+Schisto determined by unpaired Student's t test.

Next, we studied the type of intimal remodelling in these occluding lesions as described in Material and Methods. Non-plexiform and plexiform-like lesions were observed in small pulmonary vessels from both egg-exposed Wt and HIV mice (representative images in **Figure 23, B**). However, egg-treated HIV mice developed severe occlusive lesions with a plexiform-like phenotype more frequently compared to Wt counterparts **(Figure 23, C)**, in vessels in the range of OD < 100 μm and OD < 50 μm. Taken together, these results suggest that co-exposure to HIV and Schistosoma exacerbates endothelial cell proliferation and formation of plexiform-like lesions associated with faster and enhanced occlusion of small pulmonary vessels.

7.4.4. VASCULAR FIBROSIS

To analyze the impact of individual or combined HIV and Schistosoma exposure on the pulmonary vasculature, we started by assessing perivascular collagen deposition by Sirius red staining, as shown by representative images in **Figure 24, A**. Quantification of Sirius red staining **(Figure 24, B)** revealed that pulmonary vessels from HIV mice had a significantly higher degree of fibrosis compared to Wt animals. Administration of parasite eggs resulted in augmented collagen deposition in vessels from both mice, although of a greater magnitude in HIV mice. Noticeably, pulmonary vessels from untreated HIV mice demonstrated levels of fibrosis similar to those in egg-treated Wt counterparts. These findings suggest that HIV mice have an intrinsic tendency to develop pulmonary vascular fibrosis, which could be further enhanced by schistosome eggs trapped in the lung vasculature.

7.5. PULMONARY ARTERIAL PRESSURE (PAP)

Because HIV- and schistosomiasis-induced lung vascular remodelling are associated with an elevation of PAP and pulmonary vascular resistance, we analysed the impact of individual and combined HIV and Schistosoma exposure on pulmonary hemodynamic via right heart catheterization **(Figure 25, A-D)**. Untreated Wt and HIV mice had similar RVSP, systolic, diastolic and mean PAP. Egg-treated mice showed a general tendency to higher values of these hemodynamic parameters, with the differences being significant for diastolic and mean PAP in egg-treated HIV mice compared to untreated ones. Noticeably, egg-treated HIV mice demonstrated the highest values for all the hemodynamic parameters analysed.

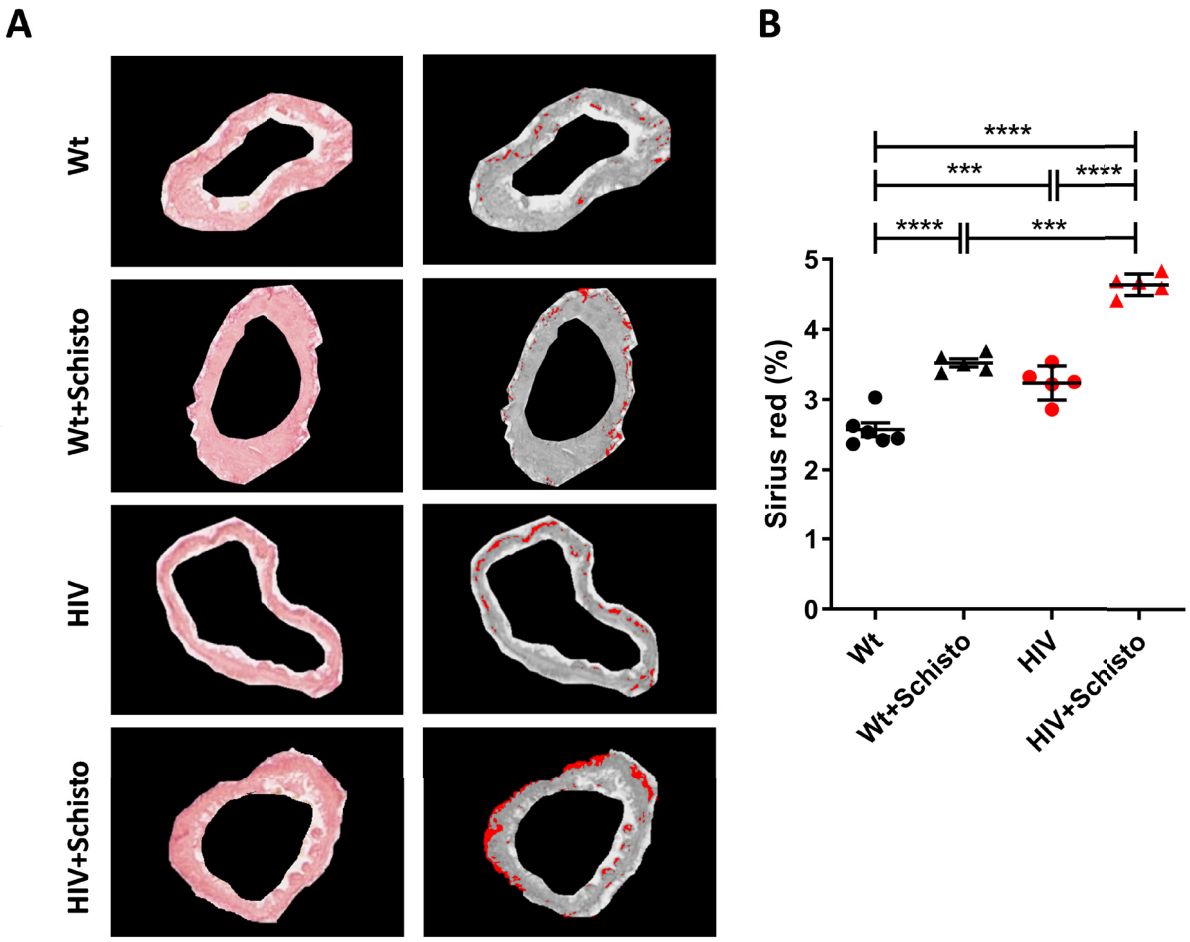

Figure 24. HIV mice show augmented pulmonary perivascular fibrosis with marked exacerbation after exposure to schistosome eggs. (A) Representative images of pulmonary vessels stained with Sirius red (left). Stained vessel areas are shown pseudo-colored in bright red (right). **(B)** Quantification of Sirius red staining as percent Sirius red-positive area fraction (as shown in A, right) in the vessel area analyzed. Mice and vessels analyzed per group were: Wt (6, 77), Wt+Schisto (5, 83), HIV (5, 53) and HIV+Schisto (5, 75). Results are expressed as mean ± SEM. ***P<0.001 and ****P<0.0001 as determined by one-way ANOVA analysis followed by Tukey post hoc test.

7.6. CARDIAC REMODELLING

We also examined the effects of HIV and Schistosoma co-exposure on cardiac remodelling. Surprisingly, we found a reduced Fulton index in HIV animals **(Figure 26, A)**, which could be associated with a modest LV hypertrophy displayed by untreated and egg-treated HIV animals compared to Wt counterparts **(Figure 26, D)**. However, when expressed in terms of body weight **(Figure 26, B)**, HIV animals had similar RV values as untreated or egg-exposed Wt mice, while a slight but significant increase was observed in egg-treated HIV compared to Wt mice **(Figure 26, C)**. Thus, in HIV and Schistosoma co-exposed mice, pulmonary vascular remodelling was associated with a consistent increase of PAP but without overt PAH or RV hypertrophy.

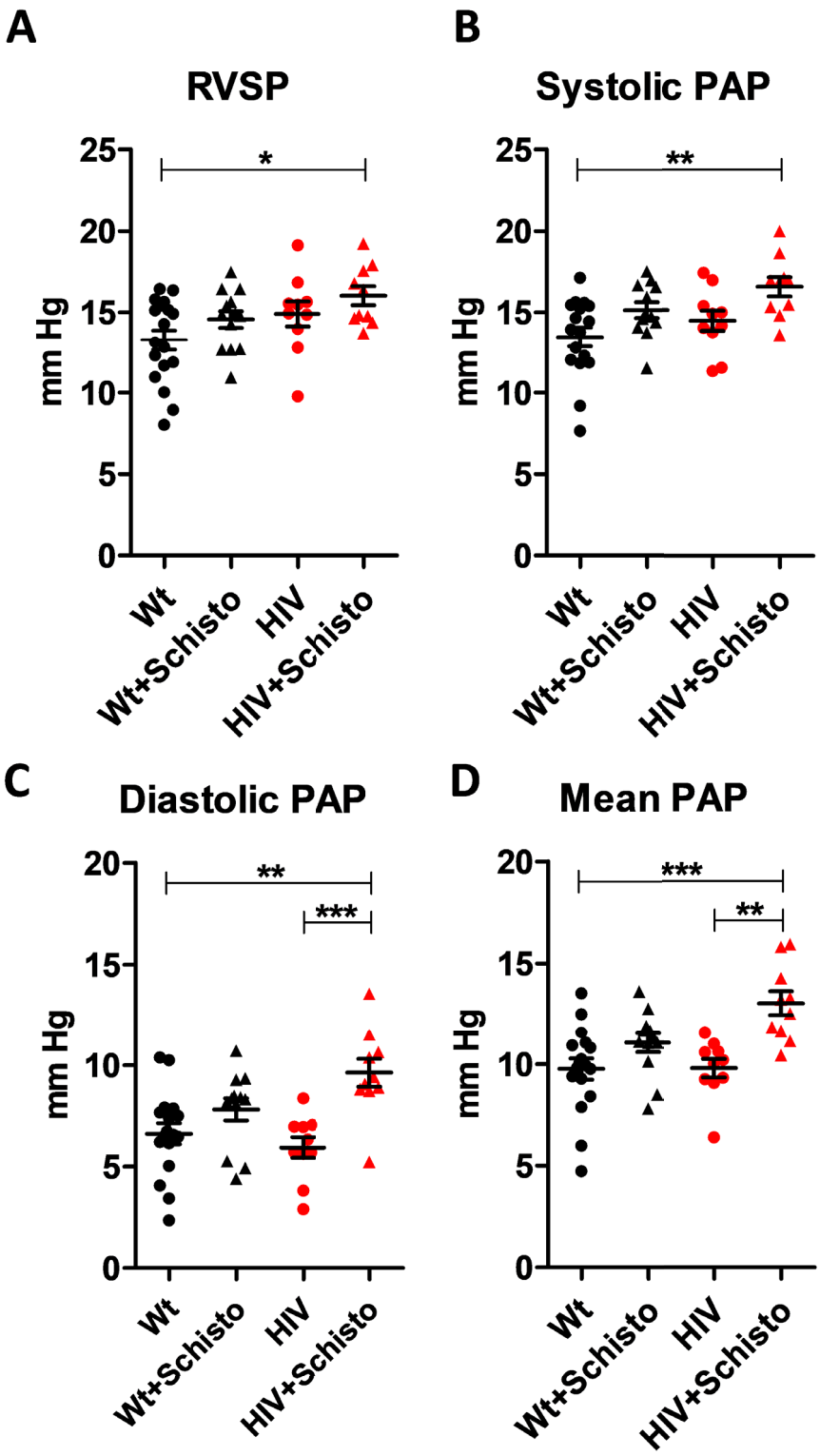

Figure 25. Schistosoma egg exposure increases pulmonary arterial pressure in HIV mice. Mean values of **(A)** right ventricular systolic pressure (RVSP), **(B)** systolic, **(C)** diastolic and **(D)** mean pulmonary arterial pressure (PAP) in Wt and HIV mice exposed or unexposed to Schistosoma. Results are expressed as means ± SEM (n=10-17). *, ** and *** indicate *P*<0.05, *P*<0.01 and *P*<0.001, respectively (one-way ANOVA analysis followed by the Tukey post hoc test).

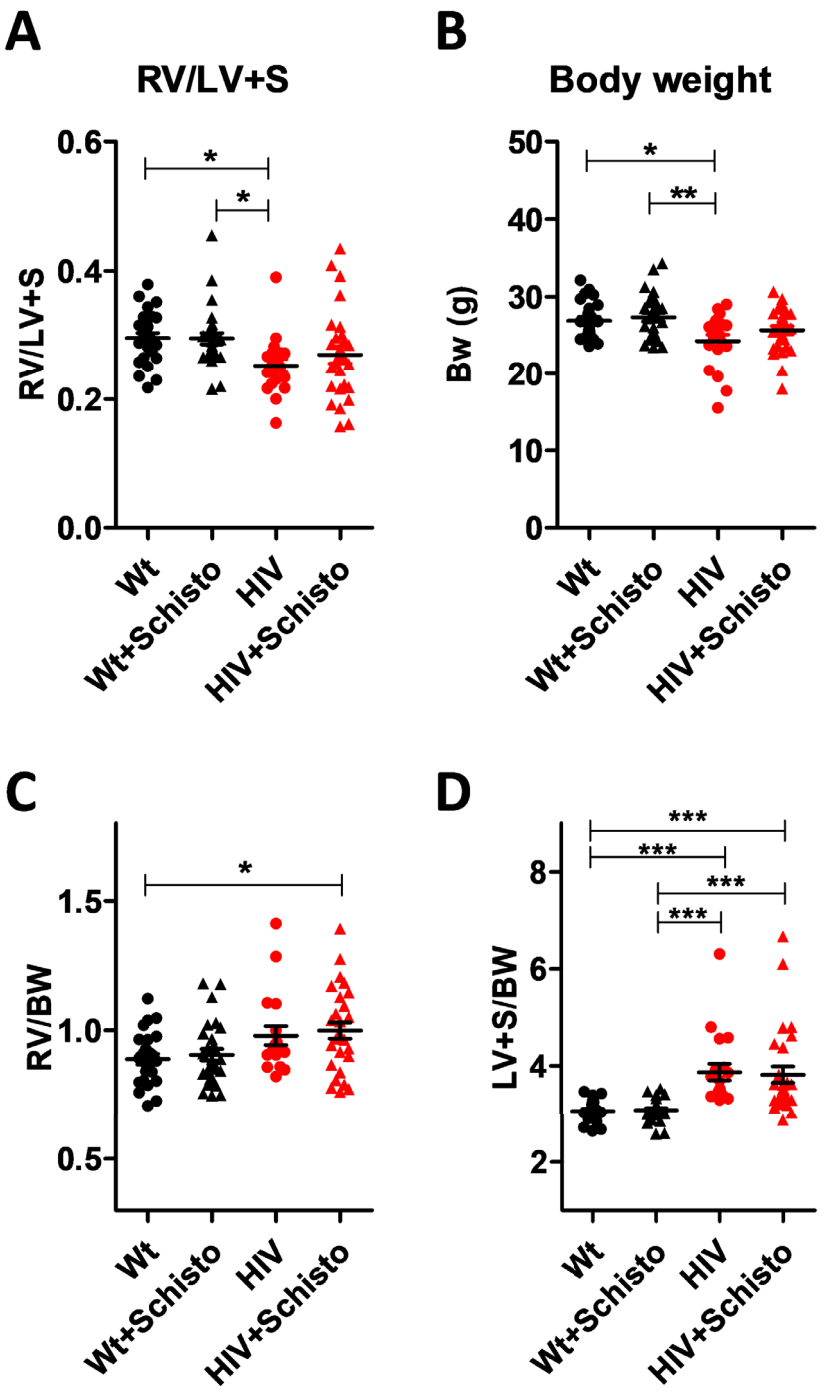

Figure 26. Cardiac remodeling in Wt and HIV mice following exposure to schistosome eggs. (A) and **(C)**: right ventricular (RV) weight relative to left ventricle + septum (LV + S) or to body weight (BW), respectively. **(B)** Body weight and **(D)** left ventricular and septum weight relative to body weight (BW) in Wt and HIV mice unexposed or exposed to schistosome eggs. Results are mean ± SEM (n=19-28). *P<0.05, **P<0.01 and ***P<0.001 (one-way ANOVA analysis followed by Tukey post hoc test).

7.7. ENDOTHELIAL CELL FUNCTION

Next, we analysed endothelial-dependent relaxation assessed following the addition of ACh to isolated PA previously stimulated with serotonin **(Figure 27, A-D)**.

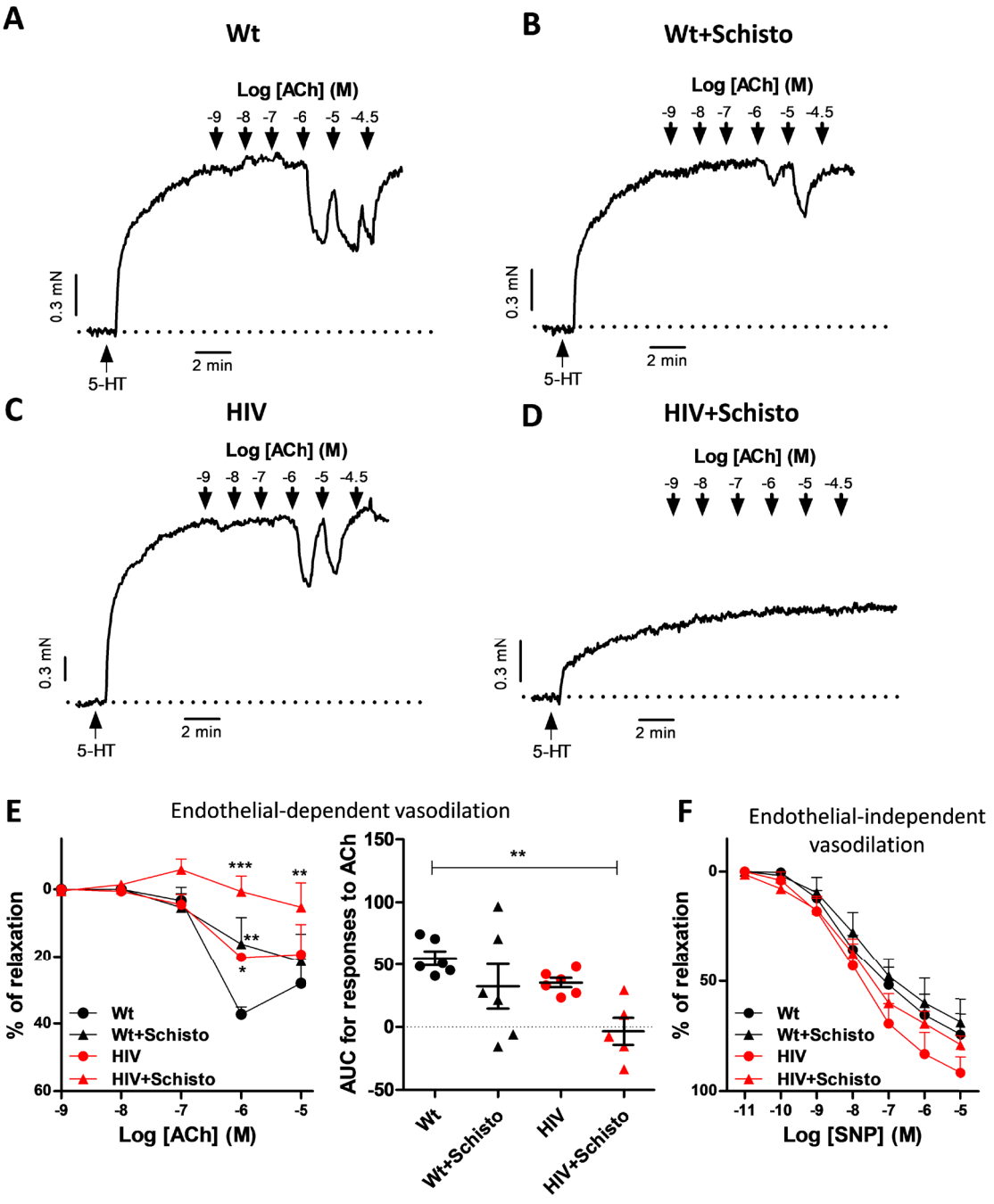

Figure 27. Endothelial dysfunction in HIV mice is aggravated by Schistosoma egg exposure. (A, B, C and D). Original recordings of the relaxation induced by Acetylcholine (ACh) in serotonin-stimulated PA from Wt and HIV mice exposed and unexposed to Schistosoma. **(E and F)** Relaxant effects of the endothelium-dependent vasodilator ACh and the endothelium independent vasodilator sodium nitroprusside (SNP), respectively, in serotonin-stimulated PA from Wt and HIV mice exposed and unexposed to Schistosoma. Panel E (right) shows the mean values of the area under the curve (AUC) of ACh-induced relaxation. The dotted line represents zero relaxant response to ACh. Values are mean ± SEM (n=5-6). **P*<0.05, ***P*<0.01 and ****P*<0.001, as determined by two-way repeated measures ANOVA analysis followed by the Bonferroni's post hoc test (panel E left) or one-way ANOVA analysis followed by Tukey post hoc test (panel E right).

The relaxation induced by ACh (10^{-6} M) was moderately attenuated in egg-treated Wt (16 ± 7%; P < 0.01) and untreated HIV (20 ± 1%; P < 0.05) mice as compared to Wt mice (37 ± 2%, **Figure 27, A-C and E left**). Remarkably, PA from egg-exposed HIV mice showed negligible endothelial-dependent vasodilation, even at the highest concentrations of ACh tested **(Figure 27, D and E left)**. In fact, the area under the curve of ACh-induced relaxation confirmed the impairment of endothelial-dependent vasodilation in egg-exposed HIV mice **(Figure 27, E right)**. In contrast, the endothelial-independent relaxation induced by SNP (**Figure 27, F**) was comparable in untreated and egg-treated Wt and HIV mice. Taken together, these findings suggest that combined exposure to HIV and Schistosoma impact the functional properties of the pulmonary vasculature partly by targeting the vascular endothelium.

7.8. THE PULMONARY IMMUNE LANDSCAPE OF MICE EXPOSED TO HIV AND SCHISTOSOMA, INDIVIDUALLY OR IN COMBINATION

Aiming at characterising the immune landscape of the lung, in terms of the phenotype of pulmonary immune cells and their cytokine expression, multi-parametric flow cytometry and immunofluorescence microscopy analyses were performed in samples from Wt and HIV mice, untreated or treated with schistosome eggs.

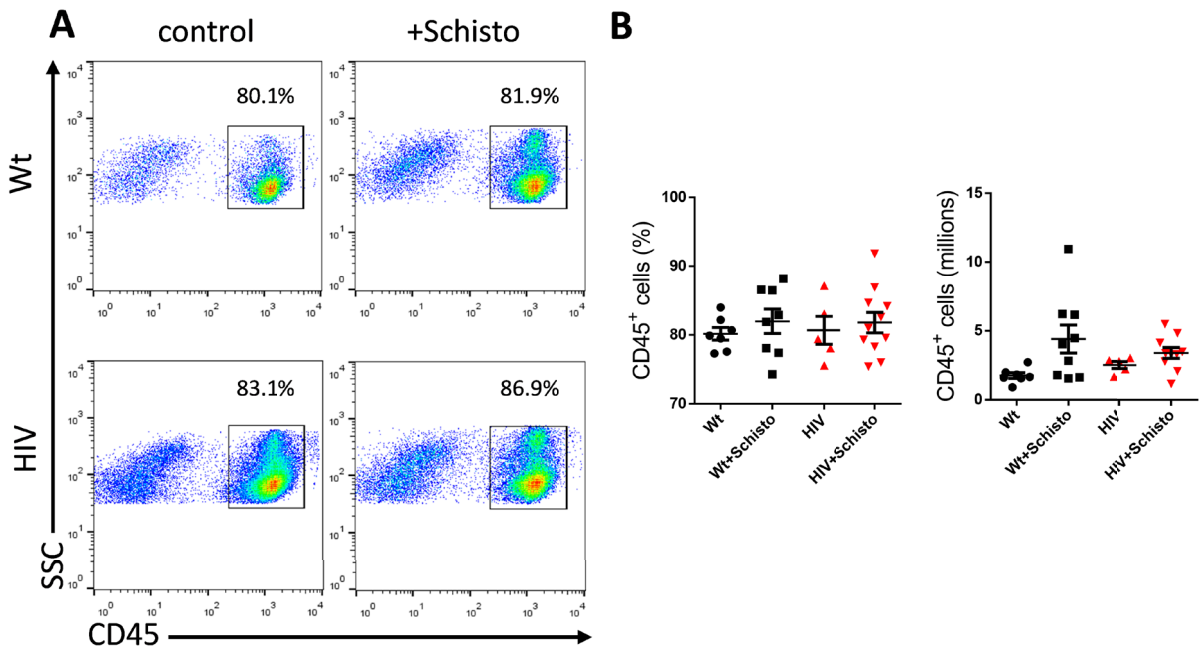

Figure 28. Pulmonary leukocytes in HIV mice exposed or not to Schistosoma eggs. (A) Flow cytometric analysis of leukocytes ($CD45^+$) in cells isolated from the lung of Wt (wild-type) and HIV mice unexposed (control) or exposed to Schistosoma eggs (+Schisto). SSC indicates side scatter. Numbers within dot plots indicate the percentage of cells in the gated region. **(B)** Frequencies and numbers of leukocytes. Results are shown as mean ± SEM (n=5-11).

7.8.1. IMMUNE CELL LANDSCAPE

Flow cytometry analyses of immune cells (identified by CD45 expression; **Figure 28, A**) in cells isolated from the lung of Wt and HIV mice showed comparable frequencies of leukocytes (CD45+ cells) which remained unaltered after administration of *S. mansoni* eggs **(Figure 28, B left)**. Leukocyte numbers **(Figure 28, B right)** were also comparable in untreated Wt and HIV mice, but with a tendency for higher leukocyte counts in the latter animals (Wt $1.63 \times 10^6 \pm 0.20 \times 10^6$; HIV $2.80 \times 10^6 \pm 0.76 \times 10^6$). Upon Schistosoma egg administration, leukocyte numbers were increased noticeably although not significantly in both Wt and HIV mice. Together, these results suggest that egg-induced leukocyte infiltration into the lung is not grossly affected by local expression of HIV proteins.

7.8.1.1. LYMPHOID CELLS

The different populations of pulmonary lymphoid cells were characterized by flow cytometry as shown in **Figure 12.**

Regarding αβ T cells, identified as $TCR\beta^+CD3^+$ **(Figure 29, A)**, similar proportions and numbers of these cells were observed in Wt and HIV mice, whereas a percent decrease but a significant increase in absolute cell number was detected in both mice after Schistosoma egg exposure **(Figure 29, B).** These data suggest that αβ T cells are recruited into the lung of Wt and HIV mice following parasite egg administration, but that other types of leukocytes predominate in the pulmonary infiltrate; which would explain the observed decrease in relative abundance.

Interestingly, surface TCRαβ expression (assessed as TCRβ/CD3 GEO-MFI) was significantly reduced in Wt but not HIV mice after Schistosoma egg administration **(Figure 29, C)**. Furthermore, CD27 expression, a marker of T cell activation, was significantly increased in αβ T cells from untreated HIV mice compared to Wt counterparts, with no further enhancement upon egg administration in either mice **(Figure 29, C).** Together, these observations suggest that αβ T cell activation could be dysregulated in HIV mice.

αβ T cells comprise two major subsets: CD4 and CD8 lymphocytes. Analysis of these subsets, identified as $TCR\beta^+CD4^+$ and $TCR\beta^+CD8^+$ cells **(Figure 30, A)**, revealed reduced proportions but increased absolute cell counts of CD4 and CD8 cells in egg-treated Wt and HIV mice compared with untreated counterparts; but less prominently for CD8 cells in egg-exposed HIV than in Wt mice **(Figure 30, B)**. Notably, both CD8 and CD4 coreceptors were overexpressed

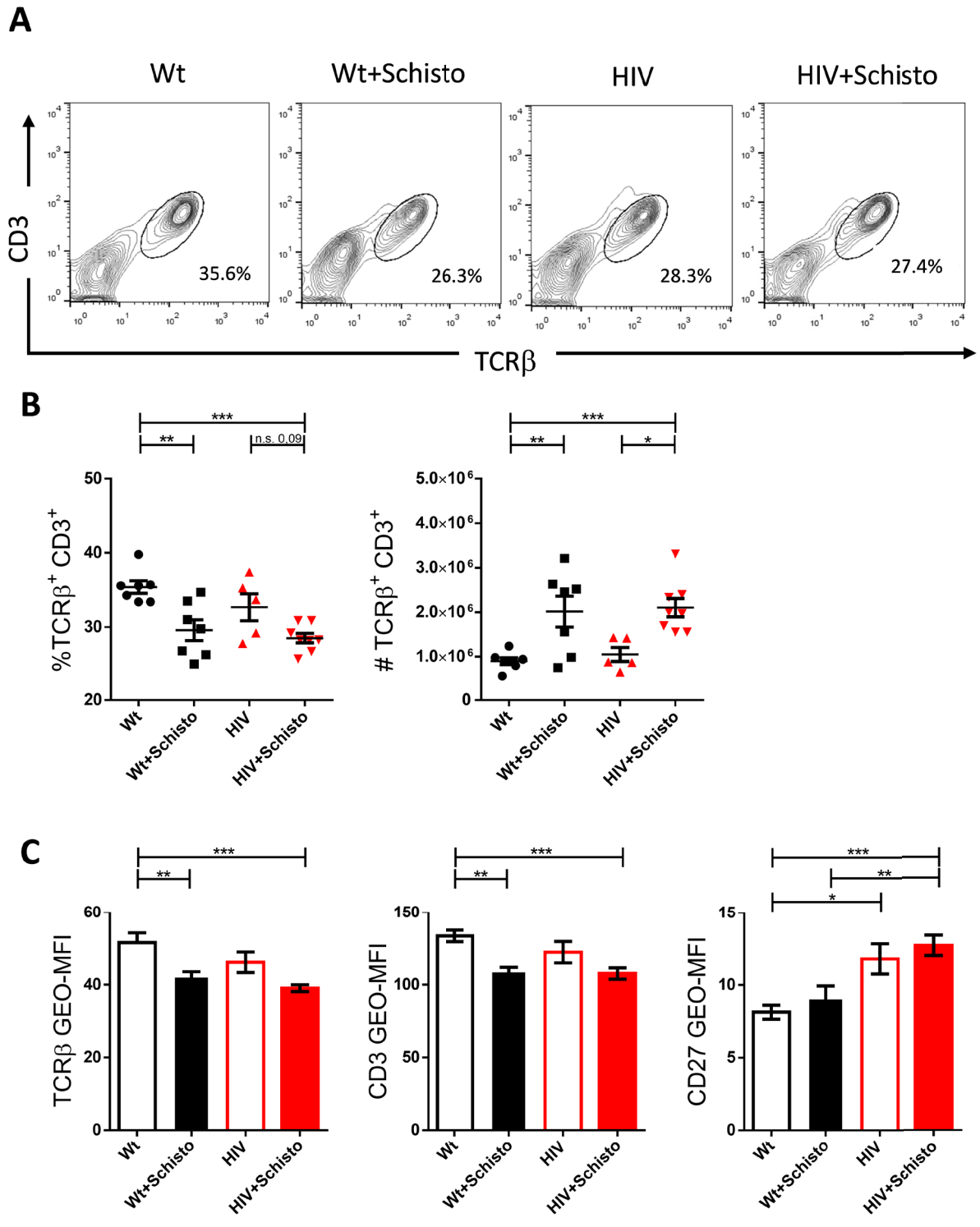

Figure 29. Pulmonary αβ T cells in HIV mice exposed or not to Schistosoma eggs. (A) Flow cytometric analysis of αβ T lymphocytes (TCRβ$^+$CD3$^+$) in the lung of Wt and HIV mice unexposed or exposed to Schistosoma eggs (+Schisto). **(B)** Frequencies (%) and numbers (#) of αβ T cells. **(C)** Surface TCR (in TCRβ$^+$ CD3$^+$) and CD27 (in TCRδ$^-$ CD3$^+$) expression. GEO-MFI: geometric mean fluorescence intensity. Results are shown as mean ± SEM (n=5-8). *P<0.05, **P<0.01 and *** P≤0.001 (one-way ANOVA).

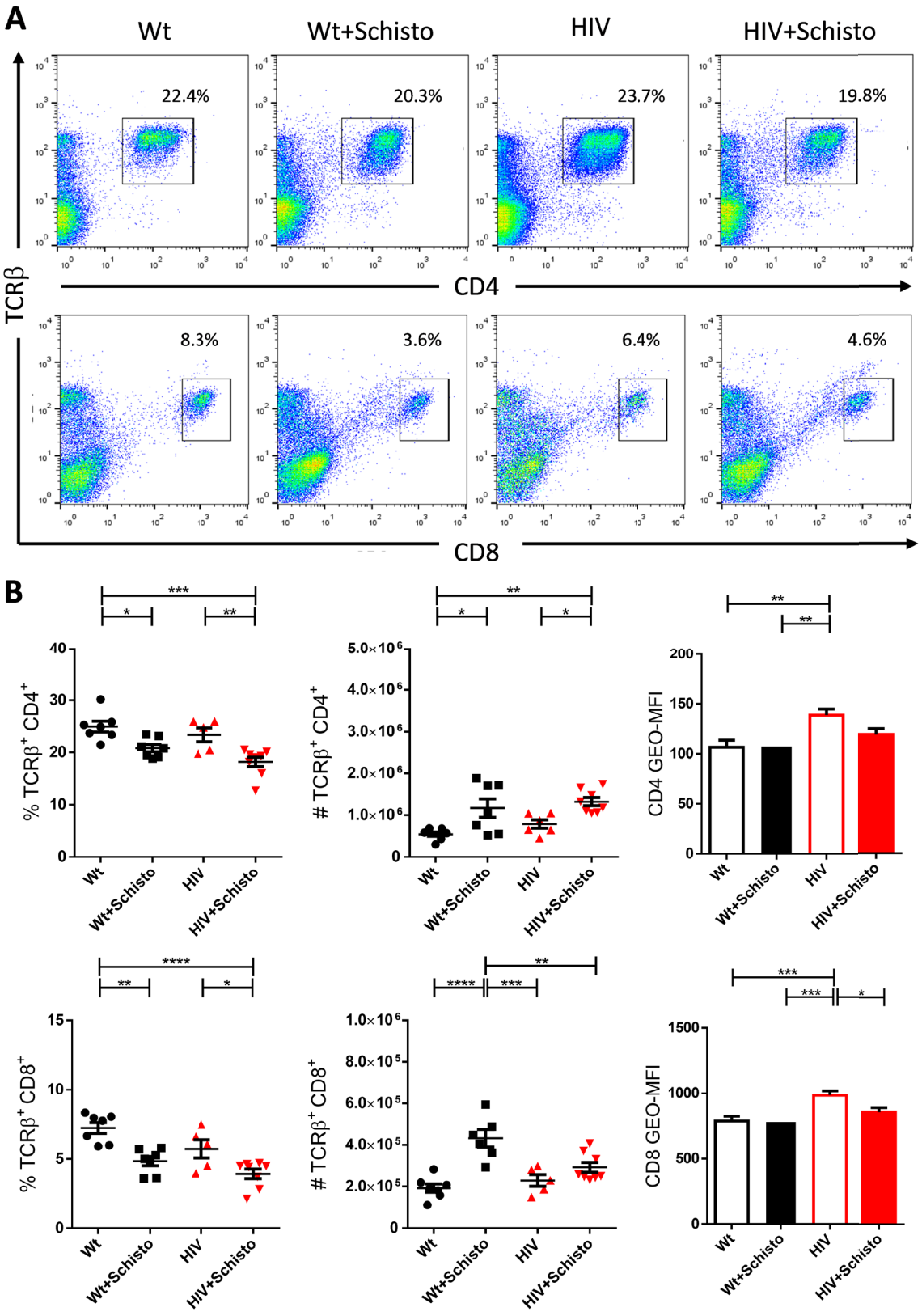

Figure 30. Pulmonary CD4 and CD8 T cells in HIV mice exposed or not to Schistosoma eggs. (A) Flow cytometric analysis of CD4 ($TCR\beta^+CD4^+$) and CD8 ($TCR\beta^+CD8^+$) T lymphocytes in the lung of Wt and HIV mice unexposed or exposed to Schistosoma eggs (+Schisto). **(B)** Frequencies (%) and numbers (#), and surface coreceptor expression (GEO-MFI). GEO-MFI: geometric mean fluorescence intensity. (n=5-8). *P<0.05, **P<0.01, ***P≤0.001 ***P≤0.0001.

in untreated HIV compared to Wt T cells. Upon parasite egg administration, surface CD8 and CD4 expression were unaltered in Wt mice; while in HIV mice surface CD8, but not CD4, was slightly but significantly reduced **(Figure 30, B)**. Together, these data suggest that expression of HIV proteins in pulmonary resident or infiltrating αβ T lymphocytes could restraint the expansion of CD8 but not CD4 cells responding to schistosome eggs, and somehow affect the surface expression of CD4 and CD8 coreceptors.

NKT lymphocytes express features of both T and NK cells, including co-expression of typical surface markers of each lineage such as TCRβ and NK1.1, which allows their identification **(Figure 31, A)**. Proportions and numbers of pulmonary NKT cells were similar in Wt and HIV animals, and were increased to a comparable extent in both mice exposed to schistosome eggs **(Figure 31, B)**; although apparently more prominently in HIV mice. This suggests that HIV exposure could potentiate the response of NKT cells to parasites eggs in the lung.

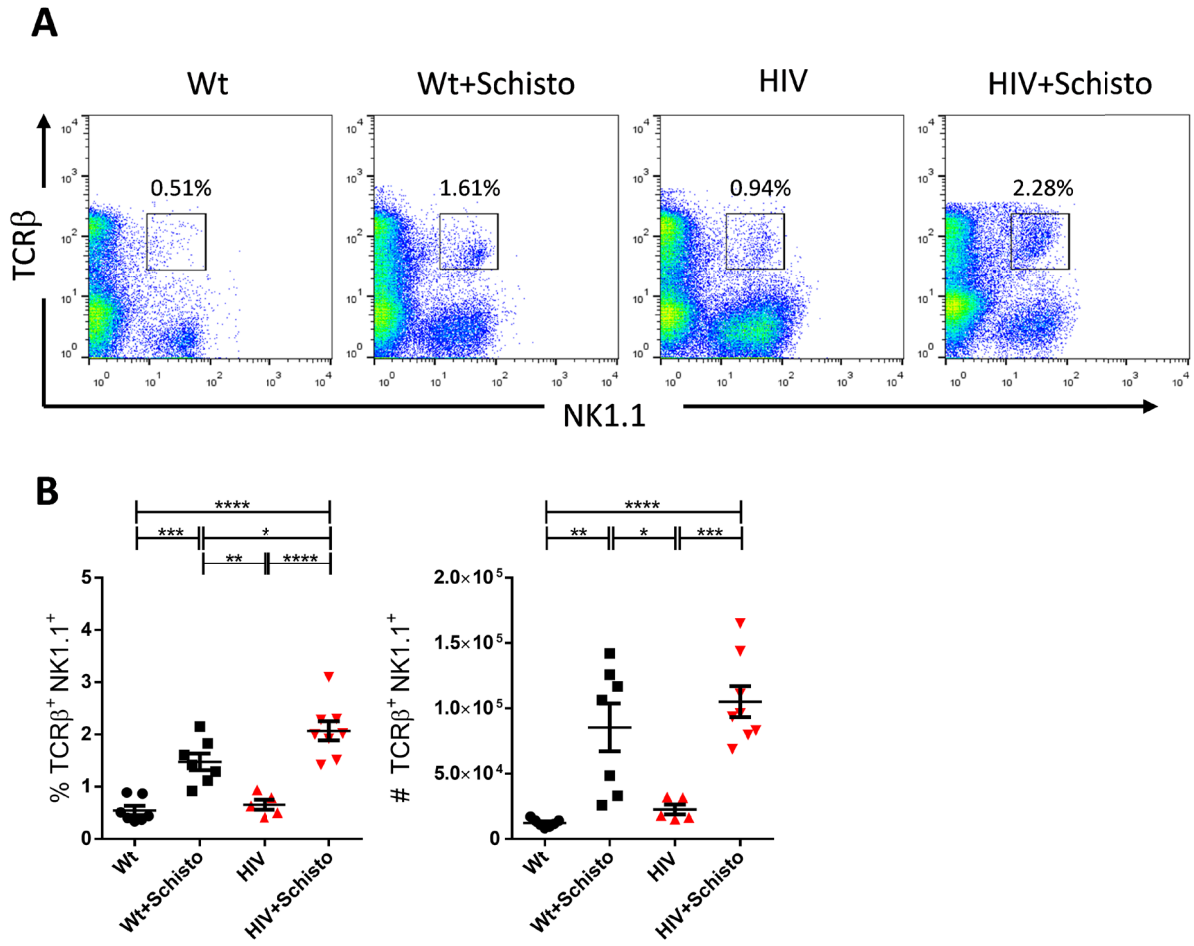

Figure 31. Pulmonary NKT cells in HIV mice exposed or not to Schistosoma eggs. (A) Flow cytometric analysis of NKT lymphocytes (TCRβ⁺NK1.1⁺) in the lung of Wt and HIV mice unexposed or exposed to Schistosoma eggs (+Schisto). **(B)** Frequencies (%) and numbers (#) (n=5-8). *P<0.05,** P<0.01, ***P≤ 0.001 ****P≤0.0001.

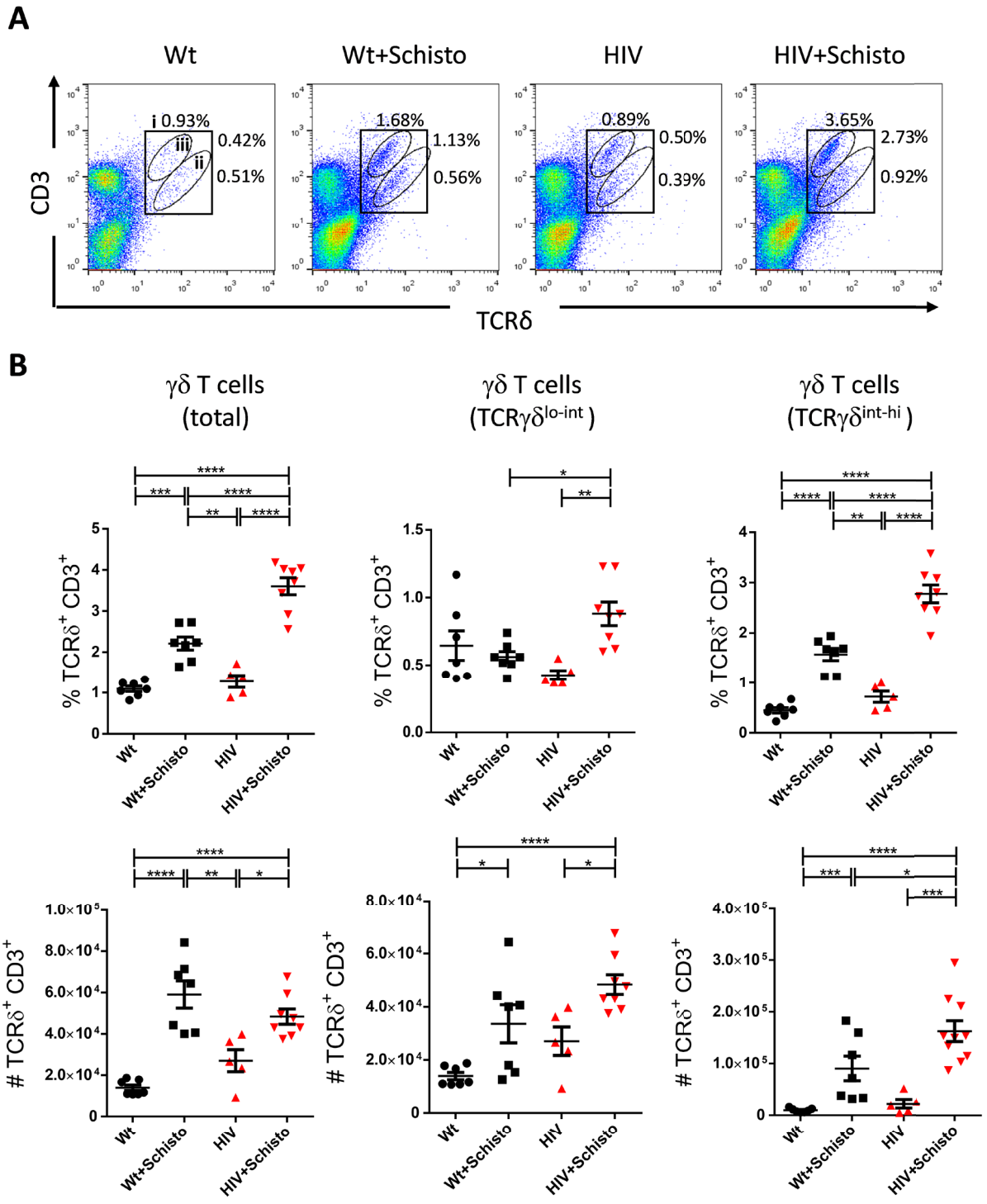

Figure 32. Pulmonary γδ T cells in HIV mice exposed or not to Schistosoma eggs. (A) Flow cytometric analysis of γδ T lymphocytes ($TCR\delta^{+}CD3^{+}$) in the lung of Wt and HIV mice unexposed or exposed to Schistosoma eggs (+Schisto). Numbers within dot plots correspond to percentage of cells in the gated regions indicated (i: total; ii: $TCR\gamma\delta^{lo\text{-}int}$; iii: $TCR\gamma\delta^{int\text{-}hi}$ **(B)** Frequencies (%) and numbers (#) of γδ T cells as gated in A (n=5-8). **P*<0.05, ***P*<0.01,****P*≤0.001 and *****P*≤0.0001.

γδ T lymphocytes, a major component of the T cell repertoire together with αβ lineage T cells, are characterized by surface expression of the TCRγδ antigen receptor. In the mouse lung, two subsets of γδ ($TCR\delta^{+}CD3^{+}$) T cells expressing distinct surface levels of the antigen receptor can be detected (Ref): $TCR\gamma\delta^{lo\text{-}int}$ and $TCR\gamma\delta^{int\text{-}hi}$ cells **(Figure 32, A)**. These two subsets were comparable in frequency and numbers in Wt and HIV mice. Upon schistosome egg administration, the abundance of either subset (and of total γδ T cells) was similarly increased in Wt and HIV mice. However, $TCR\gamma\delta^{int\text{-}hi}$ cells were augmented to a larger extent in egg-treated HIV mice compared to Wt counterparts **(Figure 32, B)**, suggesting that recruitment and/or expansion of this particular γδ T cell subset is favoured by co-exposure to HIV and parasite eggs in the lung.

In γδ T cells, the differential surface expression of CD27 and CCR6 correlates with production of a particular proinflammatory cytokine. Thus, $CD27^{+}CCR6^{-}$ cells secrete IFN-γ while $CD27^{-}CCR6^{+}$ cells produce IL-17 (Haas et al., 2009).

As shown in **Figure 33,** in Wt mice the majority of lung $TCR\gamma\delta^{lo\text{-}int}$ cells were $CD27^{-}CCR6^{-}$, with a small population of $CD27^{-}CCR6^{+}$ cells that expanded upon egg administration. In contrast, in HIV mice a prominent population (around 60%) of $TCR\gamma\delta^{lo\text{-}int}$ cells were $CD27^{-}CCR6^{+}$, which remained mostly unaltered after egg exposure. Within the pulmonary $TCR\gamma\delta^{int\text{-}hi}$ subtype, in contrast, frequency of $CD27^{-}CCR6^{+}$ was markedly increased in Wt and reduced in HIV mice compared with $TCR\gamma\delta^{lo\text{-}int}$ cells, due to the appearance in the latter mice of a prominent subpopulation of $CD27^{+}CCR6^{+}$ cells. In Wt mice, these $CD27^{+}CCR6^{+}$ cells were also detected but were minor. Interestingly, upon egg exposure, $CD27^{+}CCR6^{+}$ cells were markedly increased in Wt but less prominently in HIV mice. Taken together, these data indicate that exposure to HIV and Schistosoma, individually or in combination, alter the phenotype (and likely also the function, see below) of pulmonary γδ T cells.

NK cells represent around 10% of lymphocytes in the mouse lung (Grégoire et al., 2007). This lymphoid cell type has historically been defined as $CD3^{-}TCR\beta^{-}NK1.1^{+}$ cells to distinguish them from NKT ($CD3^{+}TCR\beta^{+}NK1.1^{+}$) lymphocytes. As shown in **Figure 34** (left panel), relative (percentage) abundance of NK cells was significantly lower in HIV compared with Wt mice, while absolute (number) abundance was not significantly different between the two mouse types; but with a tendency to lower numbers in HIV mice. Furthermore, Wt mice responded to egg administration reducing percent NK levels to those of untreated HIV counterparts, and the latter showed no changes compared to untreated ones. In either mice, absolute NK cell counts were not significantly altered by schistosome egg administration.

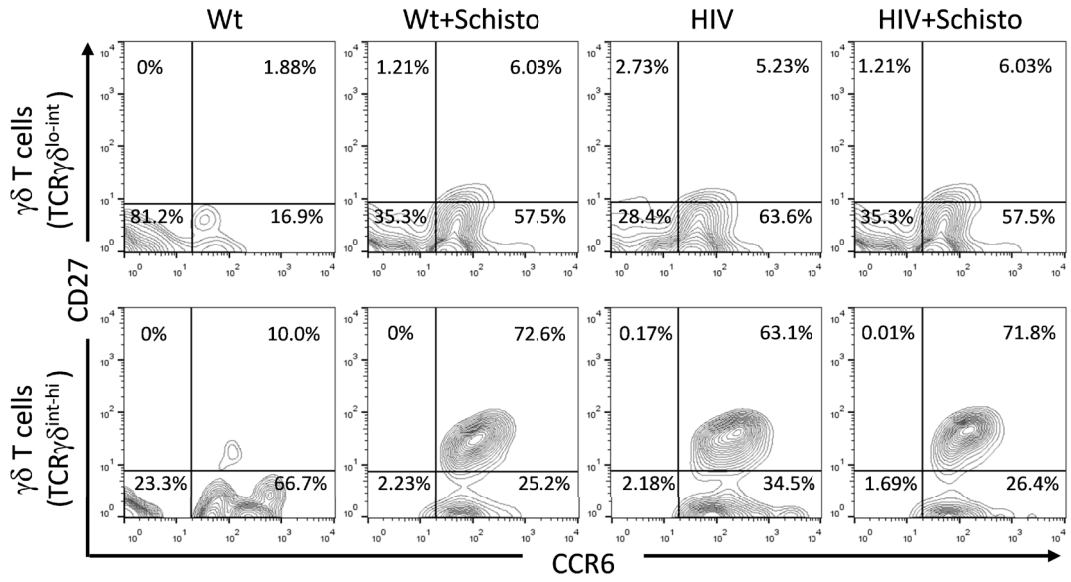

Figure 33. Pulmonary expression of CCR6 and CD27 in γδ T cells in HIV mice exposed or not to Schistosoma eggs. Flow cytometric analysis of CCR6 and CD27 expression in γδ T lymphocytes (TCRδ$^+$CD3$^+$) in the lung of Wt and HIV mice unexposed or exposed to Schistosoma eggs (+Schisto).

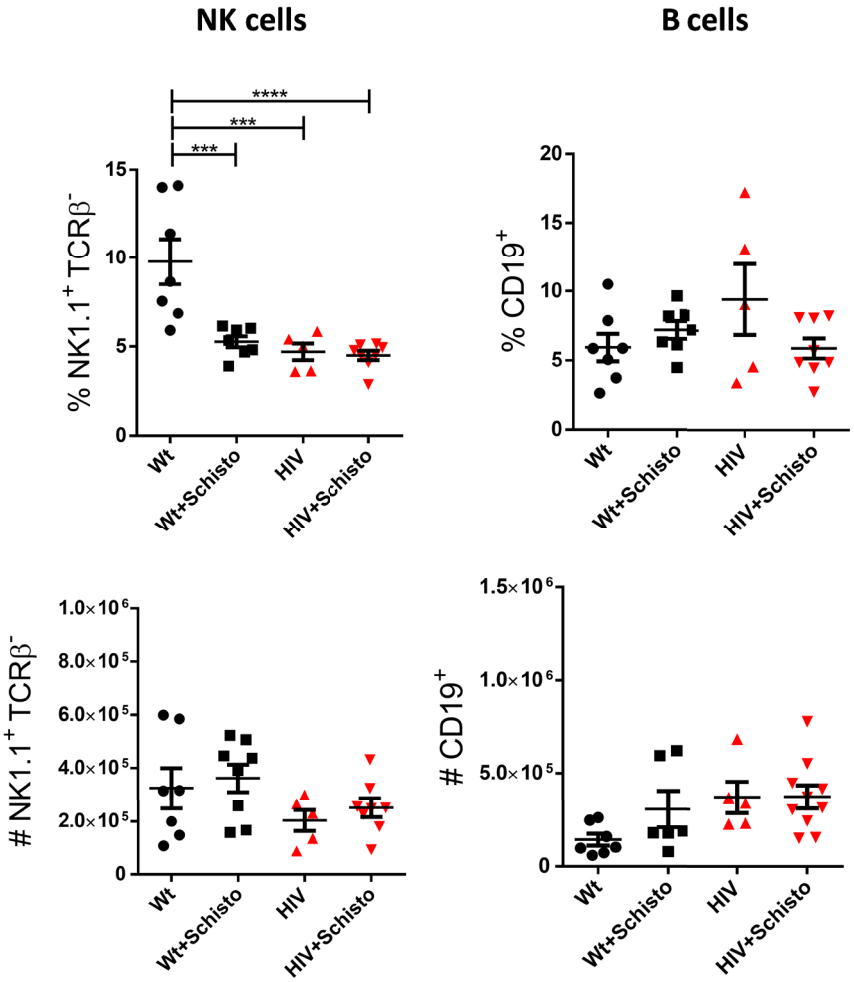

Figure 34. Pulmonary NK and B cells in HIV mice exposed or not to Schistosoma eggs. Flow cytometric analysis of NK (NK1.1$^+$TCRb$^-$) and B (CD19$^+$) lymphocytes in the lung of Wt and HIV mice unexposed or exposed to Schistosoma eggs (+Schisto)(n=5-8). Frequencies (%) and numbers (#) are shown. ***P≤0.001, ****P≤0.0001.

Regarding B lymphocytes (identified as CD19+ cells), neither frequencies nor numbers of these cells were different between Wt and HIV mice, and no alterations were detected in either mouse type following egg administration **(Figure 34)**.

7.8.1.2. MYELOID CELLS

The different populations of pulmonary myeloid cells were characterized by flow cytometry as shown in **Figure 13.**

Neutrophils and eosinophils are granulocytes sharing a distinct surface $CD11b^{+}GR1^{med}$ phenotype that allows their discrimination from monocytes, which express low or high levels of surface GR1 (Duan et al., 2016; Misharin et al., 2013). Both granulocytes participate in the immune response to multicellular parasites, and in the case of eosinophils in the granulomatous response to *S. mansoni* eggs (Pagán & Ramakrishnan, 2018).

As shown in **Figure 35**, proportions and numbers of $CD11b^{+}GR1^{med}$ cells were comparable in Wt and HIV mice. Upon schistosome egg administration, $CD11b^{+}GR1^{med}$ granulocytes were significantly increased in both frequency and cell counts in Wt but not in HIV mice; but with a tendency for higher granulocyte abundance in egg-treated compared to untreated HIV mice. These results suggest an impaired granulocyte response to parasite eggs in the lung of HIV mice.

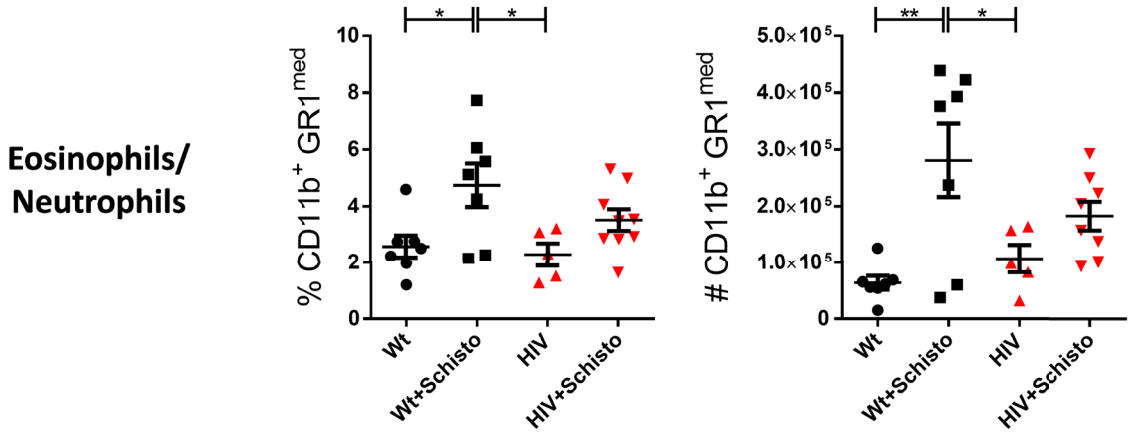

Figure 35. Pulmonary eosinophils/neutrophils in HIV mice exposed or not to Schistosoma eggs. Flow cytometric analysis of eosinophils/neutrophils ($CD11b^{+}GR1med$) in the lung of Wt and HIV mice unexposed or exposed to Schistosoma eggs (+Schisto) (n=5-8). Frequencies (%) and numbers (#) are shown. *$P \leq 0.05$, **$P \leq 0.01$.

Monocytes are $CD11b^{+}$ myeloid cells that can be further divided in two distinct functional populations based on the surface expression of the GR1 marker (Duan et al., 2016; Misharin et al., 2013). Hence, $CD11b^{+}GR1^{lo}$ monocytes are considered "patrolling" monocytes (which

patrol blood vessels), while CD11b^{+}GR1^{hi} ones represent "inflammatory" monocytes, which are robustly recruited to sites of inflammation.

As shown in **Figure 36** (upper panels), pulmonary patrolling monocytes were comparable in untreated Wt and HIV mice, and markedly increased in egg-treated HIV mice and less prominently in Wt counterparts. In regard to inflammatory monocytes **(Figure 36, lower panels)**, proportions and numbers of these cells were not significantly different in Wt compared to HIV mice, either untreated or treated with schistosome eggs. Collectively, these results show that HIV and Schistosoma co-exposure has an impact on pulmonary patrolling monocytes but not in the recruitment into the lung of inflammatory monocytes.

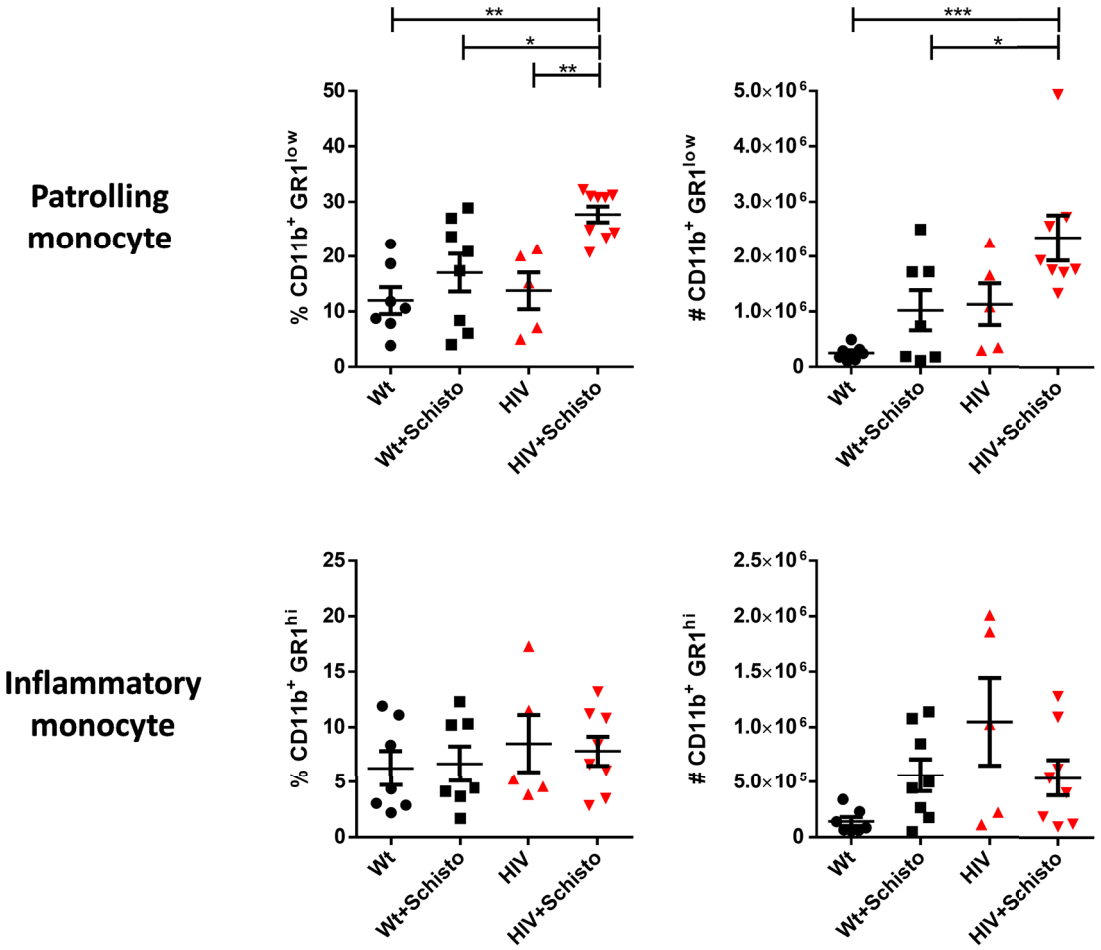

Figure 36. Pulmonary monocytes in HIV mice exposed or not to Schistosoma eggs. Flow cytometric analysis of patrolling (CD11b+GR1lo) and inflammatory (CD11b+GR1hi) monocytes in the lung of Wt and HIV mice unexposed or exposed to Schistosoma eggs (+Schisto)(n=5-8). Frequencies (%) and numbers (#) are shown. *P≤0.05, **P≤0.01, ***P≤0.001.

Pulmonary macrophages are a heterogeneous population of immune cells that fulfil a variety of specialised functions, including maintenance of pulmonary homoeostasis, removal of cellular debris, immune surveillance, microbial clearance, responses to infection and the resolution of inflammation.

Pulmonary macrophages can be traced by the surface expression of F4/80 and CD64 (although this population could contain also monocytes). Within this population, two main subsets found in the lung are interstitial and alveolar macrophages, characterised by the expression or lack of surface CD11b, respectively.

Interstitial macrophages, which are the ones that infiltrate and differentiate in the lung, were significantly increased in frequency and showed a tendency for higher cell counts in HIV mice compared with Wt counterparts **(Figure 37, left)**. Egg administration resulted in increased proportion and numbers of these macrophage subset in both Wt and HIV mice, but more prominently in the latter.

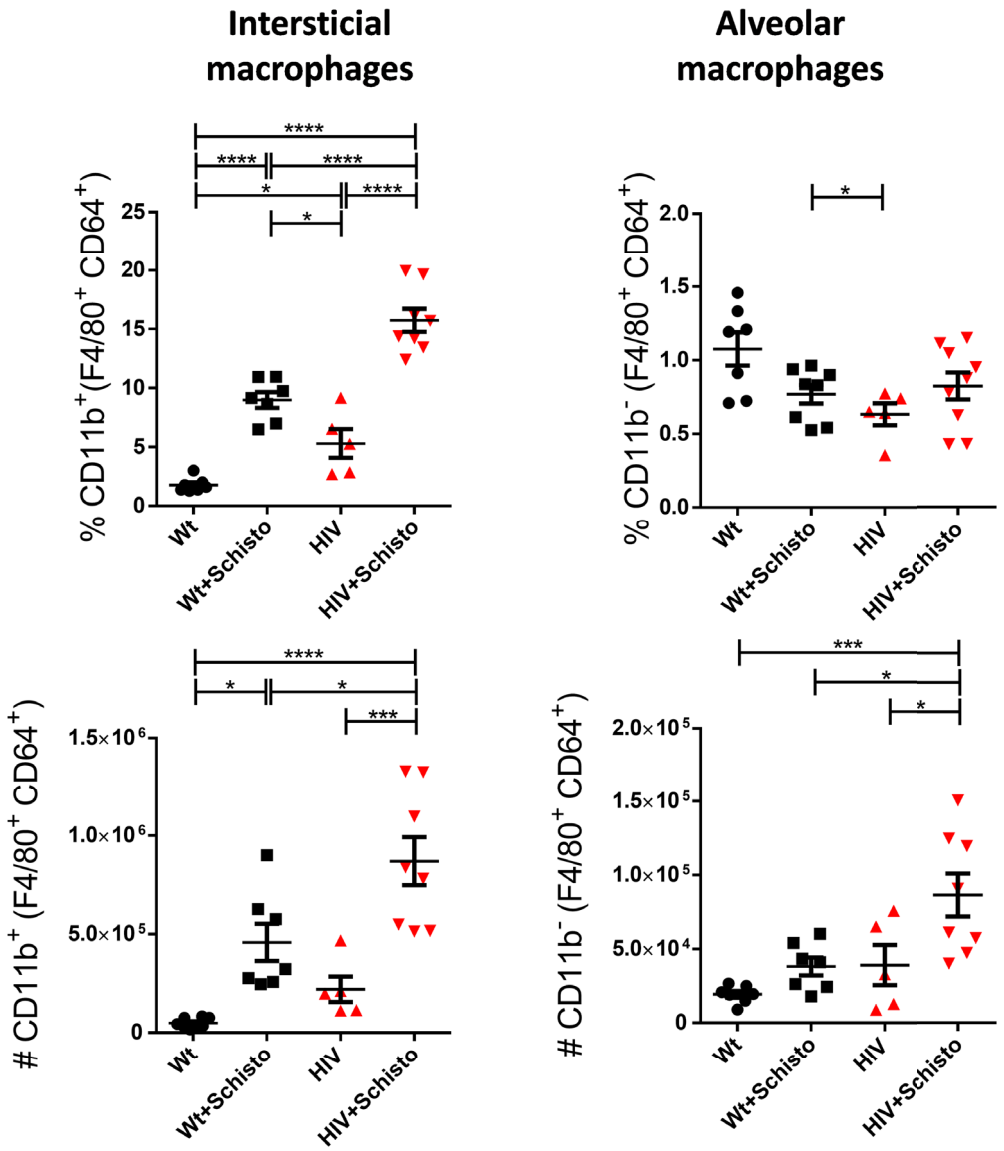

Figure 37. Pulmonary macrophages in HIV mice exposed or not to Schistosoma eggs. Flow cytometric analysis of interstitial (F4/80$^+$CD64$^+$CD11b$^+$) and alveolar (F4/80$^+$CD64$^+$CD11b$^-$) macrophages in the lung of Wt and HIV mice unexposed or exposed to Schistosoma eggs (+Schisto) (n=5-8). Frequencies (%) and numbers (#) are shown. *P≤0.05, ***P≤0.001, ****P≤0.0001.

Alveolar macrophages, the resident population of macrophages in the lung, were comparable in Wt and HIV mice, and only the latter mice responded with an increase to egg embolization into the lung; but less markedly than observed with interstitial macrophages **(Figure 37, right)**. Together, these results indicate that a prior HIV exposure potentiates the response of lung macrophages to a subsequent exposure to schistosome eggs, particularly that of interstitial macrophages.

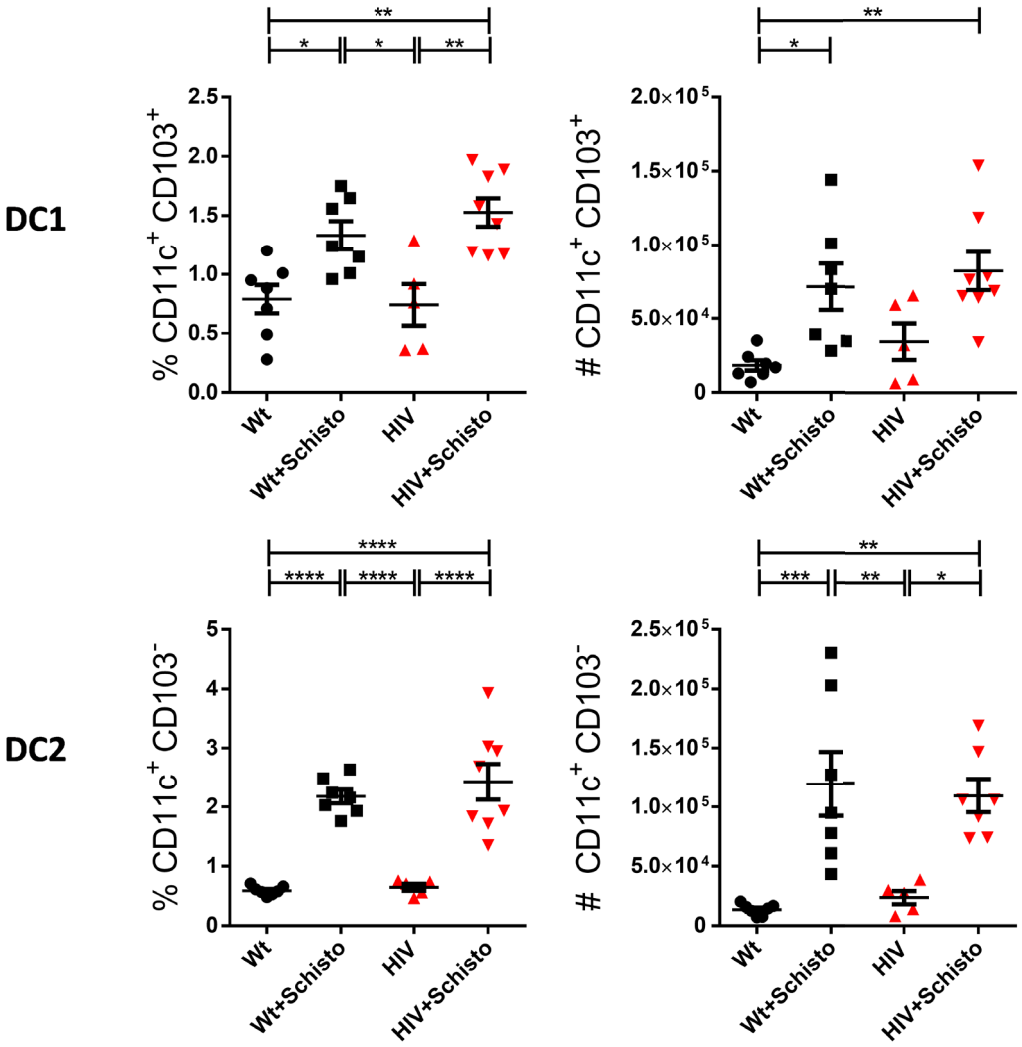

Figure 38. Pulmonary dendritic cells in HIV mice exposed or not to Schistosoma eggs. Flow cytometric analysis of DC1 ($CD11c^+CD103^+$) and DC2 ($CD11c^+CD103^-$) dendritic cells in the lung of Wt and HIV mice unexposed or exposed to Schistosoma eggs (+Schisto) (n=5-8). Frequencies (%) and numbers (#) are shown. *P≤0.05, **P≤0.01, ***P≤0.001, ****P≤0.0001.

In the mouse lung there are at least two subpopulations of dendritic cells (DC), which are defined by the expression or not of surface CD103 (Merad et al., 2013). As shown in **Figure 38**, DC1 ($CD11c^+CD103^+$) and DC2 ($CD11c^+CD103^-$) are similarly represented in the lung of Wt and HIV mice, and both DC populations are comparably increased in Wt and HIV mice following egg administration, suggesting that schistosome exposure is the dominating stimulus for expansion of pulmonary DC, with a minor contribution of exposure to HIV proteins.

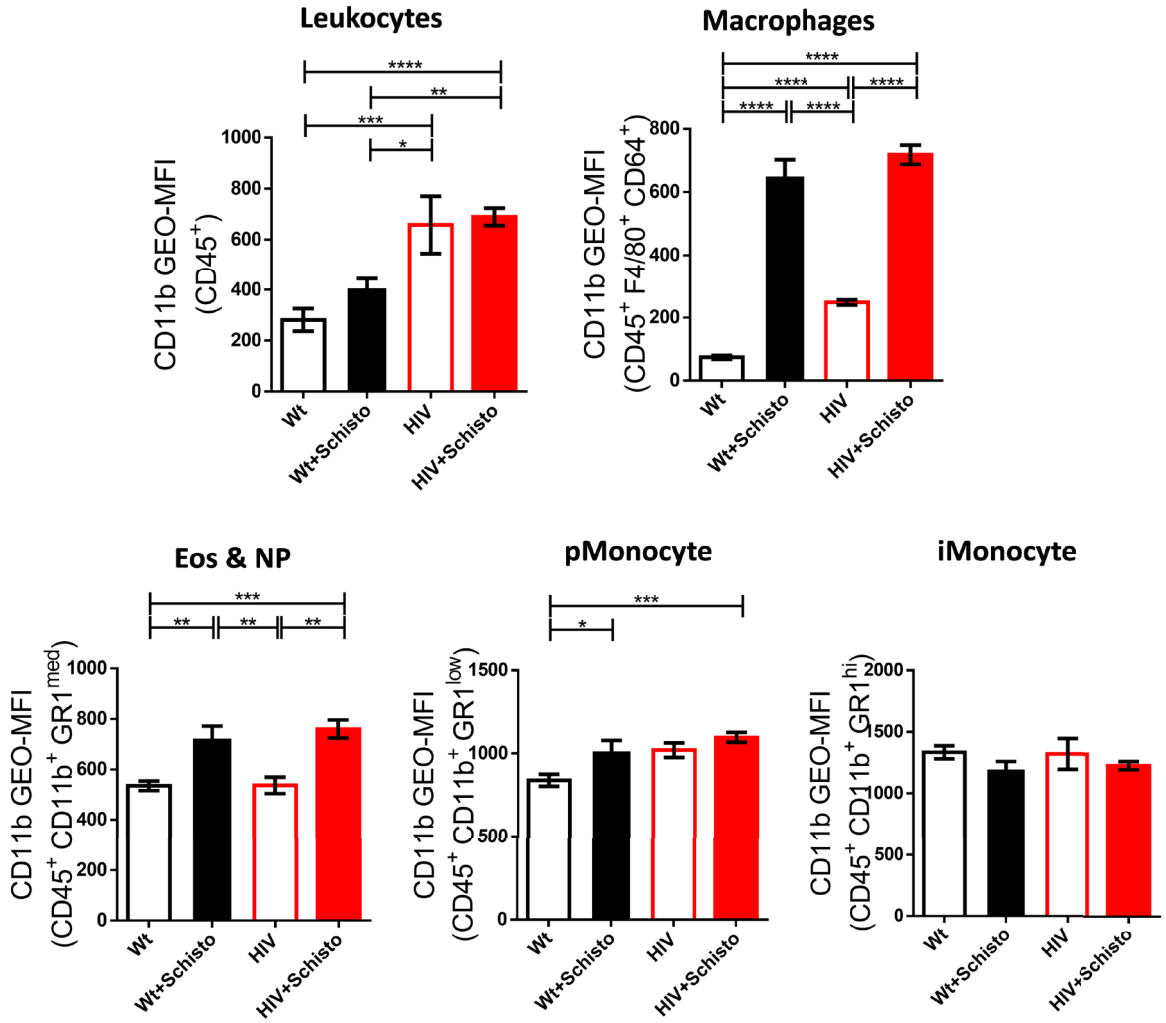

Figure 39. Surface CD11b expression in pulmonary myeloid cells from HIV mice exposed or not to Schistosoma eggs. GEO-MFI: geometric mean fluorescence intensity. (n=5-8) *P<0.05, **P<0.01, ***P≤0.001 ***P≤0.0001.

Interestingly, compared to Wt counterparts, HIV mice showed upregulated levels of surface CD11b in immune cells of the lung **(Figure 39)**, particularly in macrophages and patrolling monocytes; suggestive of an inflammatory environment occurring in the lung of HIV mice that is exacerbated upon parasite egg treatment.

7.8.1.3. GLOBAL FEATURES OF THE PULMONARY IMMUNE CELL LANDSCAPE

The global features of the pulmonary immune cell landscape, with regard to lymphoid-to-myeloid ratio and relative representation of the distinct immune cell types, are summarized and depicted in **Figure 40** and **Figure 41**, respectively; for mice exposed to HIV and Schistosoma, individually or in combination.

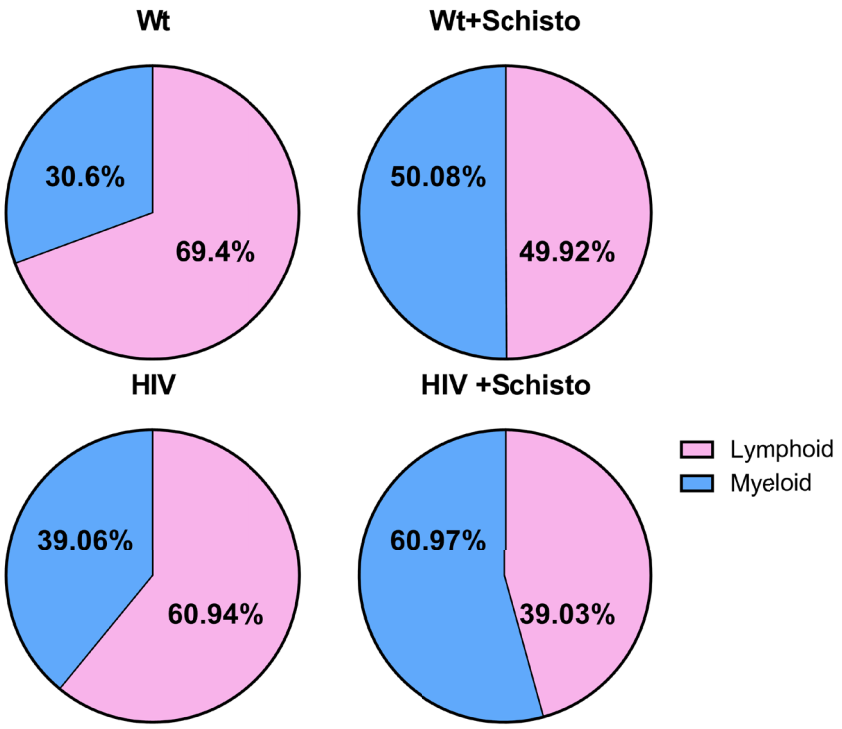

Figure 40. Lymphoid-to-myeloid ratio in Wt and HIV mice exposed or not to Schistosoma eggs.

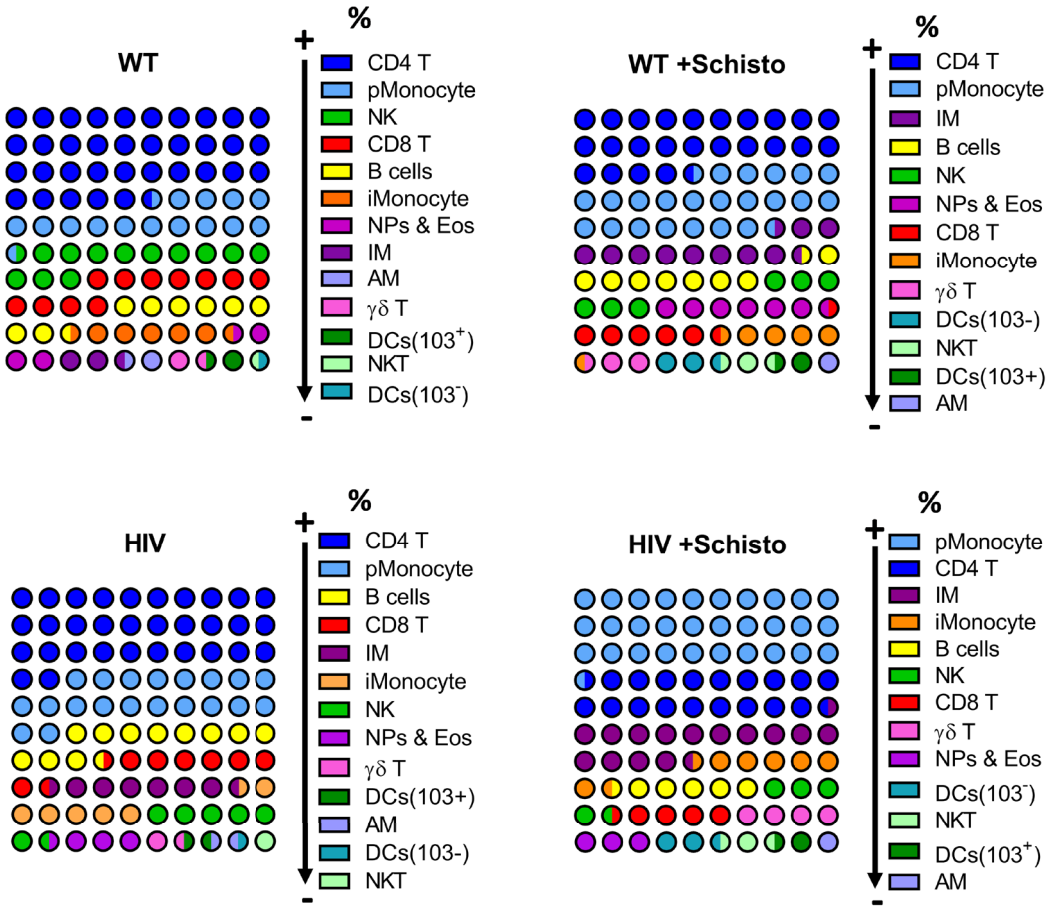

Figure 41. Relative representation of distinct immune cell types in Wt and HIV mice exposed or not to Schistosoma eggs.

7.8.1.4. IMMUNE CELLS IN GRANULOMAS

A typical phenomenon associated with schistosome infection is the formation in various tissues, including the lung, of multicellular granulomas around the trapped eggs. Although egg-treated HIV mice were able to generate granulomas, they were of smaller size and reduced egg clearance capability compared with those in Wt counterparts **(Figure 19)**.

To gain insight on the immune cell composition of granulomas in Wt and HIV mice, lung sections from these mice were analysed by immunofluorescence microscopy **(Figure 42)**. As expected, the vast majority of cells stained with DAPI (nuclei) in the granulomas of both mice also stained positive for CD45, a marker of leukocytes; with a prominent representation of macrophages (F4/80$^+$ cells) around the egg (visible in the HIV but not in the Wt granuloma). A minority of CD45$^+$F4/80$^-$ cells, most likely T cells and eosinophils, was detected in the periphery of the granuloma of both Wt and HIV mice.

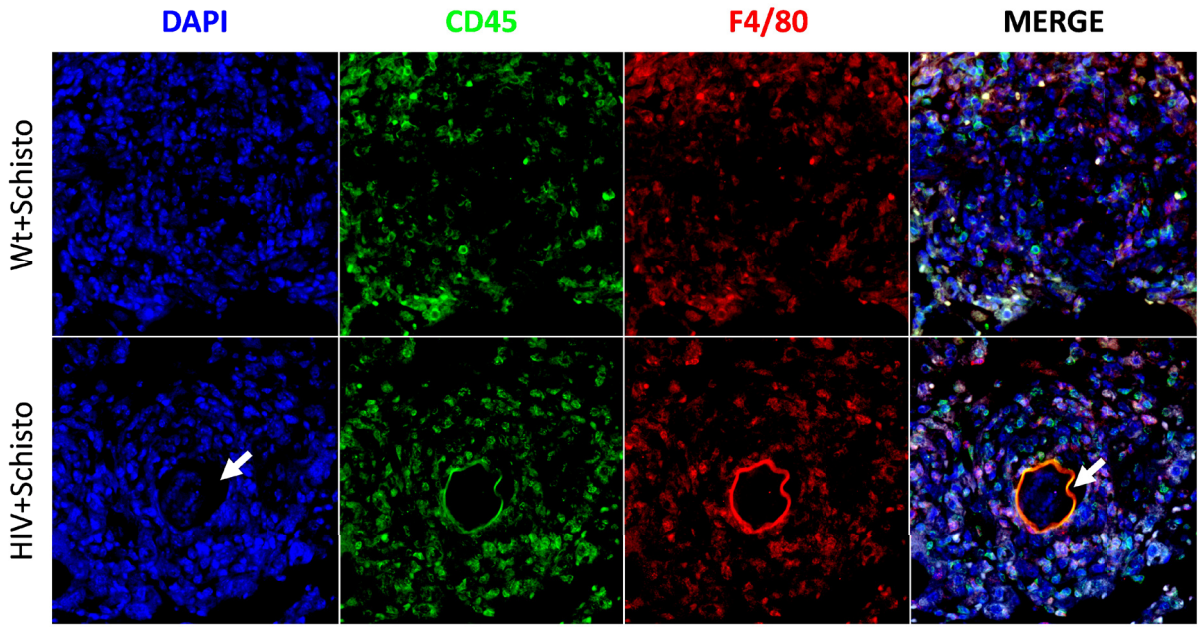

Figure 42. Total leukocytes and macrophages schistosome-induced lung granulomas. Representative examples of immunofluorescence microscopy analysis of total leukocytes (CD45$^+$) and macrophages (F4/80$^+$) in pulmonary granulomas of Wt and HIV mice exposed to Schistosoma eggs (+Schisto) (n=32-39 granuloma, from n=3-5 mice). The schistosome egg was consistently observed in HIV but not Wt mice (arrowhead).

To gain further insight about pulmonary T cells in untreated mice and in perivascular granulomas of egg-treated mice, lung sections from Wt and HIV mice were stained with specific antibodies to TCRδ and CD3. In this setting, γδ T cells can be identified as TCRδ$^+$CD3$^+$ and αβ T cells as TCRδ$^-$CD3$^+$ cells **(Figure 43)**.

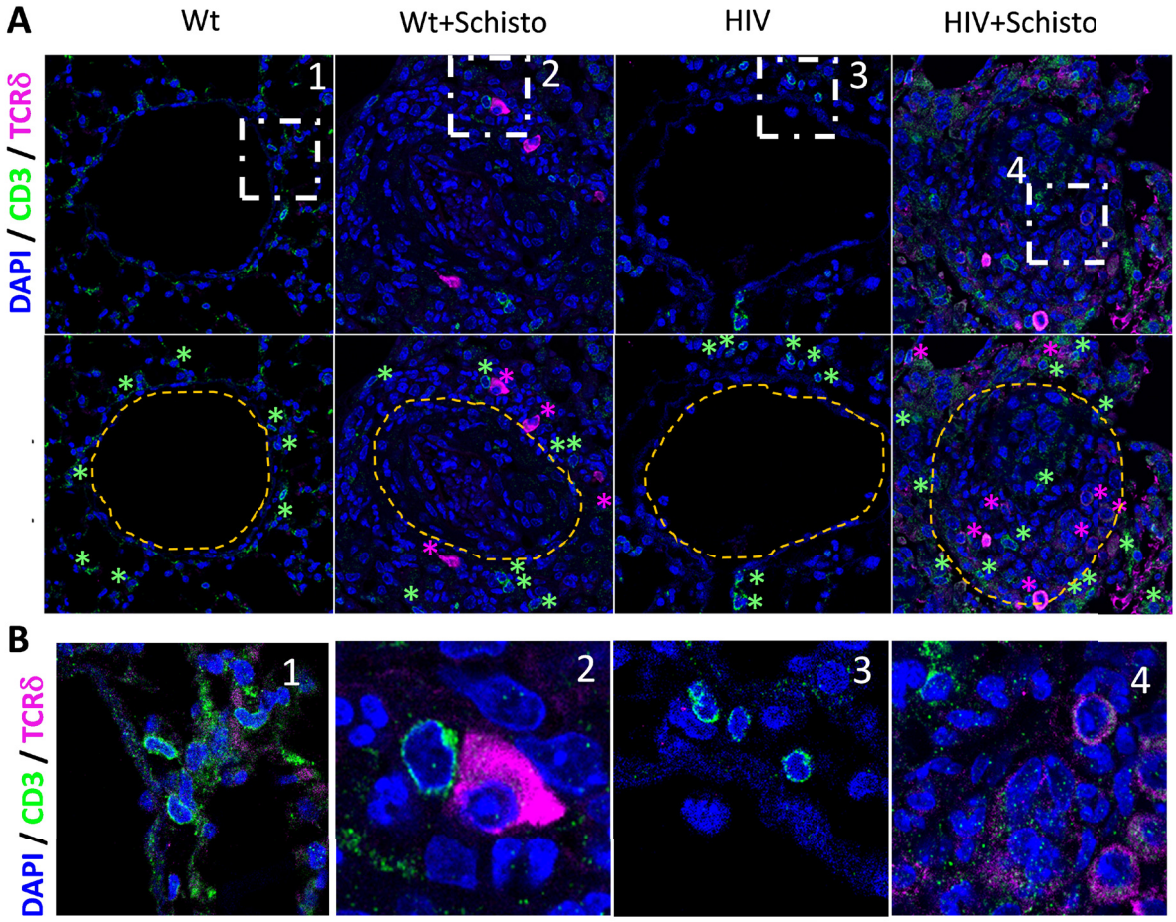

Figure 43. T cells in pulmonary perivascular granulomas in mice exposed to Schistosoma eggs. (A) Representative examples of IFM analysis of T cells (upper panels) in pulmonary perivascular granulomas of Wt and HIV mice exposed to Schistosoma eggs (+Schisto). αβ T cells and γδ T cells are marked with green and pink asterisks, respectively, in the bottom panels. Vessels are marked with a dotted line. **(B)** Magnification of the area indicated in panel A.

In untreated mice, either Wt or HIV, there were αβ T lymphocytes surrounding the vessel, but no γδ T lymphocytes. In contrast, both T cell types could be detected in the perivascular granuloma of egg-treated mice. Of note, T cells were located in the peripheral extravascular part of the granuloma in Wt mice, while in HIV mice T cells were detected in both extravascular and intravascular locations.

A more detailed analysis of T cells in perivascular granulomas of HIV mice **(Figure 44, A)** revealed two types of γδ T lymphocytes: small-sized cells expressing low levels of surface TCR (TCRγδ^{lo}) and larger ones expressing high levels of the receptor (TCRγδ^{hi}) **(Figure 44, B)**. Notably, these two populations of γδ T cells were also detected by flow cytometric analysis **(Figure 32)**.

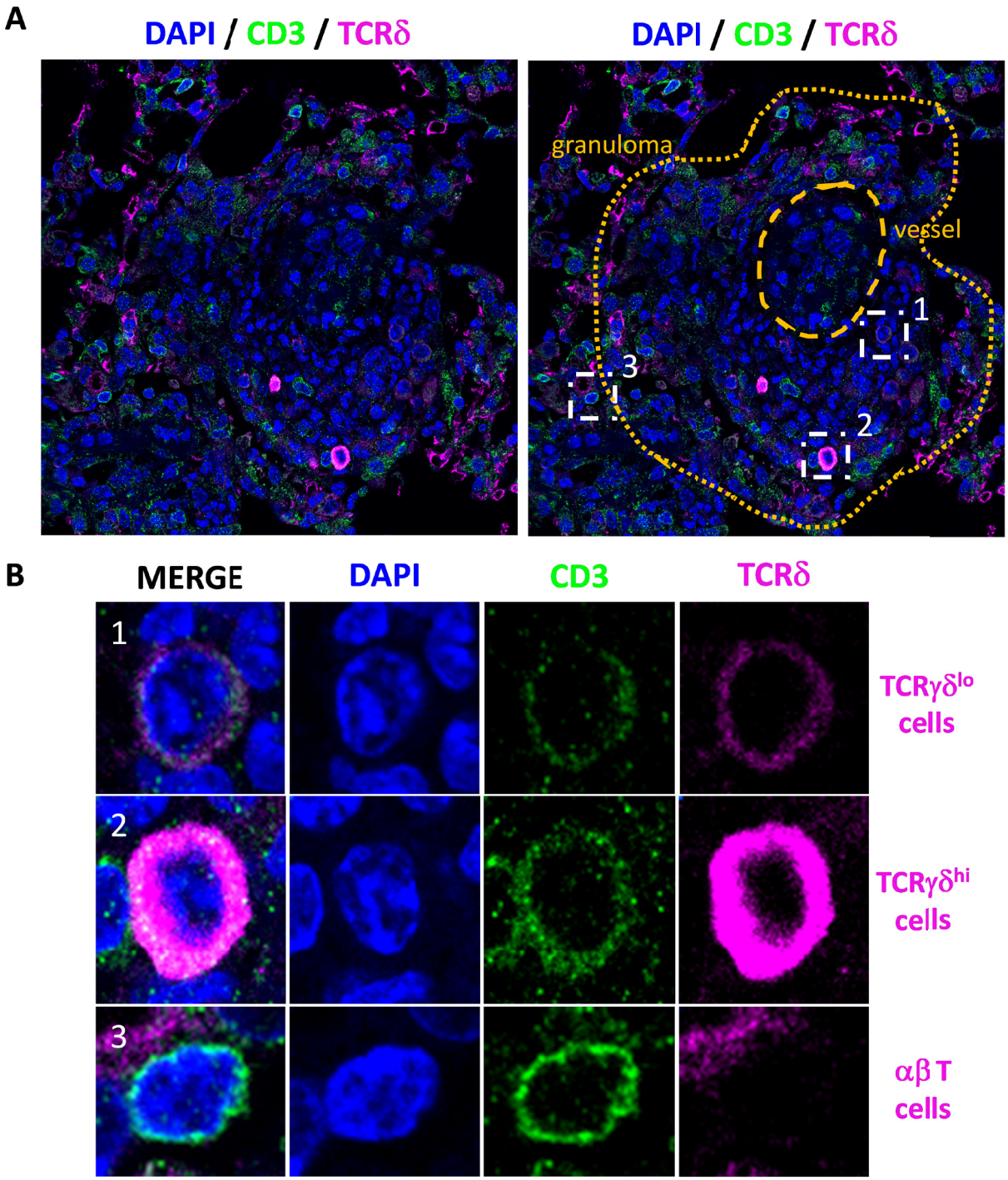

Figure 44. Differential TCRγδ expression in γδ T cells in pulmonary perivascular granulomas of HIV mice exposed to Schistosoma eggs. (A) IFM analysis of T cells (upper panels) in a pulmonary perivascular granuloma of a HIV mouse exposed to Schistosoma eggs. **(B)** TCRγδ *versus* TCRαβ expression in the single cells indicated in A; right panel.

7.8.2. CYTOKINE LANDSCAPE

For characterization of the pulmonary cytokine landscape of Wt and HIV mice, untreated or treated with schistosome, a combination of immunofluorescence microscopy and intracellular flow cytometry was used for identification of signature cytokines of Type 1 (IFN-γ), Type 2 (IL-4, IL-13) and Type 17 (IL-17A) immune responses. Intracellular cytokine expression in pulmonary T cells and myeloid cells by flow cytometry was determined following the strategies depicted in **Figure 14** and **Figure 15**, respectively.

7.8.2.1. IFN-γ

Flow cytometric analysis revealed that $CD4^+$ T cells and $TCR^{int\text{-}hi}$ γδ T cells in HIV mice **(Figure 45, A&B)** were the main cell types involved in the augmented IFN-γ response to parasite eggs, with a lesser contribution of myeloid cells **(Figure 45, C)**.

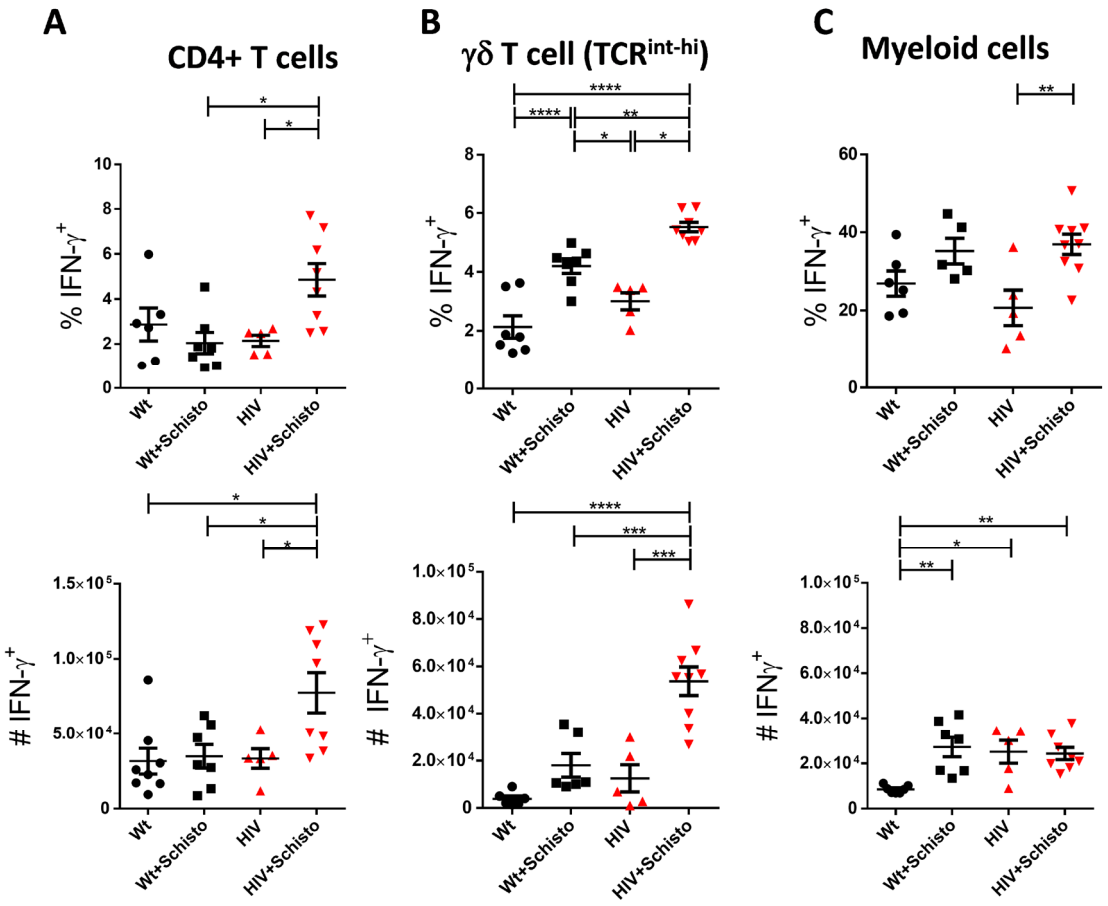

Figure 45. Flow cytometry determination of pulmonary IFN-γ expression in mice exposed or not to Schistosoma eggs. Flow cytometric analysis of intracellular IFN-γ expression in **(A)** CD4+ T cells and **(B)** γδ T cell ($TCR^{int\text{-}hi}$) **(C)** myeloid cells, gated as shown in figures 14, 14 and 15, respectively, in the lung of Wt and HIV mice unexposed or exposed to Schistosoma eggs (+Schisto)(n=5-8). Frequencies (%) and numbers (#) are shown. *P≤0.05, **P≤0.01, ***P≤0.001, **** P≤0.0001.

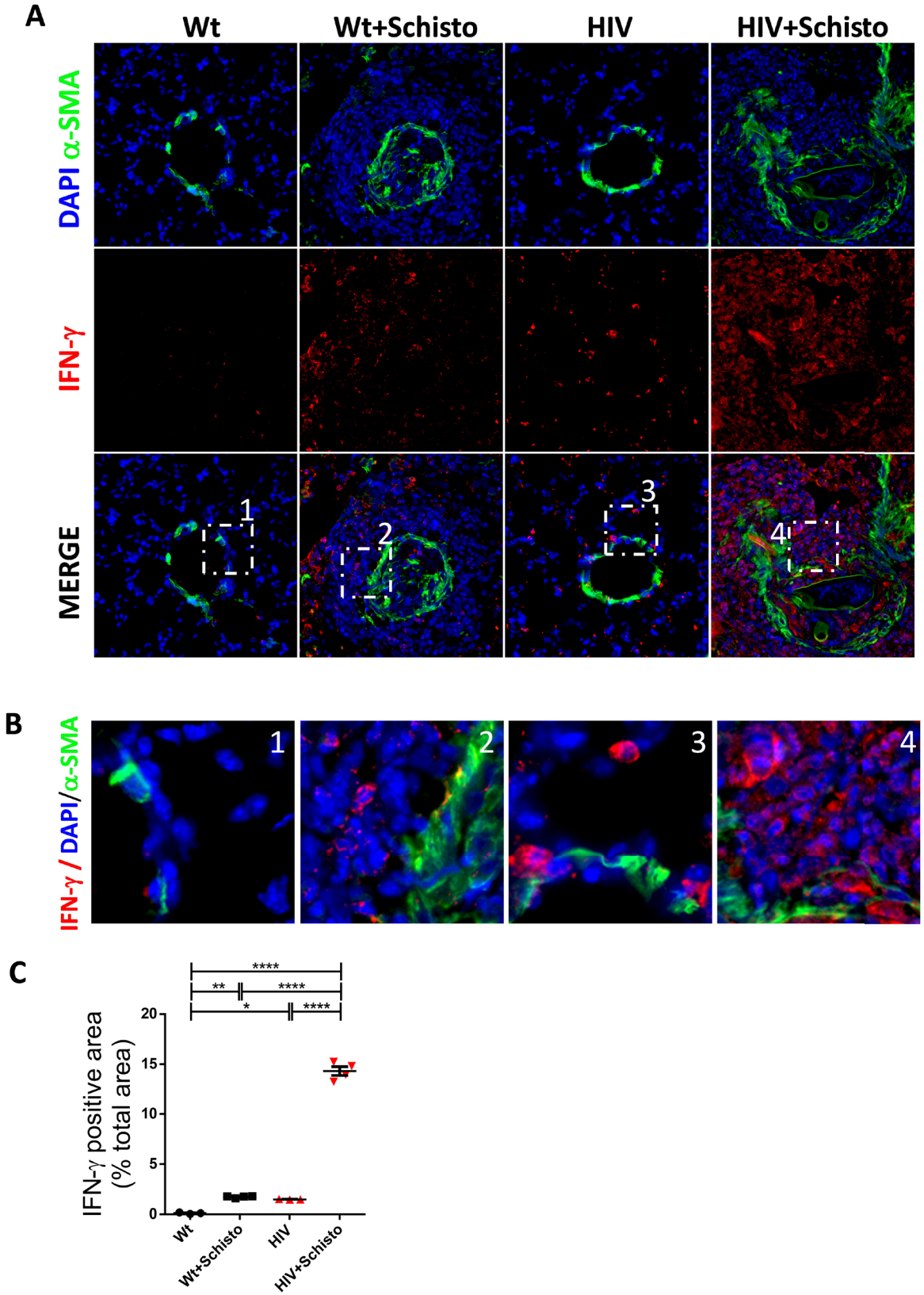

Figure 46. Immunofluorescence microscopy analysis of pulmonary IFN—γ expression in mice exposed or not to Schistosoma eggs. (A,B) Representative examples of IFM analysis. α-SMA was used as a vessel marker. (B) Magnification of the area indicated in panel A. **(C)** Quantification of IFN-γ cytokine per X40 area. Mice and vessel granuloma analyzed per group were: Wt (3; 20), Wt+Schisto (4; 27), HIV (3; 21) and HIV+Schisto (4; 29). *P≤0.05, **P≤0.01, ***P≤0.001, **** P≤0.0001.

Furthermore, immunofluorescence staining of lung sections revealed a clear IFN-γ expression in HIV but not in Wt mice. Egg administration increased IFN-γ expression in perivascular granulomas in both mice, but seemingly more in HIV mice **(Figure 46, A&B, upper panels)**; which in contrast to Wt counterparts showed not only perivascular but also markedly intravascular IFN-γ expression. Quantification of the cytokine signal confirmed this augmented IFN-γ expression in HIV compared to Wt mice, either untreated or treated with parasites eggs, but particularly in the latter **(Figure 46, C, lower panel)**.

7.8.2.2. IL-4 and IL-13

Type 2 cytokines (i.e. IL-4 and IL-13) are typically associated to the granulomatous response to parasite eggs in schistosomiasis. Intracellular flow cytometry analysis (**Figure 47**) showed that in untreated mice, either Wt or HIV, IL-4 is mainly expressed by CD4 T cells **(Figure 47A)**. After egg administration, the relative abundance of IL-4$^+$ CD4 T cells was reduced in both mice, with a concomitant increase in that of IL-4$^+$ myeloid cells; which resulted in a net increase in the number of these cells, particularly in HIV mice **(Figure 47B)**.

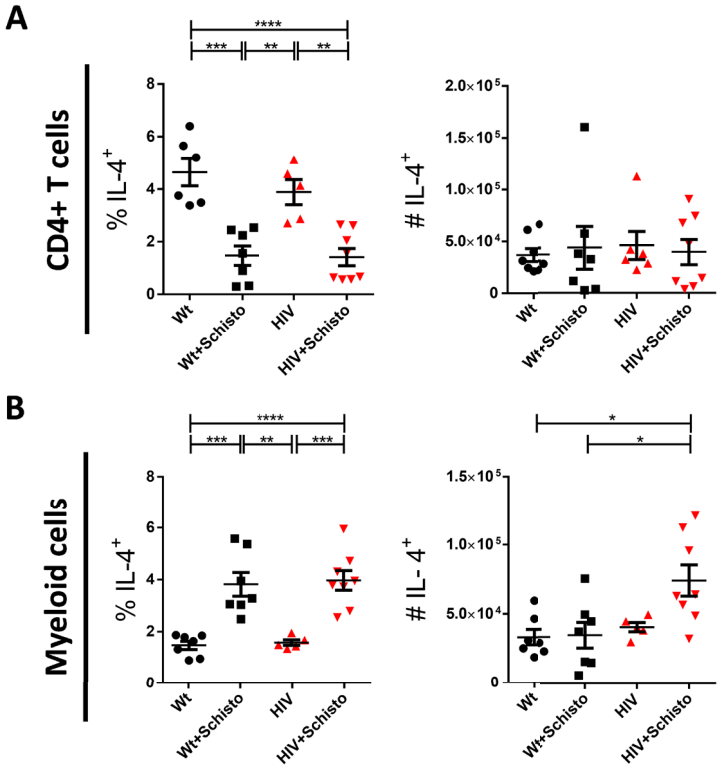

Figure 47. Flow cytometry determination of pulmonary IL-4 expression in mice exposed or not to Schistosoma eggs. Flow cytometric analysis of intracellular IL-4 expression in **(A)** CD4+ T cells and **(B)** myeloid cells, gated as shown in figures 14 and 15, respectively, in the lung of Wt and HIV mice unexposed or exposed to Schistosoma eggs (+Schisto)(n=5-8). Frequencies (%) and numbers (#) are shown. *P≤0.05, **P≤0.01, ***P≤0.001, ****P≤0.0001.

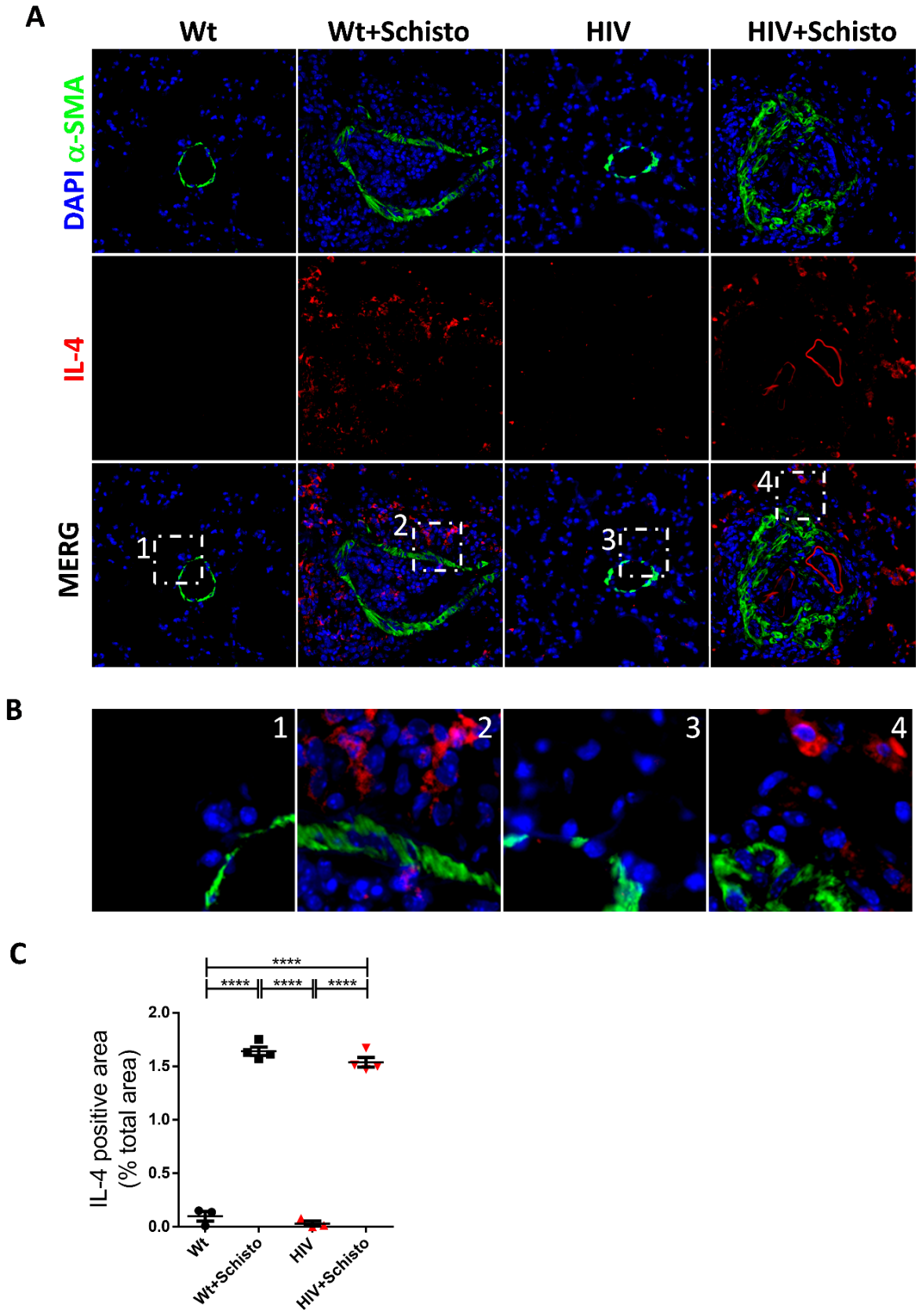

Figure 48. Immunofluorescence microscopy analysis of pulmonary IL-4 expression in mice exposed or not to Schistosoma eggs. (A) Representative examples of IFM analysis. α-SMA was used as a vessel marker. **(B)** Magnification of the area indicated in panel A. **(C)** Quantification of IL-4 cytokine per X40 area. Mice and vessel granuloma analyzed per group were: Wt (3; 21), Wt+Schisto (4; 28), HIV (3; 22) and HIV+Schisto (4; 31). *P≤0.05, **P≤0.01, ***P≤0.001, **** *P*≤0.0001.

Pulmonary IL-4 expression was hardly detected in untreated Wt and HIV mice, but strongly induced in granulomas of egg-treated mice **(Figure 48, A&B)**, and mostly in perivascular areas and to a lesser degree in intravascular locations **(Figure 48, A&B)**. Quantification of the fluorescent cytokine signal confirmed these results **(Figure 48, C).**

Analysis of pulmonary IL-13 expression by intracellular flow cytometry **(Figure 49)** showed increased relative and absolute abundance of IL-13-expressing CD4 T cells in untreated HIV mice compared to Wt counterparts. Upon parasite egg administration, these cells were decreased significantly in HIV mice and increased (but not significantly) in Wt mice **(Figure 49, A)**. Analysis of the myeloid compartment revealed higher number (but not frequency) of IL-13^{+} myeloid cells in untreated HIV compared to Wt mice **(Figure 49, B)**.

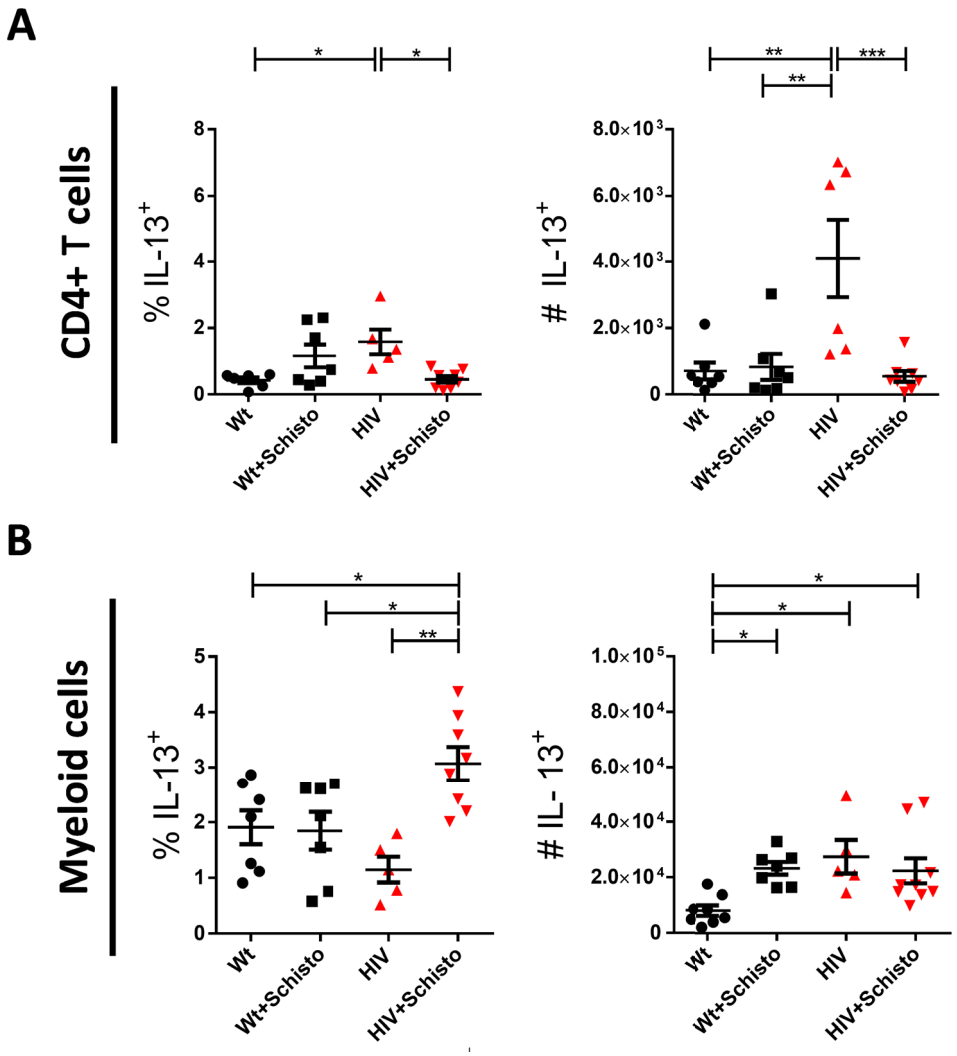

Figure 49. Flow cytometry determination of pulmonary IL-13 expression in mice exposed or not to Schistosoma eggs. Flow cytometric analysis of intracellular IL-13 expression in **(A)** CD4+ T cells and **(B)** myeloid cells, gated as shown in figures 14 and 14 and 15 respectively, in the lung of Wt and HIV mice unexposed or exposed to Schistosoma eggs (+Schisto) (n=5-8). Frequencies (%) and numbers (#) are shown. *P≤0.05, **P≤0.01, ***P≤0.001, ****P≤0.0001.

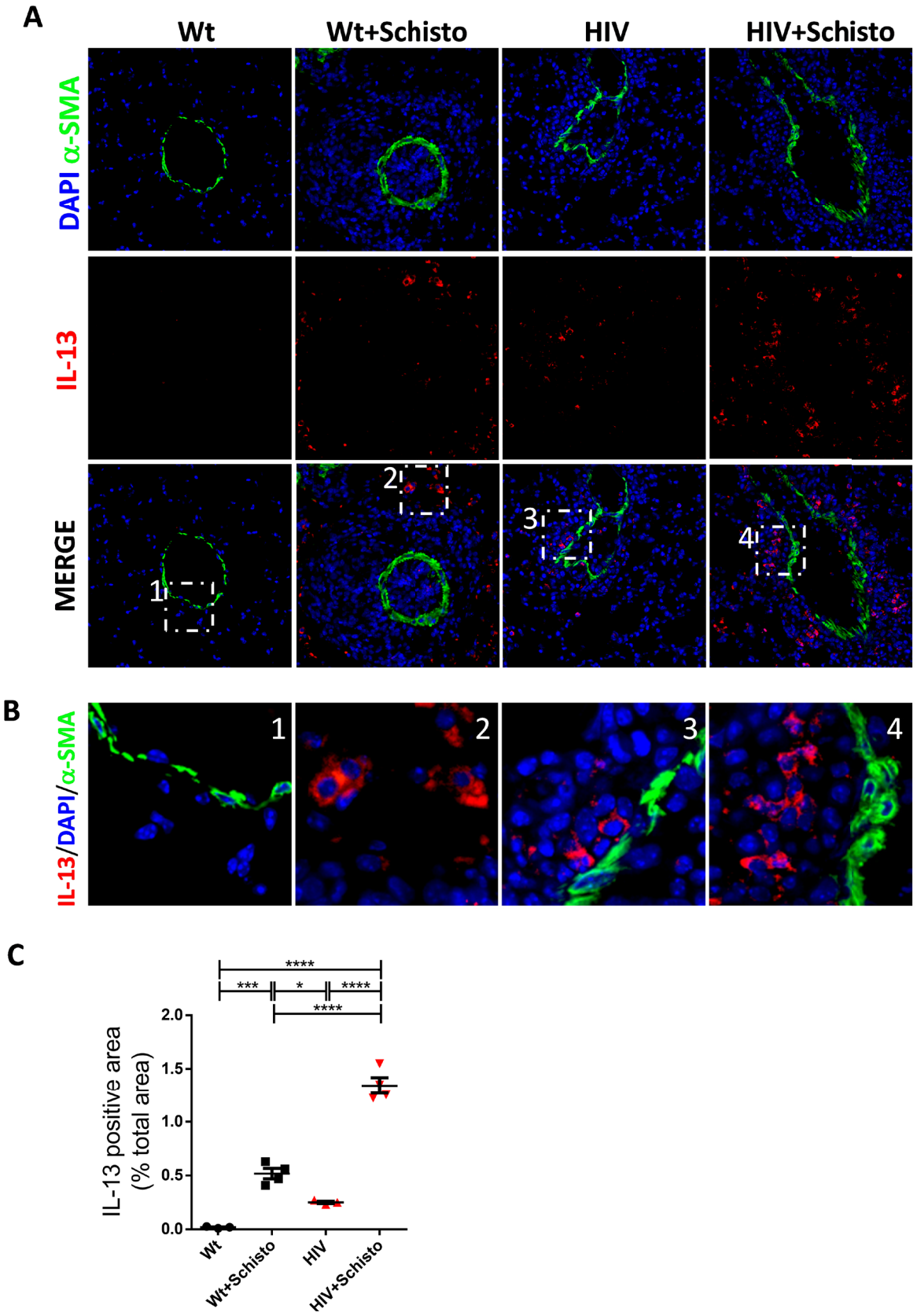

Figure 50. Immunofluorescence microscopy analysis of pulmonary IL-13 expression in mice exposed or not to Schistosoma eggs. (A) Representative examples of IFM analysis. α-SMA was used as a vessel marker. **(B)** Magnification of the area indicated in panel A. **(C)** Quantification of IL-13 cytokine per X40 area. Mice and vessel granuloma analyzed per group were: Wt (3; 21), Wt+Schisto (4; 28), HIV (3; 22) and HIV+Schisto (4; 31). *$P \leq 0.05$, **$P \leq 0.01$, ***$P \leq 0.001$, ****$P \leq 0.0001$.

Egg administration resulted in augmented percentage but not counts of these cells in HIV mice. In contrast, numbers of IL-13-expressing myeloid cells were significantly raised in egg-treated Wt mice, but to a level similar to that of untreated and egg-treated HIV counterparts. Collectively, these results reveal that IL-4 and IL-13 expression are differentially affected in pulmonary T and myeloid cells of HIV mice prior and after parasite egg administration.

In the case of IL-13, this cytokine was readily detected in the lung of untreated HIV but not in Wt mice. Egg treatment resulted in a markedly increase of IL-13 in HIV mice and less prominently in Wt counterparts **(Figure 50, A&B)**. Quantification of the IL-13 signal confirmed these observations **(Figure 50, C)**. Of note, in HIV but not Wt mice, IL-13^{+} cells were detected outside but in close proximity to the vessel wall. Cells in this location were increased in egg-treated HIV mice, along with IL-13^{+} cells in the periphery of the granuloma. In contrast, in egg-treated Wt animals, IL-13^{+} cells were present only in outer areas of the granuloma **(Figure 50, A&B).**

7.8.2.3. IL-17

Immunofluorescence analysis showed very low abundance of pro-inflammatory IL-17A-expressing cells in the lung of Wt and HIV mice. Notably, these cells were strongly augmented in perivascular granulomas of both mice, but more markedly in HIV mice; with IL-17A^{+} cells being detected both around and within the vessel **(Figure 51, A-C, upper and lower panel)**.

Intracellular flow cytometry revealed that egg-induced augmentation of pulmonary IL-17A expression was associated mainly to γδ (TCR$^{int\text{-}hi}$) T cells in Wt mice, while CD4 and γδ (TCR$^{int\text{-}hi}$) T cells contributed both to the increased expression of IL-17A in HIV mice **(Figure 52, A & B)**; with just a minor contribution from the myeloid compartment in either mice **(Figure 52, C)**.

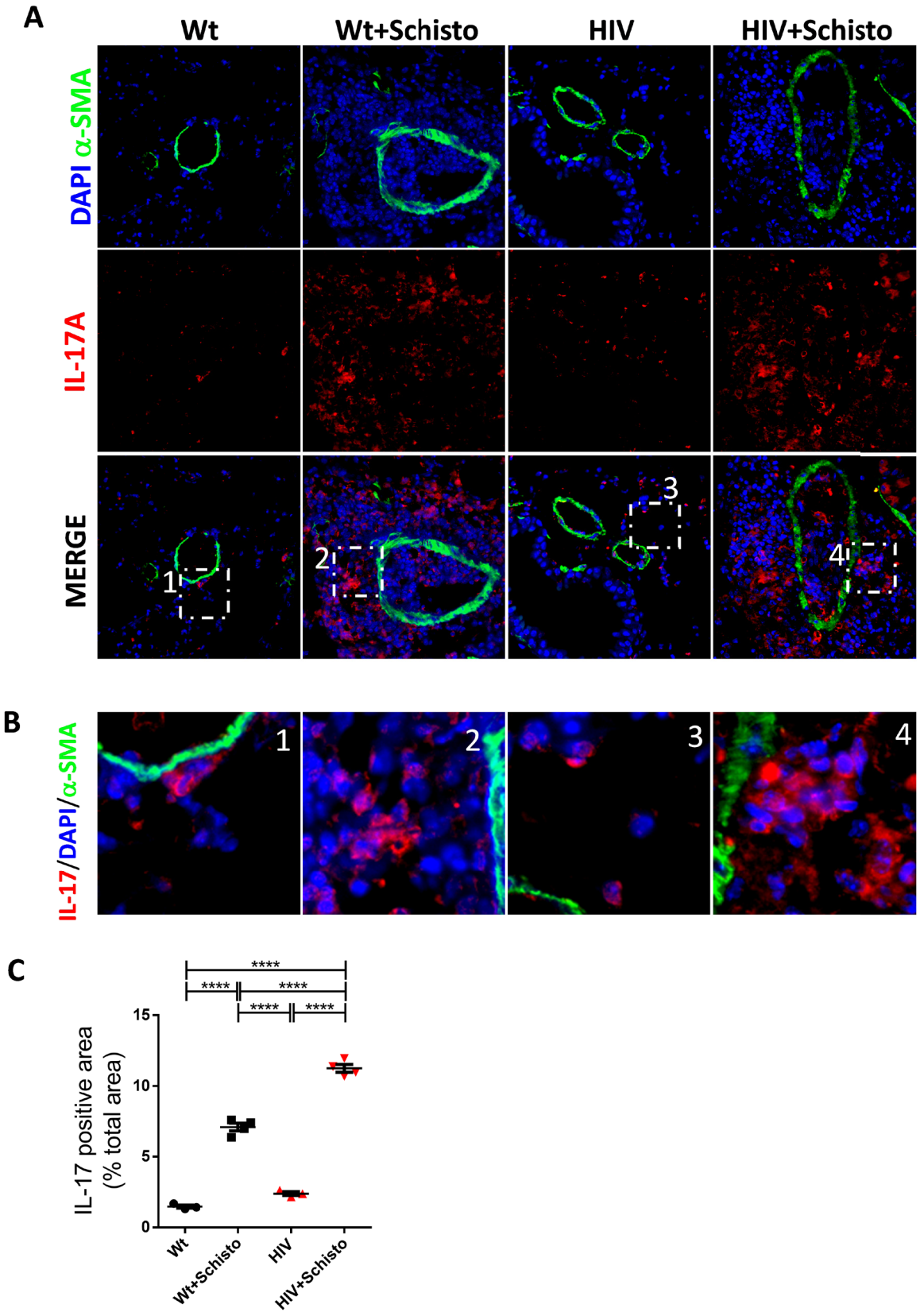

Figure 51. Immunofluorescence microscopy analysis of pulmonary IL-17 expression in mice exposed or not to Schistosoma eggs. (A) Representative examples of IFM analysis. α-SMA was used as a vessel marker. **(B)** Magnification of the area indicated in panel A. **(C)** Quantification of IL-17 cytokine per X40 area. Mice and vessel granuloma analyzed per group were: Wt (3; 20), Wt+Schisto (4; 29), HIV (3; 20) and HIV+Schisto (4; 29). **P*≤0.05, ***P*≤0.01, ****P*≤0.001, *****P*≤0.0001.

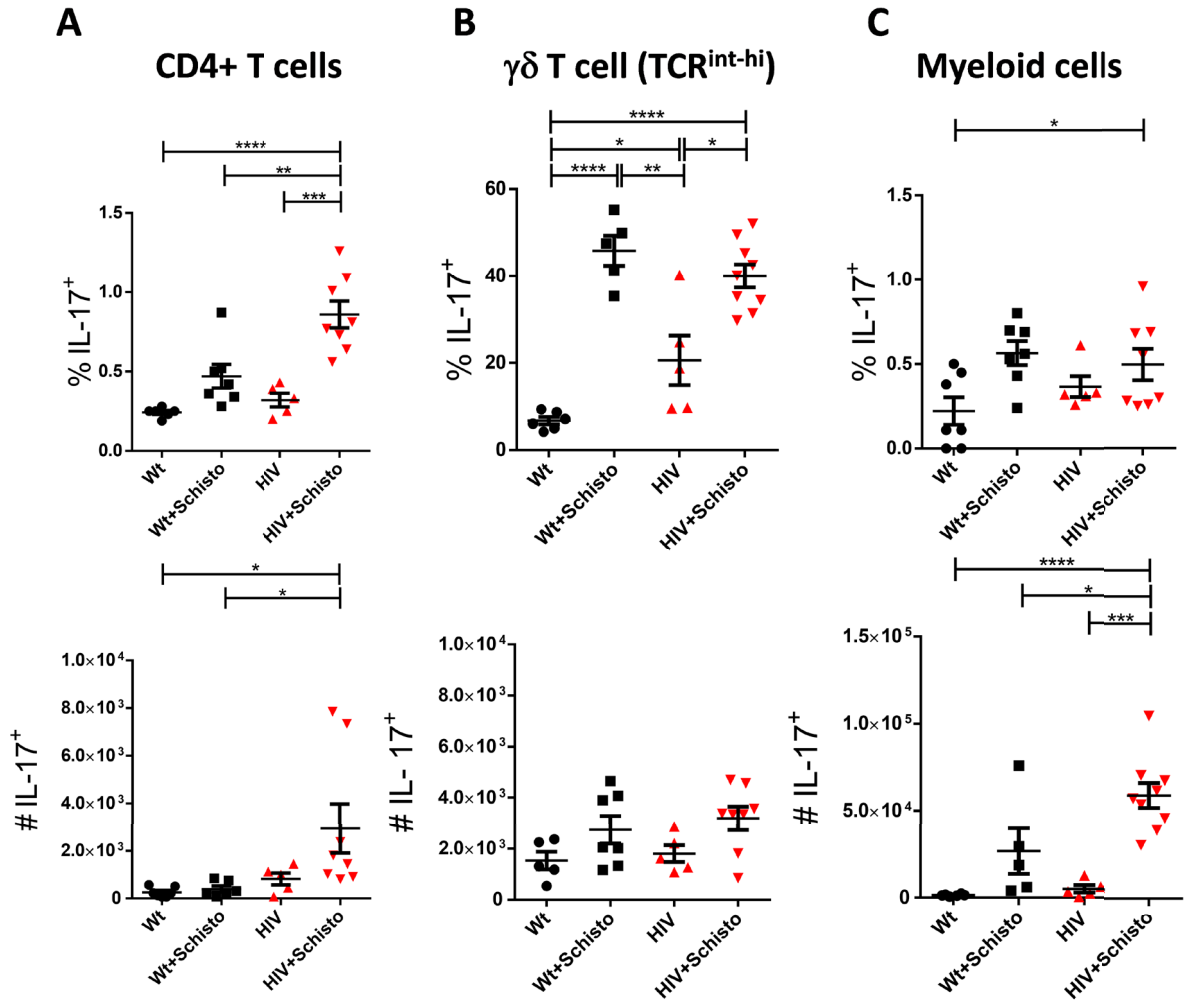

Figure 52. Flow cytometry determination of pulmonary IL-17 expression in mice exposed or not to Schistosoma eggs. Flow cytometric analysis of intracellular IL-17 expression in **(A)** CD4+ T cells and **(B)** γδ T cells and **(C)** myeloid cells, , gated as shown in figures 14, 14 and 15, respectively, in the lung of Wt and HIV mice unexposed or exposed to Schistosoma eggs (+Schisto)(n=5-8). Frequencies (%) and numbers (#) are shown. *$P \leq 0.05$, **$P \leq 0.01$, ***$P \leq 0.001$, ****$P \leq 0.0001$.

8

Discussion

Discussion

HIV and Schistosoma infections represent two major causes of morbidity and mortality globally. Among their different detrimental effects, both diseases may target the lung and contribute to the development of PVD (Butrous, 2015, 2019). Herein we report for the first time the impact of HIV and Schistosoma co-exposure on the pulmonary vasculature and development of pulmonary vascular pathology, by using a non-infectious mouse model based in HIV (Tg26) transgenic mice subjected to sensitization and embolization with *S. mansoni* eggs. This model might resemble that of HIV-infected people under ART and subsequently infected by Schistosoma. Our data showed that HIV and Schistosoma co-exposure results in an impaired immune response to parasite eggs, suppressed endothelial-dependent vasodilation, and an increased number of occluded pulmonary vessels with plexiform-like lesions, with associated augmentation of PAP.

In HIV transgenic mice, viral transcripts are expressed at low levels in immune cells such as monocytes, macrophages and lymphocytes (Bruggeman et al., 1994), similarly to HIV-infected people treated with ART (Almodovar, 2014; Cribbs et al., 2020a). Thus, HIV-related alterations in the population of lung resident immune cells (Cribbs et al., 2020a; Mwale et al., 2017a) could compromise the initiation of responses to local inflammatory stimuli (Jambo et al., 2011), such as embolized parasite eggs. Supporting this notion, we observed that untreated HIV mice showed an altered immune cell and cytokine landscape **(Figure 40-41, 45-52)**. In addition, alterations in the pulmonary recruitment of circulating inflammatory cells expressing HIV proteins could affect the progression of egg-induced immune responses in HIV mice **(Figure 19)**. In line with this, impaired macrophage infiltration into the lung and delayed resolution of lung inflammation has been reported recently in HIV Tg26 transgenic mice in response to bacterial lipopolysaccharide (LPS), with these defects being corrected by inhibition of HIV transcription

(Jerebtsova et al., 2020); suggesting an association between HIV gene expression in leukocytes and their impaired recruitment to sites of inflammation.

The granuloma induced by *Schistosoma mansoni* eggs is a compact and organized aggregate of leukocytes surrounding the egg, which is generated in response to parasite egg products and antigens. As depicted in **Figure 53** (left), the typical granuloma is mainly build by epitheloid macrophages, some of which are fused into multinucleated giant cells. These epithelioid cells are mainly located around the egg together with other cell types such as monocytes and eosinophils. T lymphocytes, both αβ and γδ T cells, are generally located in the periphery of the granuloma. Small deposits of very short collagen fibres are also found in the outer area of the granuloma. Schistosome eggs usually appear broken and with leukocytes inside (Pagán & Ramakrishnan, 2018).

In HIV mice **(Figure 53, right)**, in contrast, the size of the granuloma was considerably smaller than in Wt animals. In addition, qualitative differences in the granuloma composition were observed. Collagen fibres throughout the granuloma were longer and more abundant compared to those in Wt granulomas, and levels of collagen deposition were also higher. Of note, schistosome eggs were often found unaltered, with no evidences of egg degradation in most cases. The organization of epithelioid macrophages within the granuloma was similar to that observed in Wt counterparts, with macrophages forming tight junctions, and creating a dense network with other infiltrating leukocyte types. A main difference, however, between HIV and Wt granulomas was that αβ and γδ T lymphocytes were located throughout the granuloma in the former, and not only in the periphery as occurs in the latter. Taken together, these observations indicate a defective growth and accelerated fibrosis, and an impaired egg-clearing capability of granulomas induced by *S. mansoni* eggs in HIV mice (Kumar et al., 2019a; Pagán & Ramakrishnan, 2018a).

Thus, in egg-treated HIV mice pulmonary persistence of parasite eggs (Crosby et al., 2010; Kumar et al., 2019a) and HIV proteins could, on the one hand, sustain an inflammatory process targeting the vasculature (Almodovar, 2014; Cribbs et al., 2020a; Voelkel et al., 2016; Zahara Ali, Djuro Kosanovic, Ewa Kolosionek, Ralph T. Schermuly et al., 2017). On the other hand, HIV proteins and schistosome egg products could cause direct damage to the lung vasculature (Anand et al., 2018; Chelvanambi et al., 2019; Schwartz & Fallon, 2018). Together, this may lead to exacerbation of pulmonary vascular pathology in individuals co-exposed to HIV and Schistosoma.

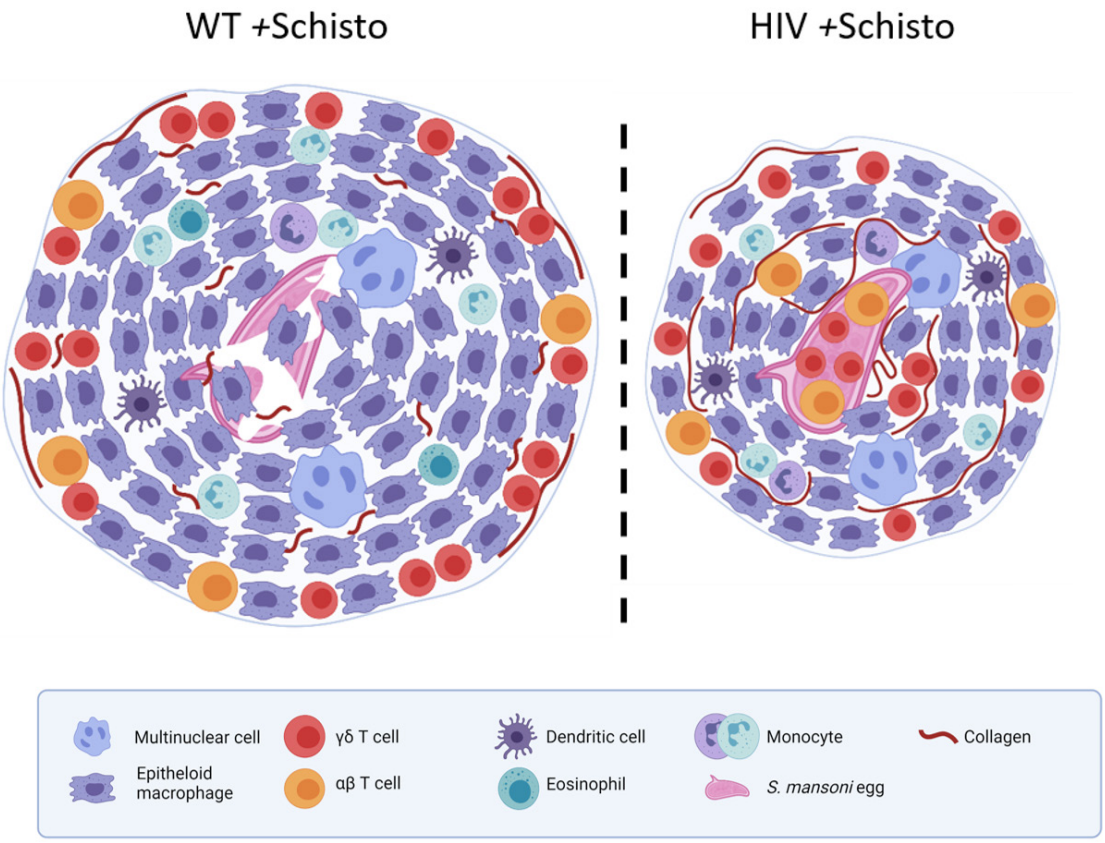

Figure 53. Features of granulomas induced by *S. mansoni* eggs in the lung of Wt (left) and HIV (right) mice.

We found that pulmonary vessels from HIV mice exhibited increased fibrosis **(Figure 24)**, which was further enhanced by lung embolization of schistosome eggs. In line with this, a recent study reported a pro-fibrotic phenotype of primary lung fibroblasts isolated from HIV (Tg26) transgenic mice and in wild-type primary lung fibroblasts cultured with HIV-1 protein gp120 (Marts et al., 2019). Because schistosomiasis and HIV infection have both been associated with lung fibrosis (Crothers et al., 2011; Knafl et al., 2020) our findings suggest that combined exposure to HIV and Schistosoma could increase the risk of developing pathological fibrotic changes in the pulmonary vasculature.

Endothelial dysfunction represents a common hallmark in HIV-infected patients regardless of antiretroviral treatment (Butrous, 2015; Cribbs et al., 2020a), and is considered a precursor of the development of HIV-associated cardiovascular and lung disease that contribute substantially to morbidity and mortality (Almodovar, 2014; Anand et al., 2018; Butrous, 2015; Cribbs et al., 2020a). In agreement with our previous work (Mondejar-Parreño et al., 2018), herein we observed that pulmonary vessels from HIV mice displayed endothelial dysfunction, which was greatly exacerbated by exposure to schistosome eggs **(Figure 27)**. Among the potential

underlying mechanisms, HIV proteins, particularly Nef, Tat and gp120, appear to be involved as they have been shown to play a key role in the development of endothelial injury (Almodovar, 2014; Anand et al., 2018; Butrous, 2015; Cribbs et al., 2020a). Gp120 induces apoptosis and endothelial dysfunction in lung microvascular endothelial cells (Green et al., 2014). Tat was also shown to induce endothelial dysfunction in porcine coronary arteries (Paladugu et al., 2003). Likewise, Nef causes endothelial dysfunction in experimental models and in human PA endothelial cells (Duffy et al., 2009). Moreover, Nef was shown to be transferred from immune cells to vascular endothelial cells resulting in endothelial activation, dysfunction and death (Wang et al., 2014). Of note, Chelvanambi et al. (Chelvanambi et al., 2019) have recently reported that Nef protein persists in the lungs of HIV patients on antiretroviral therapy, causing endothelial apoptosis and pulmonary vascular damage. Increased release of the proapoptotic endothelial monocyte-activating polypeptide II (Chelvanambi et al., 2019; Green et al., 2014) and excessive oxidative stress because of augmented reactive oxygen species (Agarwal et al., 2020; Anand et al., 2018; Wang et al., 2014) are thought to critically underlie the endothelial injury induced by HIV proteins.

It is widely accepted that endothelial dysfunction is a common initiating event that contribute to several forms of chronic lung disease as PAH (Humbert et al., 2019; Sakao et al., 2009). Indeed, endothelial dysfunction is considered an initial trigger for a number of functional and histopathological features shared in most types of PAH, such as increased vasoconstriction, muscularization, intima and media thickening, vessel obliteration and complex plexiform lesions (Abe et al., 2010; Toba et al., 2014; Tuder et al., 2013). In the present study, we show that pulmonary vessels from HIV transgenic mice display moderate endothelial dysfunction **(Figure 27)**, but only mild muscularization **(Figure 21)** and no evidence of medial thickening or vessel occlusion **(Figure 23)**. Similar results have been reported in other HIV experimental models (Agarwal et al., 2020; Porter et al., 2013a). In contrast, exposure of HIV mice to schistosome eggs led to a marked suppression of endothelial-dependent vasodilation, indicating an exacerbation of the endothelial injury. *S. mansoni* egg products have been shown to be detrimental to endothelial cells by inducing the release of IL1-β from immune cells, which in turn causes endothelial cell dysfunction and apoptosis (Ritter et al., 2010). Yet, how parasite eggs combine with HIV proteins to exacerbate pulmonary endothelial dysfunction remains to be fully determined.

Endothelial damage is critically involved in the development of obliterative pulmonary vascular lesions (Goldthorpe et al., 2015; Humbert et al., 2019; Tuder et al., 2013).

Remarkably, we found that pulmonary vessels became occluded with proliferating cells more frequently in egg-treated HIV compared to Wt mice **(Figure 23)**. Moreover, cells within the lumen-obliterating vascular lesions expressed the endothelial cell marker vWF, indicating a predominance of endothelial cells and suggestive of endothelial cell proliferation **(Figure 22)**. Our data suggest that parasite eggs in the lung, in the context of local and persistent expression of HIV proteins, aggravates endothelial injury leading to enhanced development of obliterative vascular lesions. The formation of plexiform lesions represents a morphological hallmark of the pulmonary arteriopathy in severe PAH (Abe et al., 2010; Tuder et al., 2013). While the cellular and molecular mechanisms have not been fully elucidated, the current hypothesis postulates that the lesion is initiated by endothelial apoptosis followed by proliferation of apoptosis-resistant endothelial cells (Goldthorpe et al., 2015; Humbert et al., 2019; Sakao et al., 2009; Tuder et al., 2013). Using an approach similar to that of Toba et al. (Toba et al., 2014), we detected a much higher proportion of plexiform-like lesions in egg-treated HIV than in Wt mice **(Figure 23)**. This is one novel finding very relevant to the pathophysiology of pulmonary vascular disease, as it indicates that combined exposure to HIV and Schistosoma results in the early onset of pulmonary lesions that normally occurs at advanced and severe stages of PAH (Toba et al., 2014).

In fact, plexiform-like lesions have not been consistently found in rodent models of PAH (Gomez-Arroyo et al., 2012). While the mechanisms triggering these lesions are still unknown, it is tempting to speculate that HIV proteins such as Nef, Tat and gp120 may be involved (Almodovar, 2014; Anand et al., 2018; Butrous, 2015; Cribbs et al., 2020a). Further supporting this notion, complex pulmonary vascular lesions were observed in macaques infected with chimeric simian/human immunodeficiency virus (SHIV) containing Nef and in patients with HIV-related pulmonary hypertension (Almodovar et al., 2018; Marecki et al., 2006a).

We found that exposure to parasite eggs nor HIV proteins alone affect pulmonary or RV hemodynamics **(Figure 25-26)**, and that only the exposure to both led to a clear increment in PAP and RVSP. Similarly, previous studies in other HIV models have found a requirement for a "second hit", such as cocaine (Dhillon et al., 2011), opioids (Agarwal et al., 2020) or hypoxia (Porter et al., 2013a), to elevate pulmonary pressure or exacerbate the density of pulmonary lesions (Spikes et al., 2012). As shown, exposure of HIV mice to a Schistosoma "second hit" was associated with suppression of endothelial-dependent relaxation **(Figure 27)**, increased number of vascular occlusions and plexiform-like lesions **(Figure 23)**, but not with exacerbated medial thickening **(Figure 21)** or cardiac remodelling **(Figure 26)**, compared to Wt animals treated

with parasite eggs. In line with our data, only modest hemodynamic changes were observed in animals with abundant pulmonary vascular lesions due to endothelial cell apoptosis (Goldthorpe et al., 2015). Moreover, in the hypoxia+Sugen5416 model, restoration of endothelial shear responsiveness was shown to reverse intimal occlusions but with minor consequences on medial thickening or RVSP (Szulcek et al., 2016).

In the present study, we aimed also at characterising the pulmonary immune landscape of mice exposed to HIV and Schistosoma, individually or in combination. To our knowledge, this is the first time that such a comprehensive profiling of pulmonary lymphoid and myeloid cells is performed in HIV transgenic mice, either exposed or not to schistosome eggs. These data could provide important information as to how the presence of HIV proteins in the lung could influence the composition and function of pulmonary immune cells, and also for the understanding of pulmonary pathologies associated to HIV infection and HIV comorbidities such as schistosomiasis; particularly in HIV-infected individuals treated with anti-retroviral therapy who bear a resemblance to HIV (Tg26) transgenic mice (Almodovar et al., 2017; Marecki et al., 2006b).

First, will be discuss the similarities and differences in the lung immune landscape between untreated HIV mice and Wt counterparts, and later on, will be further covered the alterations observed after schistosome egg administration in these two types of mice.

The immune characterisation by flow cytometry of the healthy lung of C57BL/6 mice, in the same range of age as FVB background mice used in our study (Yu et al., 2016), showed a lymphoid-to-myeloid ratio with predominance of lymphoid over myeloid cells (60%/40%), similar to those of Wt and HIV mice in the FVB genetic background; although it was consistently lower (but closer to C57BL/6 values) in HIV compared to Wt counterparts **(Figure 40)**. This means that, in terms of major leukocyte populations resident in the lung, FVB mice are quite comparable to the widely used C57BL/6 strain; and that HIV transgene expression does not result in a major alteration in the relative abundance of pulmonary lymphoid *versus* myeloid cells.

When comparing the gross leukocyte content in the lung of Wt and HIV mice, we observed a tendency for increased leukocyte counts in the latter animals **(Figure 28)**, suggesting increased leukocyte recruitment (in particular of myeloid cells) into the lung probably due to inflammatory signals derived from the presence of viral proteins **(Figure 17)**. Consistent

with this notion, the presence of HIV proteins in tissues leads to the recruitment of innate immune cells, such as neutrophils, monocytes, dendritic cells, and NK cells (Leite Pereira et al., 2019b). Further, it is known that an increase in blood monocytes and tissue macrophages precedes the onset of rapid progression to HIV in the macaque model of AIDS (Hasegawa et al., 2009), where increased monocyte turnover was associated with the accumulation of interstitial lung macrophages (Chelvanambi et al., 2019). In addition, an increase of myeloid lineage cells in the lung has been associated with pulmonary hypertension in HIV patients (Porter et al., 2013b). Furthermore, it is known that a viral reservoir remains stable in HIV-infected patients under prolonged antiretroviral (ART) therapy (Finzi et al., 1997; Wong et al., 1997) and HIV DNA and/or RNA has been detected in alveolar macrophages in patients under ART (Cribbs et al., 2015). HIV RNA encodes for multiple molecular patterns that can be recognised by monocytes and dendritic cells that express receptors for them, such as TLR8 and TLR7, respectively (Chang et al., 2012). Also of note, in HIV-Tat transgenic mice, expression of the viral protein in the lung resulted in increased oxidant burden and leukocyte infiltration (Cota-Gomez et al., 2011).

When individual pulmonary immune cell subsets were comparatively analysed in HIV mice, we did not observe large differences in the relative abundance of most of the cell types studied **(Figure 41)**, including T lymphocytes, eosinophils, neutrophils, monocytes and dendritic cells. However, in absolute cell counts, we did observe a tendency for increased T lymphocytes **(Figure 29)**, eosinophils/neutrophils **(Figure 35)** and DC1 ($CD103^+$) **(Figure 38)** in HIV compared to Wt counterparts.

Although B lymphocytes were not significantly affected, either in frequency or numbers in HIV mice **(Figure 34)**, they could be functionally relevant in the context of HIV proteins in the lung, as *in vitro* models have shown that viral proteins such as Nef, which is expressed in HIV mice (Dickie et al., 1991), can be accumulated by B lymphocytes (Qiao et al., 2006) and indirectly promote polyclonal B-cell activation and increased $CD4^+$ Tcell permissiveness to infection with HIV. These effects were seemingly related to Nef-induced secretion of proinflammatory cytokines by macrophages, which in turn upregulate the expression of costimulatory receptors on B lymphocytes (Swingler et al., 2003).

To be highlighted, only two leukocyte subtypes were significantly altered in the lung of HIV mice compared to Wt counterparts: NK cells **(Figure 34)** and interstitial macrophages **(Figure 37)**. Pulmonary NK cells of HIV mice were significantly decreased in frequency

and showed a tendency for reduced numbers compared to Wt mice. NK cells contribute to the clearance of HIV-infected cells during the acute phase and are key antiviral effectors of the innate immune system. Also, deficiencies of this cell type are associated with an increased likelihood of HIV infection (Mikulak et al., 2017; Scully & Alter, 2016). Decreased representation of NK cells in the pulmonary immune landscape of HIV mice could thus affect the elimination of cells expressing HIV proteins, which in turn could favour the persistence of viral proteins that could be detrimental for the integrity and/or function of different cells types in the lung.

With regard to pulmonary interstitial macrophages, a significantly increased proportion (and a tendency for higher numbers) was observed in HIV compared with Wt mice **(Figure 37)**. Interstitial macrophages (IM) are a macrophage subset located in the lung parenchyma, in contrast to the so-called alveolar macrophages (AM) residing in the airways. Hence, the increase in IM in HIV mice suggests the infiltration of the parenchyma by monocytes that differentiate later to IM. In line with this, increased monocyte turnover was associated with the accumulation of pulmonary IM in SIV-infected rhesus macaques (Cai et al., 2015). Mouse IM could exhibit some antigen-presenting capacity, as suggested by an earlier report (Gong et al., 1994). Thus, in HIV mice, a scenario could be envisaged where local expression of HIV proteins could result in the recruitment of monocytes into the lung and their differentiation in IM, which in turn could act as both proinflammatory cells and antigen-presenting cells for subsequent T cell responses. In further agreement with this notion, HIV mice showed a consistent tendency for increased abundance of monocytes of the inflammatory type in the lung **(Figure 36)**.

HIV mice also showed alterations in the surface expression of some immune cell markers in the lung, notably those of T cells such as the CD4/CD8 coreceptors and CD27 **(Figure 30)**. All these surface molecules were significantly upregulated in pulmonary αβ T cells from HIV mice compared to Wt counterparts.

CD27 is a surface protein constitutively expressed by naive T cells that plays an important role in proliferation, survival, and differentiation of T cells. In particular, CD27 promotes immune activation and enhances primary, secondary, memory and immune responses to viral infections (Grant et al., 2017). CD27 expression increases following activation of CD4 or CD8 cells via the TCR pathway. Thus, our findings strongly suggest a sustained activation of αβ T lymphocytes in the lung of HIV mice. Similar observations were made in a study with HIV patients under

ART, where the expression of CD27 on CD4 and CD8 αβ T cells was higher in ART-HIV-1 individuals compared to healthy ones (Leite Pereira et al., 2019b). In that study it was suggested that the persistent T cell activation could be associated either to residual viral replication or to HIV-dependent inflammatory mechanisms. It has been also proposed that the constitutive engagement of CD27 by CD70 promotes T cell exhaustion, and that the high levels of surface CD27 observed in HIV patients could contribute to the loss of T cell effector functions (van de Ven & Borst, 2015). Taken together, these reports would support the notion that HIV mice resemble ART-treated HIV-infected individuals in that of persistent activation and potential functional exhaustion of αβ T cells.

HIV mice also showed upregulated levels of surface CD11b in immune cells of the lung **(Figure 39)**. CD11b is the α chain of the heterodimeric integrin known as Mac-1 (macrophage-1 antigen), which is composed by the αM chain (CD11b) associated to the β2 (CD18) chain. As part of Mac-1, CD11b is expressed in myeloid-lineage cells such as monocytes/macrophages, neutrophils, eosinophils and basophils, and in lymphoid cells such as NK and peritoneal B-1 cells (Corbi et al., 1988). Mac-1 binds multiple ligands, including ICAM-1 (CD54), ICAM-2 (CD102), and fibrinogen. CD11b participates in many proinflammatory biological processes primarily associated with controlling infection. For instance, in response to inflammatory stimuli, it mediates leukocyte activation and accumulation at the sites of inflammation, by increasing leukocyte rolling, stable adhesion, crawling and transmigration across blood vessels (Khan et al., 2018). CD11b was found overexpressed in blood granulocytes, monocytes, mDCs, NK and T cells from HIV patients under ART (Leite Pereira et al., 2019a). In HIV mice, CD11b surface expression was particularly upregulated in lung macrophages and patrolling monocytes, further suggesting the occurrence of a low-intensity but persistent inflammatory process in the lung of HIV mice due likely to the local expression of HIV proteins.

We also aimed at characterizing the alterations in the pulmonary cytokine landscape of HIV mice in comparison with Wt counterparts. HIV mice showed a significant increase in global IFN-γ expression in the lung **(Figure 45-46)**, with $TCR^{int\text{-}hi}$ γδ T cells (but not CD4 αβ T cells) and myeloid cells (likely macrophages, according to the immunofluorescence images) appearing as the main contributors of this cytokine.

Increased abundance of IFN-γ in the lung of HIV mice could have indirect but relevant effects on local antigen presentation and ensuing activation of CD4 αβ T cells, not only by macrophages

but also by fibroblasts with heightened levels of MHC class II molecules (Dolei et al., 1992). Also, IFN-γ along with IL-8 have been shown to be inflammatory markers of pulmonary vascular disease, particularly in PAH (Morris et al., 2012).

With regard to pulmonary expression of Type 2 cytokines, HIV mice showed no alterations in IL-4 **(Figure 47-48)** but increased expression of IL-13 by CD4 T cells and myeloid cells **Figure 49-50)**.

In regard to IL-17A, HIV mice showed a tendency for increased pulmonary expression of this cytokine compared to WT counterparts **(Figure 51-52)**, which was associated mainly with $TCR^{int\text{-}hi}$ γδ T cells. Since IL-17A is a potent profibrotic cytokine, these observations could be related to the higher levels of perivascular fibrosis detected in HIV mice (Wynn, 2011).

The distinctive features of the pulmonary immune landscape of HIV mice and their potential relevance to development of lung disease are summarized in **Figure 54**.

(1) HIV proteins are expressed in the lung of HIV transgenic mice **(Figure 17)**. **(2,6,7)** HIV proteins, particularly Nef, Tat and gp120, have been shown to play a role in the development of endothelial injury (Almodovar, 2014; Anand et al., 2018; Butrous, 2015; Cribbs et al., 2020a). In the present study, we observed that pulmonary vessels from HIV mice displayed endothelial dysfunction **(Figure 27),** which is a precursor of the development of HIV-associated cardiovascular and lung disease **(11)** that contribute substantially to morbidity and mortality in humans (Almodovar, 2014; Anand et al., 2018; Butrous, 2015; Cribbs et al., 2020a). **(3)** In the lung, antigen presenting cells could recognize HIV-1 proteins and mediate leukocyte recruitment **(4)**. In fact, HIV mice showed a tendency for increased leukocyte counts in the lung **(Figure 28),** but with a different lymphoid/myeloid composition with increased myeloid recruitment **(Figure 40)**. Antigen presenting cells could also mediate αβ T cell activation **(5)** with upregulation of T-cell activation markers. **(9)** IL-17 production by activated leukocytes (in particular γδ T cells) **(Figure 51-52)**, could promote perivascular fibrosis **(10) (Figure 24)**. **(8)** Enhanced IFN-γ production by γδ T cells and myeloid cells **(Figure 45-46)** could counterbalance the fibrotic effect of IL-17. Nevertheless, IFN-γ production can promote endothelial injury.

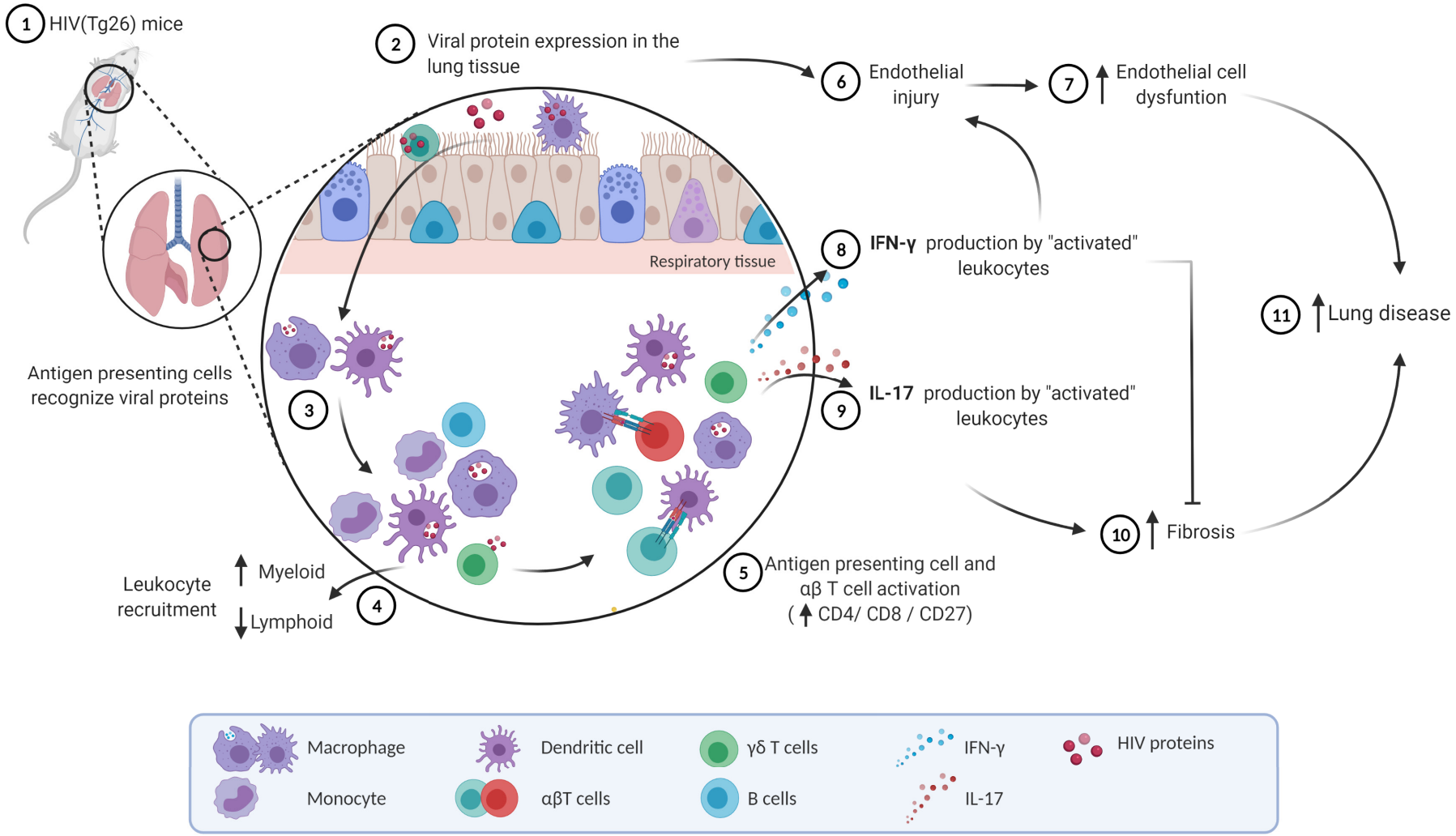

Figure 54. The pulmonary immune landscape of HIV mice and its potential relevance to development of lung pathology.

We also analyzed the impact of embolization of schistosome eggs into the lung in the pulmonary immune cell and cytokine landscape of HIV mice in comparison with Wt counterparts, aiming at defining the impact of HIV and Schistosoma co-exposure in lung pathophysiology and the specific contribution of immune cells and their products.

From the comparative analysis of schistosome egg-treated HIV mice with Wt counterparts, we first observed that parasite egg administration resulted in a noticeable increase in the pulmonary leukocyte content in both Wt and HIV mice **(Figure 28)**, most likely due to infiltration of blood leukocytes, which is in line with observations in the context of HIV infection and schistosomiasis, and mouse models of schistosome-induced PAH. Schistosome egg administration caused a similar reduction in the lymphoid-to-myeloid ratio in Wt and HIV mice when compared to untreated mice, indicating a predominance of myeloid cells in the leukocyte infiltrate in both mice; although myeloid cells were consistently more abundant in HIV than in Wt mice **(Figure 40)**. These results indicates that combined HIV and Schistosoma co-exposure favours a biased recruitment of blood myeloid cells into lung. This could be of pathological relevance as increased myeloid cells have been found in HIV-associated pulmonary hypertension (Porter et al., 2013) and fibrosis (Calabrese et al., 2013). In addition, a myeloid-to-lymphoid profile similar to that of egg-treated HIV mice has been reported for IPAH and PAH (Rabinovitch et al., 2014).

HIV and schistosome co-exposure resulted in a markedly increase of monocytes of the patrolling type **(Figure 36)**. Described "patrolling" behaviour of migrating lung monocytes as well as their localization at the interface between the capillaries and the alveoli suggested an immune surveillance function of these cells (Rodero *et al.*, 2015), although monocytic cells could also be pathogenic as inducers of fibrosis in the context of schistosomiasis (Fernandes et al., 2014). Thus, lung patrolling monocytes could be involved in the exacerbation of fibrosis observed in egg-treated HIV mice. Notably, the latter mice showed a consistent tendency for decreased abundance of lung inflammatory monocytes, likely due to their enhanced differentiation into interstitial macrophages in the context of HIV and schistosome co-exposure; as suggested by the largely increase of interstitial macrophages in egg-treated HIV mice.

Eosinophilia is a typical trait of the granulomatous response to *S. mansoni* eggs in both humans and experimental mice (Pagán & Ramakrishnan, 2018b). Levels of pulmonary eosinophils

(defined as $CD11b^{+}GR1^{med}$ cells, which could also include a minority of neutrophils), were increased to a much lesser extent in egg-treated HIV mice compared to Wt counterparts **(Figure 35)**; suggesting an impaired recruitment of eosinophil into the lung in the former animals. The reasons for this are yet to be determined.

With regard to the lymphoid immune landscape in the lung of HIV and schistosome co-exposed mice, major changes were associated with NKT and γδ T cells, with both lymphoid subsets being increased in egg-treated HIV mice compared with Wt counterparts.

NKT cells play a role in anti-infection, anti-tumoral, transplantation immunity, and autoimmune regulation. In addition, NKT cells, are able to rapidly produce cytokines, modulate the TH1/TH2 balance, and can stimulate or suppress immune responses in the lung (Rijavec *et al*., 2011). The literature about NKT cells and their involvement in PVD is scarce. In a study with *Schistosoma japonicu*m-infected mice (Cha *et al.*, 2016) the abundance of lung NKT cells was decreased compared to that of uninfected mice, which differ completely from our results with *S. mansoni* eggs **(Figure 31)**, probably due to the infectious *versus* non-infectious approach used. In other study comparing PAH patients and controls a tendency for increased blood NKT cell was observed in the former individuals, although this was not significant (Perros *et al.*, 2013).

γδ T cells are important mediators in pulmonary host defence that allow immediate responses to pathogens, being considered tissue-resident immune cells (Cheng & Hu, 2017). Lung resident γδ T cells can be activated by antigens, pathogen-associated molecular patterns (PAMPs), damage-associated molecular patterns (DAMPs), activating receptor ligands or cytokine signalling. During viral infections, activated lung γδ T cells produce several types of cytokines, among which some inhibit virus replication and some induce or inhibit lung inflammation (Cheng & Hu, 2017).

In the mouse lung, two subsets of γδ T cells are distinguished based on the surface expression of the antigen receptor: $TCR\gamma\delta^{lo\text{-}int}$ and $TCR\gamma\delta^{int\text{-}hi}$ cells (Paget et al., 2015). $TCR\gamma\delta^{hi}$ cells have been also detected in humans (El Hentati et al., 2010) and notably, they were increased in HIV-infected individuals (Dunne et al., 2018).

$TCR\gamma\delta^{lo\text{-}int}$ and $TCR\gamma\delta^{int\text{-}hi}$ cells were comparable in frequency and numbers in Wt and HIV mice **(Figure 32)**, but in the latter and not in the former mice, $TCR\gamma\delta^{int\text{-}hi}$ cells displayed

upregulated surface CD27; consistent with their being activated cells. Upon schistosome egg administration, TCRγδ$^{int\text{-}hi}$ cells were augmented more prominently in HIV mice than in Wt counterparts **(Figure 32)**. This suggests a preferential recruitment and/or expansion of TCRγδ$^{int\text{-}hi}$ cells in the context of co-exposure to HIV and parasite egg products.

γδ T cells have been implicated in various inflammatory diseases with distinct aetiology (Lu *et al.*, 2017). In HIV mice, but particularly in egg-treated ones, pulmonary TCRγδ$^{int\text{-}hi}$ cells could also act as important proinflammatory cells causing disease. In line with this, depletion of γδ T cells resulted in decreased inflammation and disease severity in a mouse model of viral lung disease (Dodd et al., 2009). Moreover, γδ T cells were detected in close proximity to arteries in the lungs of normal individuals and IPAH patients, but with higher frequency in the latter (Marsh *et al.*, 2018).

We also aimed at characterising the pulmonary cytokine landscape in the context of HIV and schistosome co-exposure in our mouse model, focusing on the tissue locations and cellular sources of various cytokines.

Type I responses are characterized by production of the signature cytokine IFN-γ. This cytokine was increased to a large extent in perivascular and intravascular locations of perivascular granulomas in egg-treated HIV mice, while only a minor increase restricted to perivascular areas was detected in Wt counterparts **(Figure 46)**. CD4^{+} T cells and TCR$^{int\text{-}hi}$ γδ T cells, and to a lesser degree myeloid cells, were the main cellular sources of IFN-γ in the lung of HIV mice **(Figure 45)**. Heightened IFN-γ expression in pulmonary γδ T cells of HIV mice is atypical, as the normal predominant population of γδ T cells in the lung are CD27^{-}CCR6^{+} cells producing solely IL-17 (Cheng & Hu, 2017). In contrast, pulmonary γδ T cells from both untreated and egg-treated HIV mice showed a mayor subset of CD27^{+}CCR6^{+} cells **(Figure 33)**. This unique phenotype appears to be associated with the expression of HIV proteins in the lung of HIV mice, where it was further favored by egg administration, while in Wt γδ T cells was only manifest upon egg treatment **(Figure 33)**.

Regarding the production of IFN-γ by pulmonary myeloid cells **(Figure 45-46)**, human macrophages derived from monocytes *in vitro*, using IL-12 and IL-18 or macrophage colony-stimulating factor (M-CSF), were able to produce IFN-γ when further stimulated with IL-12/IL-18. In addition, naturally activated alveolar macrophages immediately secreted IFN-γ upon

treatment with IL-12 and IL-18 (Darwich et al., 2009). Also, exogenous IFN-γ could induce IFN-γ mRNA expression in uninfected alveolar macrophages (Fenton et al., 2021). Therefore, lung macrophages in addition to T cells may contribute to the IFN-γ response, providing another link between the innate and acquired immune response.

Expression of IFN-γ is of relevance to pulmonary disease, as lung cells sense IFN-γ and its levels were elevated in sera from patients with systemic sclerosis associated PAH (Kirby et al., 2007). In addition, IFN-γ promotes vascular remodelling in human microvascular endothelial cells by upregulating endothelin (ET)-1 and TGF-β (Chrobak et al., 2013), which correlates with the increased presence of plexiform-like lesions observed in mice co-exposed to HIV and parasite eggs.

Type 2 responses, characterized by IL-4 and IL-13 production, have been reported to be typical in schistosomiasis, particularly during granuloma formation in the lung (Kumar *et al.*, 2019). High levels of IL-4 and IL-13 were observed in the lungs from mice treated with *S. mansoni* eggs, while mice with deficient Type 2 immunity, by combined deletion of IL-4 and IL-13, are protected from Schistosoma-induced pulmonary hypertension (Kumar *et al.*, 2015). Our data corroborates these findings to some extent, since IL-4 expression was similarly upregulated in granulomas from egg-treated HIV and Wt mice **(Figure 47-48)**; while IL-13 was more markedly increased in egg-treated HIV mice than in Wt counterparts **(Figure 49-50)**.

CD4 T cells have been directly implicated in PAH associated to schistosomiasis (SchPAH). A general concept in SchPAH pathogenesis is that an inflammatory cascade is triggered by parasite eggs, as part of the host immune response that seeks to eliminate the parasite and control the infection (Sibomana et al., 2020). Mechanistically, in this inflammatory cascade, the parasite eggs would induce the activation and antigen presentation by DCs to CD4 cells, causing their differentiation into Th2 cells producing IL-4 and IL-13, among other cytokines. These type 2 cytokines would promote monocyte recruitment and TGF-β release. TGF-β-induced production of trombospondin-1 (TSP-1) by monocytes would cause endothelial and smooth muscle cell remodelling, ultimately leading to PH (Kumar et al., 2017). Thus, CD4 Th2 cells would be instrumental at the beginning of the egg-induced immune response leading to pulmonary vascular pathology.

From the HIV side, CD4 T cells seems not to have an important role on the development of HIV-related PH, where disease progression appears to be related more to the duration of HIV infection (Farber & Loscalzo, 2004). In line with this, a recent study found that the number of alveolar CD4 T cells in HIV-infected adults was comparable to that in uninfected controls (Mwale et al., 2017b). In contrast, immunohistochemical studies in lung tissue sections from patients with iPAH and healthy donors showed a significant increase in CD4 and CD8 T cells in the adventitial space of the pulmonary vasculature (Savai et al., 2012), although their direct pathological relevance was not determined.

In contrast to the above studies, where the relevant cells expressing IL-4/IL-13 appears to be Th2 CD4 T cells, in egg-treated HIV mice these cytokines were produced mainly by pulmonary myeloid cells **(Figure 47 & 49)**. Although the precise identity of these myeloid cells is still to be established, their size, morphology and location within the granuloma is consistent with them being macrophages **(Figure 47 & 50)**.

With regard to IL-17A expression in the lung, cells expressing this cytokine were augmented in egg-induced perivascular granulomas of both HIV and WT mice, but more markedly in HIV mice; both around and within vessels **(Figure 51)**. Of note, CD4 and γδ (TCR^{int-hi}) T cells were the main producers of IL-17A in HIV mice following egg administration, while in Wt mice only γδ ($TCRi^{nt-hi}$) T cells were augmented **(Figure 52)**. This suggest that combined exposure to HIV proteins and schistosome eggs in the lung recruits and stimulates a larger variety of IL-17A-producing cells compared to the individual exposure. In line with this, IL-17 was induced in CD4, NKT, and γδ T cells following PMA/ionomycin stimulation, but γδ T cells exhibited the largest increase in expression (Chen et al., 2013).

Th17 effector cells can be induced in parallel to Th1 cells, and both types colocalize regionally and may require each other for recruitment into the region (Luger et al., 2008). HIV-1-specific IL-17-producing CD4 T cells were detectable in early HIV-1 infection, but were reduced to non-detectable levels in chronic and non-progressive HIV-1 infection patients. Of note, the virus-specific Th17 cells in early HIV-1 infection produce not only IL-17 but also co-expressed other cytokines, including IFN-γ (Yun et al., 2008). This is consistent with our data showing abundant Th1 and Th17 cells in perivascular granulomas of egg-treated HIV mice, and notably inside occluded vessels **(Figure 45 & 51)**.

In experimental animal models of hypoxia-induced PH, Th17 cells have been shown to play a pathogenic role (Hashimoto-Kataoka et al., 2015; Maston et al., 2017). Moreover, purified CD4 T cells from PAH patients expressed a higher level of IL-17 after activation than did those from control subjects (Hautefort et al., 2015). Furthermore, in a mouse model of silica-induced lung inflammation and fibrosis, it was found that IL-17A production by γδ T cells and Th17 cells was required for early lung neutrophilic inflammation and acute tissue injury (Lo Re et al., 2010). Also of note, T cells and γδ T cells in particular have been identified as proinflammatory and profibrotic mediators in the initiation and progression of pulmonary fibrosis, partly by producing IL-17 (Wynn, 2011). Indeed, reducing IL-17 activity using anti-IL-17A antibodies decreased infiltration of inflammatory cells and collagen deposition in the liver of esquistosome-infected C57BL/6 mouse (Chen et al., 2013). Taken together, these and our data suggest that IL-17 could be a critical mediator of pulmonary pathology and granuloma formation.

Collectively, the above data indicate that a markedly increase of cytokines occurs in the lung of egg-treated HIV mice compared to Wt counterparts. Thus, in HIV and Schistosoma co-exposed mice, there was an exacerbation of type 1 and 17 proinflammatory responses, in contrast to the typical response to schistosome eggs where a type 2 response is the predominant one; at least at the beginning of the response. This increase in IFN-γ and IL-17 could be underlying, at least partly, the exacerbation of fibrosis, vascular remodelling, endothelial damage and abnormal granuloma formation, which in turn could be instrumental for the development and progression of pulmonary vascular pathology associated to HIV and Schistosoma co-exposure **(Figure 55 & 56)**.

In our model, unlike previous studies (Graham et al., 2013; Kumar *et al.*, 2015a, 2019a), lung embolization of schistosome eggs was not associated with overt PH or cardiac remodeling. This resembles previous studies in mouse models of experimental schistosomiasis (Crosby et al., 2010; Graham et al., 2010) where, as in our study, an increased muscularization of small pulmonary vessels, thickening of the medial layer and even occasional plexiform-like lesions could be observed (Crosby et al., 2010). Differences in experimental conditions such as altitude (Denver *vs* Madrid) or mouse genetic background (C57BL/6 *vs* FVB) (Gharavi et al., 2004) could explain discrepancies among studies. Likely, a more overt effect on pulmonary hemodynamic would be expected with a longer pulmonary exposure to parasite eggs. However, increased mortality exhibited by untreated and particularly egg-treated HIV mice impeded analyses of a high number of animals at later time points. The causes of this higher mortality remain unknown. In any case, the number of mice and duration of the experimental protocol could be adjusted according to the increased mortality associated to HIV mice.

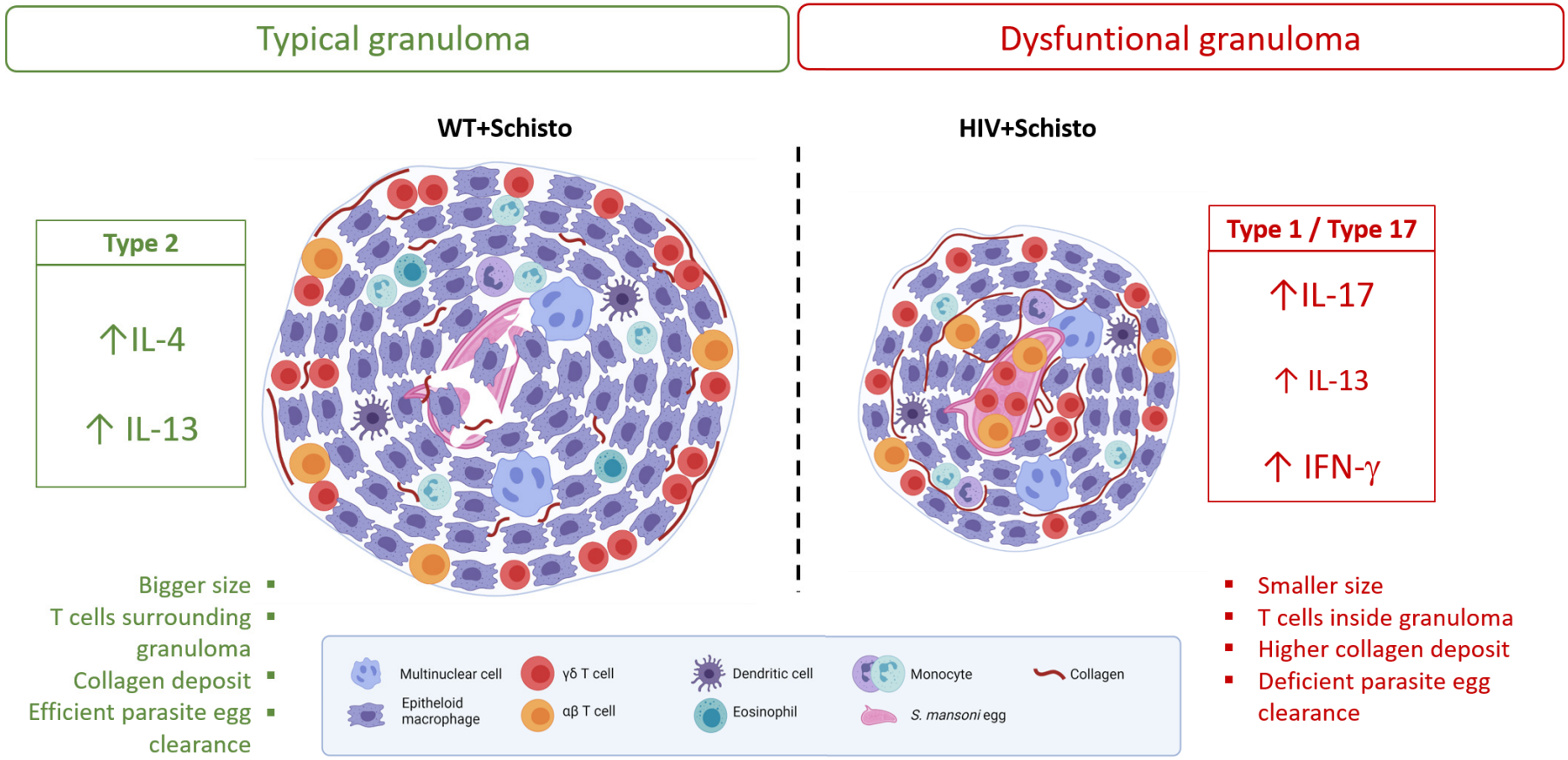

Figure 55. Alterations in the pulmonary cytokine landscape in schistosome egg-treated Wt and HIV mice and their potential impact on granuloma development.

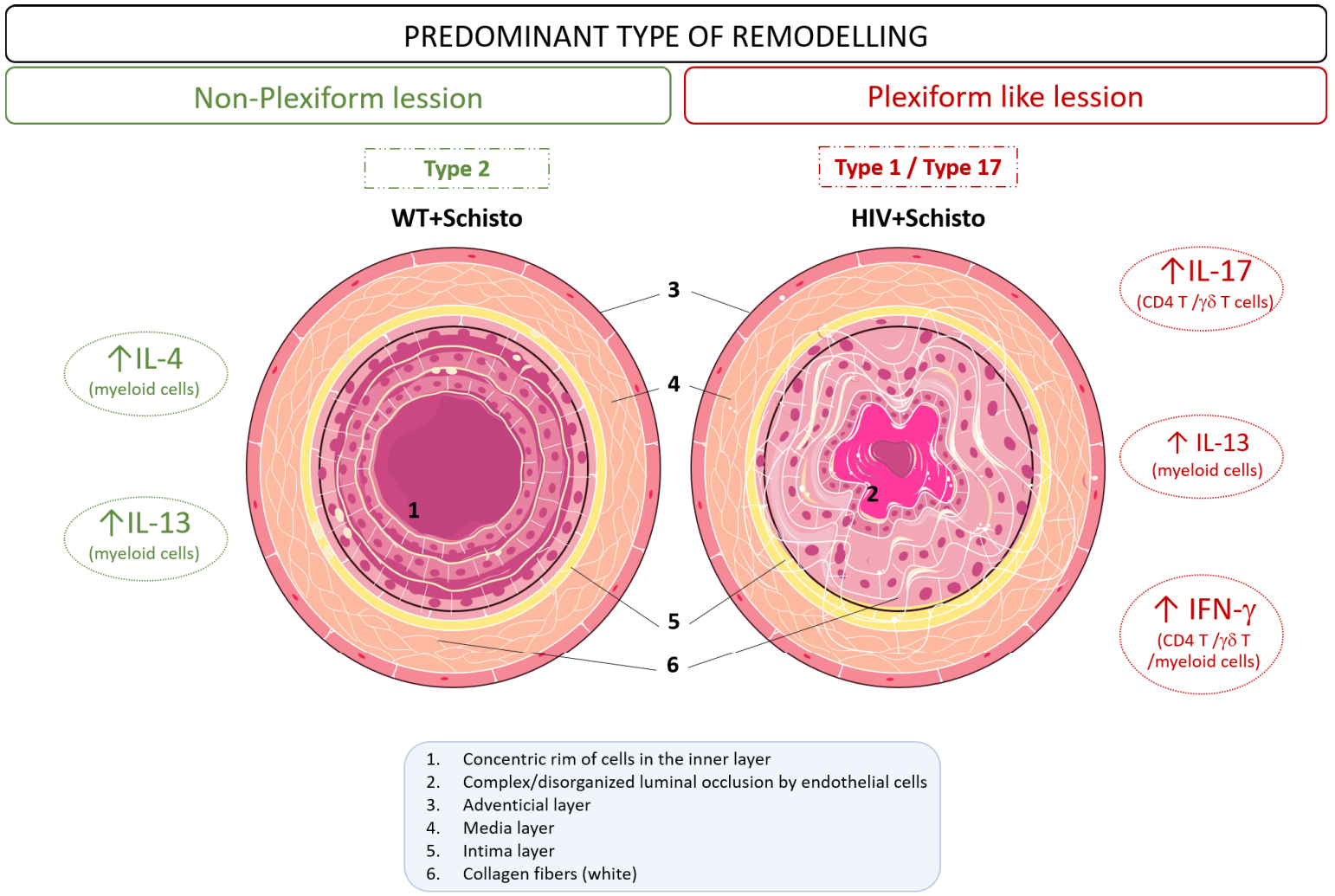

Figure 56. Alterations in the pulmonary cytokine landscape in schistosome egg-treated Wt and HIV mice and their potential impact on vascular remodeling.

Our non-infectious mouse model of HIV and Schistosome co-exposure, in contrast with other models, avoid the systemic effects associated to infection that could confound the interpretation of results (Arakelyan et al., 2019). Also, it precludes potential misleading effects due to interaction of live HIV with a live parasite, for instance, the integration of HIV-1 in the genome of *S. mansoni* (Suttiprapa et al., 2016). From the technical point of view, our model circumvent the laborious protocols and the variability of the outcome typically associated to reconstitution approaches, such as humanized mice (Cribbs et al., 2020b). The potential for long-term storage of the parasite eggs is also an advantage (Joyce et al., 2012).

Schistosomiasis and HIV infection represent two of the most common causes of pulmonary vascular pathology worldwide. Due to their high incidence globally and in endemic areas, it is conceivable that many individuals are co-infected. In the present study, we describe for the first time the impact of combined HIV and Schistosoma exposure on the pulmonary vasculature; and provide a novel insight of the structural and functional alterations occurring as a result of such HIV-Schistosoma interaction. Our work suggests that persistent expression of HIV proteins in the lungs, as occurs in ART-treated HIV-infected people, may cause an initial endothelial insult that may be aggravated in a subsequent Schistosoma infection; and foster ultimately the development of pulmonary vascular pathology.

9

Conclusions

Conclusions

A novel mouse model of HIV and Schistosoma co-exposure was analyzed to understand the impact of co-exposure on the pulmonary vasculature and development of vascular disease. Conclusions are as follows:

1. Pulmonary expression of HIV proteins, as occurs in HIV mice, impairs the granulomatous response to embolized schistosome eggs, resulting in smaller and dysfunctional granulomas with markedly reduced capability for egg clearance.

2. Persistent expression of HIV proteins in the lungs of HIV mice, as occurs in ART-treated HIV-infected people, may cause an initial endothelial insult that may be aggravated in a subsequent exposure to Schistosoma; leading ultimately to the development of overt pulmonary vascular pathology.

3. Pulmonary persistence of HIV proteins and parasite eggs in the co-exposure setting caused exacerbated endothelial dysfunction and remodelling, and associated augmentation of the pulmonary arterial pressure.

4. HIV and Schistosoma co-exposure altered the pulmonary immune cell and cytokine landscape in a manner compatible with exacerbation of inflammation, which in turn could be partly underlying the pathological alterations of the vascular endothelium.

5. The structural and functional changes in the pulmonary vasculature correlated with an altered pulmonary immune landscape in co-exposed mice, characterized by increased abundance of γδ T cells with intermediate-to-high levels of surface TCR and upregulated

CD27, patrolling-type monocytes and interstitial and alveolar macrophages, and heightened expression of IFN-γ/IL-17A by $TCR^{int\text{-}hi}$ γδ T cells and CD4 T cells, and IL-4/IL-13 in myeloid cells; which globally suggest a shift in T cells from a type 2 to a type 1/17 pro-inflammatory phenotype and enhanced local inflammation with relevance to development of vascular pathology.

6. The mouse model of HIV and Schistosoma co-exposure provides a suitable experimental model for the understanding of pulmonary vascular disease associated to the HIV and Schistosoma co-morbidity, and for testing novel therapeutical strategies for the treatment of co-infected people.

10

Future Directions

Future Directions

One of the most relevant findings of this doctoral thesis was the exacerbation of endothelial remodelling and dysfunction occurring in the pulmonary vasculature of mice co-exposed to HIV and Schistosoma. These particular vascular alterations correlated with changes in the pulmonary immune landscape and increased PAP.

Future research to solve unanswered questions posed by the thesis and to shed light on the HIV and Schistosoma pulmonary co-morbidity in humans could be focused on:

— *In vitro* studies to define the molecular and cellular mechanisms underlying the pulmonary vascular pathology in the co-exposure setting, for instance, with microvascular endothelial cells exposed or not to particular HIV proteins and parasite egg products. These studies could provide information on: 1) the identity of particular viral protein and schistosome egg molecule responsible for the endothelial damaging effects; 2) whether or not a direct interaction with the endothelium is required and 3) the potential role of specific cytokines highlighted by the thesis.

— Since there are only poor estimates of HIV and Schistosoma co-infection in humans, it would be informative to conduct population studies in collaboration with laboratories and clinicians in countries where the incidence of HIV and Schistosoma is high, such as Nigeria, Thailand or Brazil, to obtain data on co-infected patients and to assess the real extent of co-infection. It would be also of interest to obtain data on mortality and association to pulmonary vascular disease in co-infected patients. Since the clinical resources in affected countries are often limited, the aim would be to set up easy-to-perform non-invasive diagnostic tests, in combination with more specific tests such as

transthoracic echocardiography, when possible. In addition, establishment of a biobank of lung samples from individuals infected with HIV and Schistosoma, individually or in combination, could be instrumental for further understanding of the HIV and schistosomiasis pulmonary co-morbidity.

— Our mouse model of HIV and Schistosoma co-exposure revealed an altered pulmonary immune landscape that could be relevant in the development of pulmonary vascular disease. Thus, it would be interesting to assess in humans exposed to HIV and schistosome those immunological parameters particularly affected by the co-exposure. For instance, analysis of blood cytokines might corroborate the shift from a Type 2 to a pro-inflammatory Type 1/17 cytokine response observed in co-exposed mice, and serve as a marker of progression of pulmonary disease in co-infected humans. Also, as HIV (Tg26) transgenic mice somehow resemble the situation of HIV-infected ART-treated individuals, the information about the pulmonary immunological status in the mouse model could help to understand the susceptibility of these human counterparts to develop pulmonary vascular disease.

11

Bibliography

Bibliography

Abe, K., Toba, M., Alzoubi, A., Ito, M., Fagan, K. A., Cool, C. D., Voelkel, N. F., McMurtry, I. F., & Oka, M. (2010). Formation of plexiform lesions in experimental severe pulmonary arterial hypertension. *Circulation*, *121*(25), 2747–2754. https://doi.org/10.1161/CIRCULATIONAHA.109.927681

Agarwal, S., Sharma, H., Chen, L., & Dhillon, N. K. (2020). NADPH oxidase mediated endothelial injury in HIV and opioid induced pulmonary arterial hypertension. *American Journal of Physiology-Lung Cellular and Molecular Physiology*. https://doi.org/10.1152/ajplung.00480.2019

Almodovar, S. (2014). The complexity of HIV persistence and pathogenesis in the lung under antiretroviral therapy: Challenges beyond AIDS. *Viral Immunology*, *27*(5), 186–199. https://doi.org/10.1089/vim.2013.0130

Almodovar, S., Swanson, J., Giavedoni, L. D., Kanthaswamy, S., Long, C. S., Voelkel, N. F., Edwards, M. G., Folkvord, J. M., Connick, E., Westmoreland, S. V., Luciw, P. A., & Flores, S. C. (2018). Lung Vascular Remodeling, Cardiac Hypertrophy, and Inflammatory Cytokines in SHIVnef-Infected Macaques. *Viral Immunology*, *31*(3), 206–222. https://doi.org/10.1089/vim.2017.0051

Anand, A. R., Rachel, G., & Parthasarathy, D. (2018). HIV Proteins and Endothelial Dysfunction: Implications in Cardiovascular Disease. *Frontiers in Cardiovascular Medicine*, *5*(December), 1–10. https://doi.org/10.3389/fcvm.2018.00185

Arakelyan, A., Petersen, J. D., Blazkova, J., & Margolis, L. (2019). Macrophage-derived HIV-1 carries bioactive TGF-beta. *Scientific Reports*, *9*(1), 19100. https://doi.org/10.1038/s41598-019-55615-8

Bankhead, P., Loughrey, M. B., Fernández, J. A., Dombrowski, Y., McArt, D. G., Dunne, P. D., McQuaid, S., Gray, R. T., Murray, L. J., Coleman, H. G., James, J. A., Salto-Tellez, M.,

& Hamilton, P. W. (2017). QuPath: Open source software for digital pathology image analysis. *Scientific Reports*, *7*(1), 1–7. https://doi.org/10.1038/s41598-017-17204-5

Barber, D. L., Andrade, B. B., Sereti, I., & Sher, A. (2012). *Immune reconstitution inflammatory syndrome: the trouble with immunity when you had none*. https://doi.org/10.1038/nrmicro2712

Barnett, C. F., & Hsue, P. Y. (2013). Human Immunodeficiency Virus-Associated Pulmonary Arterial Hypertension. *Clinics in Chest Medicine*, *34*(2), 283–292. https://doi.org/10.1016/j.ccm.2013.01.009

Barre-Sinoussi, F., Chermann, J. C., Rey, F., Nugeyre, M. T., Chamaret, S., Gruest, J., Dauguet, C., Axler-Blin, C., Vezinet-Brun, F., Rouzioux, C., Rozenbaum, W., & Montagnier, L. (1983). Isolation of a T-lymphotropic retrovirus from a patient at risk for acquired immune deficiency syndrome (AIDS). *Science*, *220*(4599), 868 LP – 871. https://doi.org/10.1126/science.6189183

Basile, D. P., Friedrich, J. L., Spahic, J., Knipe, N., Mang, H., Leonard, E. C., Changizi-Ashtiyani, S., Bacallao, R. L., Molitoris, B. A., & Sutton, T. A. (2011). Impaired endothelial proliferation and mesenchymal transition contribute to vascular rarefaction following acute kidney injury. *American Journal of Physiology - Renal Physiology*, *300*(3). https://doi.org/10.1152/ajprenal.00546.2010

Beshay, S., Sahay, S., & Humbert, M. (2020). Evaluation and management of pulmonary arterial hypertension. *Respiratory Medicine*, *171*, 106099. https://doi.org/10.1016/J.RMED.2020.106099

Bigna, J. J. R., Sime, P. S. D., & Koulla-Shiro, S. (2015). HIV related pulmonary arterial hypertension: Epidemiology in Africa, physiopathology, and role of antiretroviral treatment. *AIDS Research and Therapy*, *12*(1), 1–8. https://doi.org/10.1186/s12981-015-0078-3

Briggs, S. D., Scholtz, B., Jacque, J. M., Swingler, S., Stevenson, M., & Smithgall, T. E. (2001). HIV-1 Nef Promotes Survival of Myeloid Cells by a Stat3-dependent Pathway. *Journal of Biological Chemistry*, *276*(27), 25605–25611. https://doi.org/10.1074/jbc.M103244200

Bruggeman, L. A., Thomson, M. M., Nelson, P. J., Kopp, J. B., Rappaport, J., Klotman, P. E., & Klotman, M. E. (1994). Patterns of HIV-1 mRNA Expression in Transgenic Mice Are Tissue-Dependent. *Virology*, *202*(2), 940–948. https://doi.org/10.1006/viro.1994.1416

Bustinduy, A., King, C., Scott, J., Appleton, S., Sousa-Figueiredo, J. C., Betson, M., & Stothard, J. R. (2014). HIV and schistosomiasis co-infection in African children. *The Lancet Infectious Diseases*, *14*(7), 640–649. https://doi.org/10.1016/S1473-3099(14)70001-5

Butrous, G., Ghofrani, H. A., & Grimminger, F. (2008). Pulmonary vascular disease in the developing world. *Circulation*, *118*(17), 1758–1766. https://doi.org/10.1161/CIRCULATIONAHA.107.727289

Butrous, G. (2015). Human immunodeficiency virus-associated pulmonary arterial hypertension considerations for pulmonary vascular diseases in the developing world. *Circulation*, *131*(15), 1361–1370. https://doi.org/10.1161/CIRCULATIONAHA.114.006978

Butrous, G. (2019). Schistosome infection and its effect on pulmonary circulation. *Global Cardiology Science and Practice*, *2019*(1). https://doi.org/10.21542/gcsp.2019.5

Butrous, G., & Mathie, A. (2019). Infection in pulmonary vascular diseases: Would another consortium really be the way to go? *Global Cardiology Science and Practice*, *2019*(1), 1–5. https://doi.org/10.21542/gcsp.2019.1

Cai, Y., Sugimoto, C., Liu, D. X., Midkiff, C. C., Alvarez, X., Lackner, A. A., Kim, W.-K., Didier, E. S., & Kuroda, M. J. (2015). Increased monocyte turnover is associated with interstitial macrophage accumulation and pulmonary tissue damage in SIV-infected rhesus macaques. *Journal of Leukocyte Biology*, *97*(6), 1147–1153. https://doi.org/10.1189/jlb.4a0914-441r

Calabrese, F., Kipar, A., Lunardi, F., Balestro, E., Perissinotto, E., Rossi, E., Nannini, N., Marulli, G., Stewart, J. P., & Rea, F. (2013). Herpes virus infection is associated with vascular remodeling and pulmonary hypertension in idiopathic pulmonary fibrosis. *PloS One*, *8*(2), e55715. https://doi.org/10.1371/journal.pone.0055715

Caldwell, R. L., Gadipatti, R., Lane, K. B., & Shepherd, V. L. (2006). HIV-1 TAT represses transcription of the bone morphogenic protein receptor-2 in U937 monocytic cells. *Journal of Leukocyte Biology*, *79*(1), 192–201. https://doi.org/10.1189/jlb.0405194

Cha, H., Qin, W., Yang, Q., Xie, H., Qu, J., Wang, M., Chen, D., Wang, F., Dong, N., Chen, L., & Huang, J. (n.d.). Differential pulmonic NK and NKT cell responses in Schistosoma japonicum-infected mice. *Parasitology Research*. https://doi.org/10.1007/s00436-016-5320-y

Chang, J. J., Lacas, A., Lindsay, R. J., Doyle, E. H., Axten, K. L., Pereyra, F., Rosenberg, E. S., Walker, B. D., Allen, T. M., & Altfeld, M. (2012). Differential regulation of toll-like receptor pathways in acute and chronic HIV-1 infection. *Aids*, *26*(5), 533–541. https://doi.org/10.1097/QAD.0b013e32834f3167

Cheever, A. W., Macedonia, J. G., Mosimann, J. E., & Cheever, E. A. (1994). Kinetics of egg production and egg excretion by Schistosoma mansoni and S. japonicum in mice infected with a single pair of worms. *American Journal of Tropical Medicine and Hygiene*, *50*(3), 281–295. https://doi.org/10.4269/ajtmh.1994.50.281

Cheever, A. W., Mosimann, J. E., Deb, S., Cheever, E. A., & Duvall, R. H. (1994). Natural history of Schistosoma mansoni infection in mice: Egg production, egg passage in the feces, and contribution of host and parasite death to changes in worm numbers. *American Journal of Tropical Medicine and Hygiene*, *50*(3), 269–280. https://doi.org/10.4269/ajtmh.1994.50.269

Chelvanambi, S., Bogatcheva, N. V., Bednorz, M., Agarwal, S., Maier, B., Alves, N. J., Li, W., Syed, F., Saber, M. M., Dahl, N., Lu, H., Day, R. B., Smith, P., Jolicoeur, P., Yu, Q., Dhillon, N. K., Weissmann, N., Twigg, H. L., & Clauss, M. (2019). HIV-Nef protein persists in the lungs of aviremic patients with HIV and induces endothelial cell death. *American Journal of Respiratory Cell and Molecular Biology*, *60*(3), 357–366. https://doi.org/10.1165/rcmb.2018-0089OC

Chen, D., Luo, X., Xie, H., Gao, Z., Fang, H., & Huang, J. (2013). Characteristics of IL-17 induction by Schistosoma japonicum infection in C57BL/6 mouse liver. *Immunology*, *139*(4), 523–532. https://doi.org/https://doi.org/10.1111/imm.12105

Cheng, M., & Hu, S. (2017). Lung-resident γδ T cells and their roles in lung diseases. *Immunology*, *151*(4), 375–384. https://doi.org/10.1111/imm.12764

Chrobak, I., Lenna, S., Stawski, L., & Trojanowska, M. (2013). Interferon-γ promotes vascular remodeling in human microvascular endothelial cells by upregulating endothelin (ET)-1 and transforming growth factor (TGF) β2. *Journal of Cellular Physiology*, *228*(8), 1774–1783. https://doi.org/10.1002/jcp.24337

Colley, D. G., & Secor, W. E. (2014). Immunology of human schistosomiasis. *Parasite Immunology*, *36*(8), 347–357. https://doi.org/10.1111/pim.12087

Cooper, A. M. (2009). Cell-mediated immune responses in tuberculosis. *Annual Review of Immunology*, *27*, 393–422. https://doi.org/10.1146/annurev.immunol.021908.132703

Corbi, A. L., Kishimoto, T. K., Miller, L. J., & Springer, T. A. (1988). The human leukocyte adhesion glycoprotein Mac-1 (complement receptor type 3, CD11b) alpha subunit. Cloning, primary structure, and relation to the integrins, von Willebrand factor and factor B. *The Journal of Biological Chemistry*, *263*(25), 12403–12411.

Costiniuk, C. T., Kovacs, C., Routy, J.-P., Singer, J., Gurunathan, S., Sekaly, R.-P., & Angel, J. B. (2012). Short Communication: Human Immunodeficiency Virus Rebound in Blood and Seminal Plasma Following Discontinuation of Antiretroviral Therapy. *AIDS Research and Human Retroviruses*, *29*(2), 266–269. https://doi.org/10.1089/aid.2011.0343

Cota-Gomez, A., Flores, A. C., Ling, X.-F., Varella-Garcia, M., & Flores, S. C. (2011). HIV-1 Tat increases oxidant burden in the lungs of transgenic mice. *Free Radical Biology & Medicine*, *51*(9), 1697–1707. https://doi.org/10.1016/j.freeradbiomed.2011.07.023

Cribbs, S. K., Crothers, K., & Morris, A. (2020a). Pathogenesis of hiv-related lung disease: Immunity, infection, and inflammation. *Physiological Reviews*, *100*(2), 603–632. https://doi.org/10.1152/physrev.00039.2018

Cribbs, S. K., Lennox, J., Caliendo, A. M., Brown, L. A., & Guidot, D. M. (2015). Healthy HIV-1-infected individuals on highly active antiretroviral therapy harbor HIV-1 in their alveolar macrophages. *AIDS Research and Human Retroviruses*, *31*(1), 64–70. https://doi.org/10.1089/AID.2014.0133

Crosby, A., Jones, F. M., Southwood, M., Stewart, S., Schermuly, R., Butrous, G., Dunne, D. W., & Morrell, N. W. (2010). Pulmonary vascular remodeling correlates with lung eggs and cytokines in murine schistosomiasis. *American Journal of Respiratory and Critical Care Medicine*, *181*(3), 279–288. https://doi.org/10.1164/rccm.200903-0355OC

Crothers, K., Huang, L., Goulet, J. L., Goetz, M. B., Brown, S. T., Rodriguez-Barradas, M. C., Oursler, K. K., Rimland, D., Gibert, C. L., Butt, A. A., & Justice, A. C. (2011). HIV infection and risk for incident pulmonary diseases in the combination antiretroviral therapy era. *American Journal of Respiratory and Critical Care Medicine*, *183*(3), 388–395. https://doi.org/10.1164/rccm.201006-0836OC

Dam, V., Microbiology, M., Sciences, H., Foundation, E., Aids, I., Medicine, T., Title, U. K. R., Keywords, U., & Ekii, O. A. (n.d.). *Effect of Schistosoma mansoni Infection on Innate and HIV-1-Specific T-Cell Immune Responses in HIV-1-Infected Ugandan Fisher Folk*. 1–28.

Darwich, L., Coma, G., Peña, R., Bellido, R., Blanco, E. J. J., Este, J. A., Borras, F. E., Clotet, B., Ruiz, L., Rosell, A., Andreo, F., Parkhouse, R. M. E., & Bofill, M. (2009). Secretion of interferon-γ by human macrophages demonstrated at the single-cell level after costimulation with interleukin (IL)-12 plus IL-18. *Immunology*, *126*(3), 386–393. https://doi.org/https://doi.org/10.1111/j.1365-2567.2008.02905.x

Dessein, A., Kouriba, B., Eboumbou, C., Dessein, H., Argiro, L., Marquet, S., Elwali, N. E. M. A., Rodrigues, V., Li, Y., Doumbo, O., & Chevillard, C. (2004). Interleukin-13 in the skin and interferon-γ in the liver are key players in immune protection in human schistosomiasis. *Immunological Reviews*, *201*(4), 180–190. https://doi.org/10.1111/j.0105-2896.2004.00195.x

Dhillon, N. K., Li, F., Xue, B., Tawfik, O., Morgello, S., Buch, S., & Ladner, A. O. B. (2011). Effect of cocaine on human immunodeficiency virus-mediated pulmonary endothelial and smooth muscle dysfunction. *American Journal of Respiratory Cell and Molecular Biology*, *45*(1), 40–52. https://doi.org/10.1165/rcmb.2010-0097OC

Dickie, P., Felser, J., Eckhaus, M., Bryant, J., Silver, J., Marinos, N., & Notkins, A. L. (1991a). HIV-associated nephropathy in transgenic mice expressing HIV-1 genes. *Virology*, *185*(1), 109–119. https://doi.org/10.1016/0042-6822(91)90759-5

Dodd, J., Riffault, S., Kodituwakku, J. S., Hayday, A. C., & Openshaw, P. J. M. (2009). Pulmonary V gamma 4+ gamma delta T cells have proinflammatory and antiviral effects in viral lung disease. *Journal of Immunology (Baltimore, Md. : 1950)*, *182*(2), 1174–1181. https://doi.org/10.4049/jimmunol.182.2.1174

Dolei, A., Serra, C., Arca, M. V, & Toniolo, A. (1992). Acute HIV-1 infection of CD4+ human lung fibroblasts. In *AIDS (London, England)* (Vol. 6, Issue 2, pp. 232–234).

Duan, M., Steinfort, D. P., Smallwood, D., Hew, M., Chen, W., Ernst, M., Irving, L. B., Anderson, G. P., & Hibbs, M. L. (2016). CD11b immunophenotyping identifies inflammatory profiles in the mouse and human lungs. *Mucosal Immunology*, *9*(2), 550–563. https://doi.org/10.1038/mi.2015.84

Duffy, P., Wang, X., Lin, P. H., Yao, Q., & Chen, C. (2009). HIV Nef Protein Causes Endothelial Dysfunction in Porcine Pulmonary Arteries and Human Pulmonary Artery Endothelial Cells1. *Journal of Surgical Research*, *156*(2), 257–264. https://doi.org/10.1016/j.jss.2009.02.005

Dunne, P. J., Maher, C. O., Freeley, M., Dunne, K., Petrasca, A., Orikiiriza, J., Dunne, M. R., Reidy, D., O'Dea, S., Loy, A., Woo, J., Long, A., Rogers, T. R., Mulcahy, F., & Doherty, D. G. (2018). CD3ε Expression defines functionally distinct subsets of Vδ1 T cells in patients with human immunodeficiency virus infection. *Frontiers in Immunology*, *9*(MAY). https://doi.org/10.3389/fimmu.2018.00940

Ehrenreich, H., Rieckmann, P., Sinowatz, F., Weih, K. A., Arthur, L. O., Goebel, F. D., Burd, P. R., Coligan, J. E., & Clouse, K. A. (1993). Potent stimulation of monocytic endothelin-1 production by HIV-1 glycoprotein 120. *The Journal of Immunology*, *150*(10), 4601 LP – 4609. http://www.jimmunol.org/content/150/10/4601.abstract

Ehrlich, M., Gutman, O., Knaus, P., & Henis, Y. I. (2012). Oligomeric interactions of TGF-β and BMP receptors. *FEBS Letters*, *586*(14), 1885–1896. https://doi.org/10.1016/J.FEBSLET.2012.01.040

El Hentati, F. Z., Gruy, F., Iobagiu, C., & Lambert, C. (2010). Variability of CD3 membrane expression and T cell activation capacity. *Cytometry Part B - Clinical Cytometry*, *78*(2), 105–114. https://doi.org/10.1002/cyto.b.20496

El Ridi, R., Wagih, A., Salem, R., Mahana, N., El Demellawy, M., & Tallima, H. (2006). Impact of interleukin-1 and interleukin-6 in murine primary schistosomiasis. *International Immunopharmacology*, *6*(7), 1100–1108. https://doi.org/10.1016/j.intimp.2006.01.021

Eming, S. A., Wynn, T. A., & Martin, P. (2017). Inflammation and metabolism in tissue repair and regeneration. *Science (New York, N.Y.)*, *356*(6342), 1026—1030. https://doi.org/10.1126/science.aam7928

Everts, B., Hussaarts, L., Driessen, N. N., Meevissen, M. H. J., Schramm, G., van der Ham, A. J., van der Hoeven, B., Scholzen, T., Burgdorf, S., Mohrs, M., Pearce, E. J., Hokke, C. H., Haas, H., Smits, H. H., & Yazdanbakhsh, M. (2012). Schistosome-derived omega-1 drives Th2 polarization by suppressing protein synthesis following internalization by the mannose receptor. *Journal of Experimental Medicine*, *209*(10), 1753–1767. https://doi.org/10.1084/jem.20111381

Fallon, P. G., Richardson, E. J., McKenzie, G. J., & McKenzie, A. N. J. (2000). Schistosome Infection of Transgenic Mice Defines Distinct and Contrasting Pathogenic Roles for IL-4 and IL-13: IL-13 Is a Profibrotic Agent. *The Journal of Immunology*, *164*(5), 2585–2591. https://doi.org/10.4049/jimmunol.164.5.2585

Farber, H. W., & Loscalzo, J. (2004). Pulmonary arterial hypertension. *The New England Journal of Medicine*, *351*(16), 1655–1665. https://doi.org/10.1056/NEJMra035488

Feng, Y., Broder, C. C., Kennedy, P. E., & Berger, E. A. (1996). HIV-1 Entry Cofactor: Functional cDNA Cloning of a Seven-Transmembrane, G Protein-Coupled Receptor. *Science*, *272*(5263), 872 LP – 877. https://doi.org/10.1126/science.272.5263.872

Fenton, M. J., Vermeulen, M. W., Kim, S., Burdick, M., Strieter, R. M., & Kornfeld, H. (2021). Induction of gamma interferon production in human alveolar macrophages by Mycobacterium tuberculosis. *Infection and Immunity*, *65*(12), 5149–5156. https://doi.org/10.1128/iai.65.12.5149-5156.1997

Fernandes, J. S., Araujo, M. I., Lopes, D. M., Da Paixão De Souza, R., Carvalho, E. M., & Santos Cardoso, L. (2014). *Monocyte Subsets in Schistosomiasis Patients with Periportal Fibrosis*. https://doi.org/10.1155/2014/703653

Finzi, D., Hermankova, M., Pierson, T., Carruth, L. M., Buck, C., Chaisson, R. E., Quinn, T. C., Chadwick, K., Margolick, J., Brookmeyer, R., Gallant, J., Markowitz, M., Ho, D. D., Richman, D. D., & Siliciano, R. F. (1997). Identification of a reservoir for HIV-1 in patients on highly active antiretroviral therapy. *Science (New York, N.Y.)*, *278*(5341), 1295–1300. https://doi.org/10.1126/science.278.5341.1295

Gallo, R. C., Sarin, P. S., Gelmann, E. P., Robert-Guroff, M., Richardson, E., Kalyanaraman, V. S., Mann, D., Sidhu, G. D., Stahl, R. E., Zolla-Pazner, S., Leibowitch, J., & Popovic, M. (1983). Isolation of human T-cell leukemia virus in acquired immune deficiency syndrome (AIDS). *Science*, *220*(4599), 865 LP – 867. https://doi.org/10.1126/science.6601823

Gelfand, M. (1948). *A clinico-pathological study of schistosomiasis in South Central Africa*.

Gharavi, A. G., Ahmad, T., Wong, R. D., Hooshyar, R., Vaughn, J., Oller, S., Frankel, R. Z., Bruggeman, L. A., D'Agati, V. D., Klotman, P. E., & Lifton, R. P. (2004). Mapping a locus for susceptibility to HIV-1-associated nephropathy to mouse chromosome 3. *Proceedings of the National Academy of Sciences of the United States of America*, *101*(8), 2488–2493. https://doi.org/10.1073/pnas.0308649100

Gobbi, F., Tamarozzi, F., Buonfrate, D., van Lieshout, L., Bisoffi, Z., & Bottieau, E. (2020). New Insights on Acute and Chronic Schistosomiasis: Do We Need a Redefinition? *Trends in Parasitology*, *36*(8), 660–667. https://doi.org/10.1016/J.PT.2020.05.009

Goldthorpe, H., Jiang, J. Y., Taha, M., Deng, Y., Sinclair, T., Ge, C. X., Jurasz, P., Turksen, K., Mei, S. H. J., & Stewart, D. J. (2015). Occlusive lung arterial lesions in endothelial-targeted, fas-induced apoptosis transgenic mice. *American Journal of Respiratory Cell and Molecular Biology*, *53*(5), 712–718. https://doi.org/10.1165/rcmb.2014-0311OC

Gomez-Arroyo, J., Saleem, S. J., Mizuno, S., Syed, A. A., Bogaard, H. J., Abbate, A., Taraseviciene-Stewart, L., Sung, Y., Kraskauskas, D., Farkas, D., Conrad, D. H., Nicolls, M. R., & Voelkel, N. F. (2012). A brief overview of mouse models of pulmonary arterial hypertension: Problems and prospects. *American Journal of Physiology - Lung Cellular and Molecular Physiology*, *302*(10). https://doi.org/10.1152/ajplung.00362.2011

Gong, J. L., McCarthy, K. M., Rogers, R. A., & Schneeberger, E. E. (1994). Interstitial lung macrophages interact with dendritic cells to present antigenic peptides derived from particulate antigens to T cells. *Immunology*, *81*(3), 343–351.

Good, R. B., Gilbane, A. J., Trinder, S. L., Denton, C. P., Coghlan, G., Abraham, D. J., & Holmes, A. M. (2015). Endothelial to Mesenchymal Transition Contributes to Endothelial Dysfunction in Pulmonary Arterial Hypertension. *American Journal of Pathology*, *185*(7), 1850–1858. https://doi.org/10.1016/j.ajpath.2015.03.019

Goujard, C., Emilie, D., Roussillon, C., Godot, V., Rouzioux, C., Venet, A., Colin, C., Pialoux, G., Girard, P. M., Boilet, V., Chaix, M. L., Galanaud, P., & Chene, G. (2012). Continuous versus intermittent treatment strategies during primary HIV-1 infection: The randomized ANRS INTERPRIM Trial. *Aids*, *26*(15), 1895–1905. https://doi.org/10.1097/QAD.0b013e32835844d9

Graham, B. B., Chabon, J., Gebreab, L., Poole, J., Debella, E., Davis, L., Tanaka, T., Sanders, L., Dropcho, N., Bandeira, A., Vandivier, R. W., Champion, H. C., Butrous, G., Wang, X. J., Wynn, T. A., & Tuder, R. M. (2013). Transforming growth factor-β signaling promotes pulmonary hypertension caused by schistosoma mansoni. *Circulation*, *128*(12), 1354–1364. https://doi.org/10.1161/CIRCULATIONAHA.113.003072

Graham, B. B., Mentink-Kane, M. M., El-Haddad, H., Purnell, S., Zhang, L., Zaiman, A., Redente, E. F., Riches, D. W. H., Hassoun, P. M., Bandeira, A., Champion, H. C., Butrous,

G., Wynn, T. A., & Tuder, R. M. (2010). Schistosomiasis-induced experimental pulmonary hypertension: Role of interleukin-13 signaling. *American Journal of Pathology*, *177*(3), 1549–1561. https://doi.org/10.2353/ajpath.2010.100063

Grant, E. J., Nüssing, S., Sant, S., Clemens, E. B., & Kedzierska, K. (2017). The role of CD27 in anti-viral T-cell immunity. *Current Opinion in Virology*, *22*, 77–88. https://doi.org/10.1016/j.coviro.2016.12.001

Green, L. A., Yi, R., Petrusca, D., Wang, T., Elghouche, A., Gupta, S. K., Petrache, I., & Clauss, M. (2014). HIV envelope protein gp120-induced apoptosis in lung microvascular endothelial cells by concerted upregulation of EMAP II and its receptor, CXCR3. *American Journal of Physiology - Lung Cellular and Molecular Physiology*, *306*(4), 372–382. https://doi.org/10.1152/ajplung.00193.2013

Grégoire, C., Chasson, L., Luci, C., Tomasello, E., Geissmann, F., Vivier, E., & Walzer, T. (2007). The trafficking of natural killer cells. *Immunological Reviews*, *220*(1), 169–182. https://doi.org/https://doi.org/10.1111/j.1600-065X.2007.00563.x

Haas, J. D., González, F. H. M., Schmitz, S., Chennupati, V., Föhse, L., Kremmer, E., Förster, R., & Prinz, I. (2009). CCR6 and NK1.1 distinguish between IL-17A and IFN-γ-producing γδ effector T cells. *European Journal of Immunology*, *39*(12), 3488–3497. https://doi.org/https://doi.org/10.1002/eji.200939922

Hasegawa, A., Liu, H., Ling, B., Borda, J. T., Alvarez, X., Sugimoto, C., Vinet-Oliphant, H., Kim, W. K., Williams, K. C., Ribeiro, R. M., Lackner, A. A., Veazey, R. S., & Kuroda, M. J. (2009). The level of monocyte turnover predicts disease progression in the macaque model of AIDS. *Blood*, *114*(14), 2917–2925. https://doi.org/10.1182/blood-2009-02-204263

Hashimoto-Kataoka, T., Hosen, N., Sonobe, T., Arita, Y., Yasui, T., Masaki, T., Minami, M., Inagaki, T., Miyagawa, S., Sawa, Y., Murakami, M., Kumanogoh, A., Yamauchi-Takihara, K., Okumura, M., Kishimoto, T., Komuro, I., Shirai, M., Sakata, Y., & Nakaoka, Y. (2015). Interleukin-6/interleukin-21 signaling axis is critical in the pathogenesis of pulmonary arterial hypertension. *Proceedings of the National Academy of Sciences of the United States of America*, *112*(20), E2677-86. https://doi.org/10.1073/pnas.1424774112

Hautefort, A., Girerd, B., Montani, D., Cohen-Kaminsky, S., Price, L., Lambrecht, B. N., Humbert, M., & Perros, F. (2015). T-helper 17 cell polarization in pulmonary arterial hypertension. *Chest*, *147*(6), 1610–1620. https://doi.org/10.1378/chest.14-1678

Helming, L., & Gordon, S. (2008). The molecular basis of macrophage fusion. *Immunobiology*, *212*(9–10), 785–793. https://doi.org/10.1016/j.imbio.2007.09.012

Honeycutt, J. B., Thayer, W. O., Baker, C. E., Ribeiro, R. M., Lada, S. M., Cao, Y., Cleary, R. A., Hudgens, M. G., Richman, D. D., & Garcia, J. V. (2017). HIV persistence in tissue

macrophages of humanized myeloid-only mice during antiretroviral therapy. *Nature Publishing Group*, *23*. https://doi.org/10.1038/nm.4319

Horiike, M., Iwami, S., Kodama, M., Sato, A., Watanabe, Y., Yasui, M., Ishida, Y., Kobayashi, T., Miura, T., & Igarashi, T. (2012). Lymph nodes harbor viral reservoirs that cause rebound of plasma viremia in SIV-infected macaques upon cessation of combined antiretroviral therapy. *Virology*, *423*(2), 107–118. https://doi.org/10.1016/J.VIROL.2011.11.024

Humbert, M., Guignabert, C., Bonnet, S., Dorfmüller, P., Klinger, J. R., Nicolls, M. R., Olschewski, A. J., Pullamsetti, S. S., Schermuly, R. T., Stenmark, K. R., & Rabinovitch, M. (2019). Pathology and pathobiology of pulmonary hypertension: state of the art and research perspectives. *The European Respiratory Journal*, *53*(1). https://doi.org/10.1183/13993003.01887-2018

Jambo, K. C., Sepako, E., Fullerton, D. G., Mzinza, D., Glennie, S., Wright, A. K., Heyderman, R. S., & Gordon, S. B. (2011). Bronchoalveolar CD4+ T cell responses to respiratory antigens are impaired in HIV-infected adults. *Thorax*, *66*(5), 375–382. https://doi.org/10.1136/thx.2010.153825

James, C. O., Huang, M.-B., Khan, M., Garcia-Barrio, M., Powell, M. D., & Bond, V. C. (2004). Extracellular Nef protein targets CD4+ T cells for apoptosis by interacting with CXCR4 surface receptors. *Journal of Virology*, *78*(6), 3099–3109. https://doi.org/10.1128/jvi.78.6.3099-3109.2004

Jerebtsova, M., Ahmad, A., Niu, X., Rutagarama, O., & Nekhai, S. (2020). HIV-1 transcription inhibitor 1E7-03 restores LPS-induced alteration of lung leukocytes' infiltration dynamics and resolves inflammation in HIV transgenic mice. *Viruses*, *12*(2). https://doi.org/10.3390/v12020204

Joint United Nations Programme on HIV/AIDS (UNAIDS). (2019). AIDS data 2019. *Science*, *268*(5209), 350–350.

Joyce, K. L., Morgan, W., Greenberg, R., & Nair, M. G. (2012). Using eggs from Schistosoma mansoni as an in vivo model of helminth-induced lung inflammation. *Journal of Visualized Experiments*, *64*, 1. https://doi.org/10.3791/3905

Kanmogne, G. D., Primeaux, C., & Grammas, P. (2005). Induction of apoptosis and endothelin-1 secretion in primary human lung endothelial cells by HIV-1 gp120 proteins. *Biochemical and Biophysical Research Communications*, *333*(4), 1107–1115. https://doi.org/10.1016/J.BBRC.2005.05.198

Khan, S. Q., Khan, I., & Gupta, V. (2018). CD11b Activity Modulates Pathogenesis of Lupus Nephritis. *Frontiers in Medicine*, *5*, 52. https://doi.org/10.3389/fmed.2018.00052

Kilkenny, C., Browne, W., Cuthill, I. C., Emerson, M., & Altman, D. G. (2010). Animal research: Reporting in vivo experiments: The ARRIVE guidelines. *British Journal of Pharmacology*, *160*(7), 1577–1579. https://doi.org/10.1111/j.1476-5381.2010.00872.x

Kirby, A. C., Newton, D. J., Carding, S. R., & Kaye, P. M. (2007). Evidence for the involvement of lung-specific γδ T cell subsets in local responses to Streptococcus pneumoniae infection. *European Journal of Immunology*, *37*(12), 3404–3413. https://doi.org/10.1002/eji.200737216

Kline, E. R., & Sutliff, R. L. (2008). The Roles of HIV-1 Proteins and Antiretroviral Drug Therapy in HIV-1-Associated Endothelial Dysfunction. *Journal of Investigative Medicine*, *56*(5), 752 LP – 769. https://doi.org/10.1097/JIM.0b013e3181788d15

Knafl, D., Gerges, C., King, C. H., Humbert, M., & Bustinduy, A. L. (2020). Schistosomiasis-associated pulmonary arterial hypertension: A systematic review. *European Respiratory Review*, *29*(155). https://doi.org/10.1183/16000617.0089-2019

Knox, K. S., Vinton, C., Hage, C. A., Kohli, L. M., Twigg, H. L., Klatt, N. R., Zwickl, B., Waltz, J., Goldman, M., Douek, D. C., & Brenchley, J. M. (2010). Reconstitution of CD4 T Cells in Bronchoalveolar Lavage Fluid after Initiation of Highly Active Antiretroviral Therapy. *Journal of Virology*, *84*(18), 9010–9018. https://doi.org/10.1128/jvi.01138-10

Kumar, R., Mickael, C., Chabon, J., Gebreab, L., Rutebemberwa, A., Garcia, A. R., Koyanagi, D. E., Sanders, L., Gandjeva, A., Kearns, M. T., Barthel, L., Janssen, W. J., Mauad, T., Bandeira, A., Schmidt, E., Tuder, R. M., & Graham, B. B. (2015). The causal role of IL-4 and IL-13 in schistosoma mansoni pulmonary hypertension. *American Journal of Respiratory and Critical Care Medicine*, *192*(8), 998–1008. https://doi.org/10.1164/rccm.201410-1820OC

Kumar, R., Mickael, C., Kassa, B., Gebreab, L., Robinson, J. C., Koyanagi, D. E., Sanders, L., Barthel, L., Meadows, C., Fox, D., Irwin, D., Li, M., McKeon, B. A., Riddle, S., Dale Brown, R., Morgan, L. E., Evans, C. M., Hernandez-Saavedra, D., Bandeira, A., … Graham, B. B. (2017). TGF-β activation by bone marrow-derived thrombospondin-1 causes Schistosoma- and hypoxia-induced pulmonary hypertension. *Nature Communications*, *8*, 15494. https://doi.org/10.1038/ncomms15494

Kumar, R., Mickael, C., Kassa, B., Sanders, L., Koyanagi, D., Hernandez-Saavedra, D., Freeman, S., Morales-Cano, D., Cogolludo, A., McKee, A. S., Fontenot, A. P., Butrous, G., Tuder, R. M., & Graham, B. B. (2019a). Th2 CD4+ T Cells Are Necessary and Sufficient for Schistosoma-Pulmonary Hypertension. *Journal of the American Heart Association*, *8*(15). https://doi.org/10.1161/JAHA.119.013111

Kumar, R., Mickael, C., Kassa, B., Sanders, L., Koyanagi, D., Hernandez-Saavedra, D., Freeman, S., Morales-Cano, D., Cogolludo, A., McKee, A. S., Fontenot, A. P., Butrous, G., Tuder, R. M., & Graham, B. B. (2019b). Th2 CD4(+) T Cells Are Necessary and Sufficient for Schistosoma-Pulmonary Hypertension. *Journal of the American Heart Association*, *8*(15), e013111. https://doi.org/10.1161/JAHA.119.013111

Lawn, S. D., Wainwright, H., & Orrell, C. (2009). Fatal unmasking tuberculosis immune reconstitution disease with bronchiolitis obliterans organizing pneumonia: The role of macrophages. *Aids*, *23*(1), 143–145. https://doi.org/10.1097/QAD.0b013e32831d2a98

Leite Pereira, A., Tchitchek, N., Lambotte, O., Le Grand, R., & Cosma, A. (2019). Characterization of Leukocytes From HIV-ART Patients Using Combined Cytometric Profiles of 72 Cell Markers. *Frontiers in Immunology*, *10*, 1777. https://doi.org/10.3389/fimmu.2019.01777

Linke, M., Pham, H. T. T., Katholnig, K., Schnöller, T., Miller, A., Demel, F., Schütz, B., Rosner, M., Kovacic, B., Sukhbaatar, N., Niederreiter, B., Blüml, S., Kuess, P., Sexl, V., Müller, M., Mikula, M., Weckwerth, W., Haschemi, A., Susani, M., … Weichhart, T. (2017). Chronic signaling via the metabolic checkpoint kinase mTORC1 induces macrophage granuloma formation and marks sarcoidosis progression. *Nature Immunology*, *18*(3), 293–302. https://doi.org/10.1038/ni.3655

Lo Re, S., Dumoutier, L., Couillin, I., Van Vyve, C., Yakoub, Y., Uwambayinema, F., Marien, B., van den Brûle, S., Van Snick, J., Uyttenhove, C., Ryffel, B., Renauld, J.-C., Lison, D., & Huaux, F. (2010). IL-17A-producing gammadelta T and Th17 lymphocytes mediate lung inflammation but not fibrosis in experimental silicosis. *Journal of Immunology (Baltimore, Md. : 1950)*, *184*(11), 6367–6377. https://doi.org/10.4049/jimmunol.0900459

Lu, H., Li, D.-J., Jin, L.-P., & Li-Ping Jin, C. (2017). *γδT Cells and Related Diseases*. https://doi.org/10.1111/aji.12495

Luger, D., Silver, P. B., Tang, J., Cua, D., Chen, Z., Iwakura, Y., Bowman, E. P., Sgambellone, N. M., Chan, C.-C., & Caspi, R. R. (2008). Either a Th17 or a Th1 effector response can drive autoimmunity: conditions of disease induction affect dominant effector category. *The Journal of Experimental Medicine*, *205*(4), 799–810. https://doi.org/10.1084/jem.20071258

Machado, R. D., Pauciulo, M. W., Thomson, J. R., Lane, K. B., Morgan, N. V., Wheeler, L., Phillips, J. A., Newman, J., Loyd, J. E., Galieè, N., Manes, A., McNeil, K., Yacoub, M., Mikhail, G., Rogers, P., Corris, P., Humbert, M., Martensson, G., Tranebjaerg, L., … Nichols, W. C. (2001). BMPR2 Haploinsufficiency as the Inherited Molecular Mechanism for Primary Pulmonary Hypertension. *The American Journal of Human Genetics*, *68*(1), 92–102. https://doi.org/10.1086/316947

Maddon, P. J., Dalgleish, A. G., McDougal, J. S., Clapham, P. R., Weiss, R. A., & Axel, R. (1986). The T4 gene encodes the AIDS virus receptor and is expressed in the immune system and the brain. *Cell*, *47*(3), 333–348. https://doi.org/10.1016/0092-8674(86)90590-8

Madsen, J., Gaiha, G. D., Palaniyar, N., Dong, T., Mitchell, D. A., & Clark, H. W. (2013). *Surfactant Protein D Modulates HIV Infection of Both T-Cells and Dendritic Cells*. https://doi.org/10.1371/journal.pone.0059047

Marecki, J. C., Cool, C. D., Parr, J. E., Beckey, V. E., Luciw, P. A., Tarantal, A. F., Carville, A., Shannon, R. P., Cota-Gomez, A., Tuder, R. M., Voelkel, N. F., & Flores, S. C. (2006). HIV-1 nef is associated with complex pulmonary vascular lesions in SHIV-nef-infected macaques. *American Journal of Respiratory and Critical Care Medicine*, *174*(4), 437–445. https://doi.org/10.1164/rccm.200601-005OC

Marsh, L. M., Jandl, K., Grünig, G., Foris, V., Bashir, M., Ghanim, B., Klepetko, W., Olschewski, H., Olschewski, A., & Kwapiszewska, G. (2018). The inflammatory cell landscape in the lungs of patients with idiopathic pulmonary arterial hypertension. *European Respiratory Journal*, *51*(1). https://doi.org/10.1183/13993003.01214-2017

Marts, L. T., Guidot, D. M., & Sueblinvong, V. (2019). HIV-1 Protein gp120 Induces Mouse Lung Fibroblast-to-Myofibroblast Transdifferentiation via CXCR4 Activation. *American Journal of the Medical Sciences*, *357*(6), 483–491. https://doi.org/10.1016/j.amjms.2019.03.006

Masse-Ranson, G., Mouquet, H., & Di Santo, J. P. (2018). Humanized mouse models to study pathophysiology and treatment of HIV infection. *Current Opinion in HIV and AIDS*, *13*(2), 143–151. https://doi.org/10.1097/COH.0000000000000440

Maston, L. D., Jones, D. T., Giermakowska, W., Howard, T. A., Cannon, J. L., Wang, W., Wei, Y., Xuan, W., Resta, T. C., & Gonzalez Bosc, L. V. (2017). Central role of T helper 17 cells in chronic hypoxia-induced pulmonary hypertension. *American Journal of Physiology. Lung Cellular and Molecular Physiology*, *312*(5), L609–L624. https://doi.org/10.1152/ajplung.00531.2016

Mavilio, D., Benjamin, J., Daucher, M., Lombardo, G., Kottilil, S., Planta, M. A., Marcenaro, E., Bottino, C., Moretta, L., Moretta, A., & Fauci, A. S. (2003). Natural killer cells in HIV-1 infection: Dichotomous effects of viremia on inhibitory and activating receptors and their functional correlates. *Proceedings of the National Academy of Sciences*, *100*(25), 15011 LP – 15016. https://doi.org/10.1073/pnas.2336091100

Merad, M., Sathe, P., Helft, J., Miller, J., & Mortha, A. (2013). *The Dendritic Cell Lineage: Ontogeny and Function of Dendritic Cells and Their Subsets in the Steady State and the Inflamed Setting*. https://doi.org/10.1146/annurev-immunol-020711-074950

Mi, S., Li, Z., Yang, H.-Z., Liu, H., Wang, J.-P., Ma, Y.-G., Wang, X.-X., Liu, H.-Z., Sun, W., & Hu, Z.-W. (2011). Blocking IL-17A Promotes the Resolution of Pulmonary Inflammation and Fibrosis Via TGF-β1–Dependent and –Independent Mechanisms. *The Journal of Immunology*, *187*(6), 3003–3014. https://doi.org/10.4049/jimmunol.1004081

Mikulak, J., Oriolo, F., Zaghi, E., Di Vito, C., & Mavilio, D. (2017). Natural killer cells in HIV-1 infection and therapy. In *Aids* (Vol. 31, Issue 17). https://doi.org/10.1097/QAD.0000000000001645

Misharin, A. V., Morales-Nebreda, L., Mutlu, G. M., Budinger, G. R. S., & Perlman, H. (2013). Flow cytometric analysis of macrophages and dendritic cell subsets in the mouse lung. *American Journal of Respiratory Cell and Molecular Biology*, *49*(4), 503–510. https://doi.org/10.1165/rcmb.2013-0086MA

Moir, S., Malaspina, A., Ho, J., Wang, W., DiPoto, A. C., O'Shea, M. A., Roby, G., Mican, J. A. M., Kottilil, S., Chun, T. W., Proschan, M. A., & Fauci, A. S. (2008). Normalization of B cell counts and subpopulations after antiretroviral therapy in chronic HIV disease. *Journal of Infectious Diseases*, *197*(4), 572–579. https://doi.org/10.1086/526789

Mondejar-Parreño, G., Morales-Cano, D., Barreira, B., Callejo, M., Ruiz-Cabello, X. J., Moreno, L., Esquivel-Ruiz, S., Mathie, A., Butrous, G., Perez-Vizcaino, F., & Cogolludo, A. (2018). HIV transgene expression impairs K+ channel function in the pulmonary vasculature. *American Journal of Physiology - Lung Cellular and Molecular Physiology*, *315*(5), L711–L723. https://doi.org/10.1152/ajplung.00045.2018

Moreno, J. L., Mikhailenko, I., Tondravi, M. M., & Keegan, A. D. (2007). IL-4 promotes the formation of multinucleated giant cells from macrophage precursors by a STAT6-dependent, homotypic mechanism: contribution of E-cadherin. *Journal of Leukocyte Biology*, *82*(6), 1542–1553. https://doi.org/10.1189/jlb.0107058

Morris, A., Gingo, M. R., George, M. P., Lucht, L., Kessinger, C., Singh, V., Hillenbrand, M., Busch, M., McMahon, D., Norris, K. A., Champion, H. C., Gladwin, M. T., Zhang, Y., Steele, C., & Sciurba, F. C. (2012). Cardiopulmonary function in individuals with HIV infection in the antiretroviral therapy era. *AIDS (London, England)*, *26*(6), 731–740. https://doi.org/10.1097/QAD.0b013e32835099ae

Mutapi, F., Winborn, G., Midzi, N., Taylor, M., Mduluza, T., & Maizels, R. M. (2007). Cytokine responses to Schistosoma haematobium in a Zimbabwean population: Contrasting profiles for IFN-γ, IL-4, IL-5 and IL-10 with age. *BMC Infectious Diseases*, *7*, 1–11. https://doi.org/10.1186/1471-2334-7-139

Mwale, A., Hummel, A., Mvaya, L., Kamng'ona, R., Chimbayo, E., Phiri, J., Malamba, R., Kankwatira, A., Mwandumba, H. C., & Jambo, K. C. (2017). B cell, CD8+ T cell and gamma delta T cell lymphocytic alveolitis alters alveolar immune cell homeostasis in HIV-infected Malawian adults. *Wellcome Open Research*, *2*, 105. https://doi.org/10.12688/wellcomeopenres.12869.1

Ndeffo Mbah, M., Poolman, E. M., Drain, P. K., Coffee, M. P., Werf, M. J. van der, & GalvaniMartial, and A. P. (2016). HIV prevalence correlates with Schistosoma haematobium in sub-Saharan Africa. *Trop Med Int Health*, *18*(10), 1174–1179. https://doi.org/10.1111/tmi.12165.HIV

Neff, C. P., Chain, J. L., MaWhinney, S., Martin, A. K., Linderman, D. J., Flores, S. C., Campbell, T. B., Palmer, B. E., & Fontenot, A. P. (2014). Lymphocytic Alveolitis Is Associated with the Accumulation of Functionally Impaired HIV-Specific T Cells in the Lung of Antiretroviral Therapy–Naive Subjects. *American Journal of Respiratory and Critical Care Medicine*, *191*(4), 464–473. https://doi.org/10.1164/rccm.201408-1521OC

Nelwan, M. L. (2019). Schistosomiasis: Life Cycle, Diagnosis, and Control. In *Current Therapeutic Research - Clinical and Experimental* (Vol. 91, pp. 5–9). Excerpta Medica Inc. https://doi.org/10.1016/j.curtheres.2019.06.001

Pagán, A. J., & Ramakrishnan, L. (2018). The Formation and Function of Granulomas. *Annual Review of Immunology*, *36*, 639–665. https://doi.org/10.1146/annurev-immunol-032712-100022

Paget, C., Chow, M. T., Gherardin, N. A., Beavis, P. A., Uldrich, A. P., Duret, H., Hassane, M., Souza-Fonseca-Guimaraes, F., Mogilenko, D. A., Staumont-Sallé, D., Escalante, N. K., Hill, G. R., Neeson, P., Ritchie, D. S., Dombrowicz, D., Mallevaey, T., Trottein, F., Belz, G. T., Godfrey, D. I., & Smyth, M. J. (2015). CD3 bright signals on γδ T cells identify IL-17A-producing Vγ6Vδ1+T cells. *Immunology and Cell Biology*, *93*(2), 198–212. https://doi.org/10.1038/icb.2014.94

Paladugu, R., Fu, W., Conklin, B. S., Lin, P. H., Lumsden, A. B., Yao, Q., Chen, C., & Geary, R. (2003). HIV Tat protein causes endothelial dysfunction in porcine coronary arteries. *Journal of Vascular Surgery*, *38*(3), 549–555. https://doi.org/10.1016/S0741-5214(03)00770-5

Pearce, E. J. (2005). Priming of the immune response by schistosome eggs. *Parasite Immunology*, *27*(7–8), 265–270. https://doi.org/10.1111/j.1365-3024.2005.00765.x

Pearce, E. J., Cheever, A., Leonard, S., Covalesky, M., Fernandez-Botran, R., Kohler, G., & Kopf, M. (1996). Schistosoma mansoni in IL-4-deficient mice. *International Immunology*, *8*(4), 435–444. https://doi.org/10.1093/intimm/8.4.435

Perros, F., Cohen-Kaminsky, S., Gambaryan, N., Girerd, B., Raymond, N., Klingelschmitt, I., Huertas, A., Mercier, O., Fadel, E., Simonneau, G., Humbert, M., Dorfmüller, P., & Montani, D. (n.d.). *Cytotoxic Cells and Granulysin in Pulmonary Arterial Hypertension and Pulmonary Veno-occlusive Disease*. https://doi.org/10.1164/rccm.201208-1364OC

Popescu, I., Drummond, M. B., Gama, L., Lambert, A., Hoji, A., Coon, T., Merlo, C. A., Wise, R. A., Keruly, J., Clements, J. E., Kirk, G. D., & McDyer, J. F. (2016). HIV suppression restores the lung mucosal CD4+ T-cell viral immune response and resolves CD8+ T-cell alveolitis in patients at risk for HIV-associated chronic obstructive pulmonary disease. *Journal of Infectious Diseases*, *214*(10), 1520–1530. https://doi.org/10.1093/infdis/jiw422

Porter, K. M., Walp, E. R., Elms, S. C., Raynor, R., Mitchell, P. O., Guidot, D. M., & Sutliff, R. L. (2013). Human immunodeficiency virus-1 transgene expression increases pulmonary vascular

resistance and exacerbates hypoxia-induced pulmonary hypertension development. *Pulmonary Circulation*, *3*(1), 58–67. https://doi.org/10.4103/2045-8932.109915

Qiao, X., He, B., Chiu, A., Knowles, D. M., Chadburn, A., & Cerutti, A. (2006). Human immunodeficiency virus 1 Nef suppresses CD40-dependent immunoglobulin class switching in bystander B cells. *Nature Immunology*, *7*(3), 302–310. https://doi.org/10.1038/ni1302

Rabinovitch, M., Guignabert, C., Humbert, M., & Nicolls, M. R. (2014). Inflammation and immunity in the pathogenesis of pulmonary arterial hypertension. *Circulation Research*, *115*(1), 165–175. https://doi.org/10.1161/CIRCRESAHA.113.301141

Rijavec, M., Volarevic, S., Osolnik, K., & Kosnik, M. (2011). Natural killer T cells in pulmonary disorders. *Respiratory Medicine*, *105*, S20–S25. https://doi.org/10.1016/S0954-6111(11)70006-3

Ritter, M., Gross, O., Kays, S., Ruland, J., Nimmerjahn, F., Saijo, S., Tschopp, J., Layland, L. E., & Da Costa, C. P. (2010). Schistosoma mansoni triggers Dectin-2, which activates the Nlrp3 inflammasome and alters adaptive immune responses. *Proceedings of the National Academy of Sciences of the United States of America*, *107*(47), 20459–20464. https://doi.org/10.1073/pnas.1010337107

Rodero, M. P., Poupel, L., Loyher, P.-L., Hamon, P., Licata, F., Pessel, C., Hume, D. A., Combadì Ere, C., & Boissonnas, A. (n.d.). *Immune surveillance of the lung by migrating tissue monocytes*. https://doi.org/10.7554/eLife.07847.001

Sakao, S., Tatsumi, K., & Voelkel, N. F. (2009). Endothelial cells and pulmonary arterial hypertension: Apoptosis, proliferation, interaction and transdifferentiation. *Respiratory Research*, *10*, 1–9. https://doi.org/10.1186/1465-9921-10-95

Satoh, T., Nakagawa, K., Sugihara, F., Kuwahara, R., Ashihara, M., Yamane, F., Minowa, Y., Fukushima, K., Ebina, I., Yoshioka, Y., Kumanogoh, A., & Akira, S. (2017). Identification of an atypical monocyte and committed progenitor involved in fibrosis. *Nature*, *541*(7635), 96–101. https://doi.org/10.1038/nature20611

Savai, R., Pullamsetti, S. S., Kolbe, J., Bieniek, E., Voswinckel, R., Fink, L., Scheed, A., Ritter, C., Dahal, B. K., Vater, A., Klussmann, S., Ghofrani, H. A., Weissmann, N., Klepetko, W., Banat, G. A., Seeger, W., Grimminger, F., & Schermuly, R. T. (2012). Immune and inflammatory cell involvement in the pathology of idiopathic pulmonary arterial hypertension. *American Journal of Respiratory and Critical Care Medicine*, *186*(9), 897–908. https://doi.org/10.1164/rccm.201202-0335OC

Schwartz, C., & Fallon, P. G. (2018). Schistosoma "Eggs-iting" the host: Granuloma formation and egg excretion. *Frontiers in Immunology*, *9*(October), 1–16. https://doi.org/10.3389/fimmu.2018.02492

Scully, E., & Alter, G. (2016). NK Cells in HIV Disease. *Current HIV/AIDS Reports*, *13*(2), 85–94. https://doi.org/10.1007/s11904-016-0310-3

Secor, W. E. (2012). The effects of schistosomiasis on HIV/AIDS infection, progression and transmission. *Current Opinion in HIV and AIDS*, *7*(3), 254–259. https://doi.org/10.1097/COH.0b013e328351b9e3

Shaw, A. F. B., & Ghareeb, A. A. (1938). The pathogenesis of pulmonary schistosomiasis in Egypt with special reference to Ayerza's disease. *The Journal of Pathology and Bacteriology*, *46*(3), 401–424. https://doi.org/10.1002/path.1700460302

Sibomana, J. P., Campeche, A., Carvalho-Filho, R. J., Correa, R. A., Duani, H., Pacheco Guimaraes, V., Hilton, J. F., Kassa, B., Kumar, R., Lee, M. H., Loureiro, C. M. C., Mazimba, S., Mickael, C., Oliveira, R. K. F., Ota-Arakaki, J. S., Rezende, C. F., Silva, L. C. S., Sinkala, E., Ahmed, H. Y., & Graham, B. B. (2020). Schistosomiasis Pulmonary Arterial Hypertension. *Frontiers in Immunology*, *11*(December), 1–18. https://doi.org/10.3389/fimmu.2020.608883

Spikes, L., Dalvi, P., Tawfik, O., Gu, H., Voelkel, N. F., Cheney, P., O'Brien-Ladner, A., & Dhillon, N. K. (2012). Enhanced pulmonary arteriopathy in simian immunodeficiency virus-infected macaques exposed to morphine. *American Journal of Respiratory and Critical Care Medicine*, *185*(11), 1235–1243. https://doi.org/10.1164/rccm.201110-1909OC

Suttiprapa, S., Rinaldi, G., Tsai, I. J., Mann, V. H., Dubrovsky, L., Yan, H. Bin, Holroyd, N., Huckvale, T., Durrant, C., Protasio, A. V., Pushkarsky, T., Iordanskiy, S., Berriman, M., Bukrinsky, M. I., & Brindley, P. J. (2016). HIV-1 Integrates Widely throughout the Genome of the Human Blood Fluke Schistosoma mansoni. *PLoS Pathogens*, *12*(10), 1–26. https://doi.org/10.1371/journal.ppat.1005931

Swingler, S., Brichacek, B., Jacque, J. M., Ulich, C., Zhou, J., & Stevenson, M. (2003). HIV-1 Nef intersects the macrophage CD40L signalling pathway to promote resting-cell infection. *Nature*, *424*(6945), 213–219. https://doi.org/10.1038/nature01749

Szulcek, R., Happe, C. M., Rol, N., Fontijn, R. D., Dickhoff, C., Hartemink, K. J., Grünberg, K., Tu, L., Timens, W., Nossent, G. D., Paul, M. A., Leyen, T. A., Horrevoets, A. J., De Man, F. S., Guignabert, C., Yu, P. B., Vonk-Noordegraaf, A., Amerongen, G. P. V. N., & Bogaard, H. J. (2016). Delayed microvascular shear adaptation in pulmonary arterial hypertension: Role of platelet endothelial cell adhesion molecule-1 cleavage. *American Journal of Respiratory and Critical Care Medicine*, *193*(12), 1410–1420. https://doi.org/10.1164/rccm.201506-1231OC

Tachado, S. D., Zhang, J., Zhu, J., Patel, N., & Koziel, H. (2005). HIV Impairs TNF-α Release in Response to Toll-Like Receptor 4 Stimulation in Human Macrophages In Vitro. *American Journal of Respiratory Cell and Molecular Biology*, *33*(6), 610–621. https://doi.org/10.1165/rcmb.2004-0341OC

Terunuma, H., Deng, X., Dewan, Z., Fujimoto, S., & Yamamoto, N. (2008). Potential role of NK cells in the induction of immune responses: Implications for NK cell-based immunotherapy for cancers and viral infections. *International Reviews of Immunology*, *27*(3), 93–110. https://doi.org/10.1080/08830180801911743

Toba, M., Alzoubi, A., O'Neill, K. D., Gairhe, S., Matsumoto, Y., Oshima, K., Abe, K., Oka, M., & McMurtry, I. F. (2014). Temporal hemodynamic and histological progression in Sugen5416/hypoxia/ normoxia-exposed pulmonary arterial hypertensive rats. *American Journal of Physiology - Heart and Circulatory Physiology*, *306*(2), 243–250. https://doi.org/10.1152/ajpheart.00728.2013

Tuder, R. M., Stacher, E., Robinson, J., Kumar, R., & Graham, B. B. (2013). Pathology of pulmonary hypertension. *Clinics in Chest Medicine*, *34*(4), 639–650. https://doi.org/10.1016/j.ccm.2013.08.009

Van de Ven, K., & Borst, J. (2015). Targeting the T-cell co-stimulatory CD27/CD70 pathway in cancer immunotherapy: rationale and potential. *Immunotherapy*, *7*(6), 655–667. https://doi.org/10.2217/imt.15.32

Van Den Bossche, J., Bogaert, P., Van Hengel, J., Guérin, C. J., Berx, G., Movahedi, K., Van Den Bergh, R., Pereira-Fernandes, A., Geuns, J. M. C., Pircher, H., Dorny, P., Grooten, J., De Baetselier, P., & Van Ginderachter, J. A. (2009). Alternatively activated macrophages engage in homotypic and heterotypic interactions through IL-4 and polyamine-induced E-cadherin/catenin complexes. *Blood*, *114*(21), 4664–4674. https://doi.org/10.1182/blood-2009-05-221598

Voelkel, N. F., Tamosiuniene, R., & Nicolls, M. R. (2016). Challenges and opportunities in treating inflammation associated with pulmonary hypertension. *Expert Review of Cardiovascular Therapy*, *14*(8), 939–951. https://doi.org/10.1080/14779072.2016.1180976

Wall, K. M., Kilembe, W., Vwalika, B., Dinh, C., Livingston, P., Lee, Y. M., Lakhi, S., Boeras, D., Naw, H. K., Brill, I., Chomba, E., Sharkey, T., Parker, R., Shutes, E., Tichacek, A., Secor, W. E., & Allen, S. (2018). Schistosomiasis is associated with incident HIV transmission and death in Zambia. *PLoS Neglected Tropical Diseases*, *12*(12), 1–17. https://doi.org/10.1371/journal.pntd.0006902

Wallace, J. M., Hansen, N. I., Lavange, L., Glassroth, J., Browdy, B. L., Rosen, M. J., Kvale, P. A., Mangura, B. T., Reichman, L. B., & Hopewell, P. C. (1997). Respiratory disease trends in the Pulmonary Complications of HIV Infection Study cohort. Pulmonary Complications of HIV Infection Study Group. *American Journal of Respiratory and Critical Care Medicine*, *155*(1), 72–80. https://doi.org/10.1164/ajrccm.155.1.9001292

Wang, T., Green, L. A., Gupta, S. K., Kim, C., Wang, L., Almodovar, S., Flores, S. C., Prudovsky, I. A., Jolicoeur, P., Liu, Z., & Clauss, M. (2014). Transfer of intracellular HIV Nef to

endothelium causes endothelial dysfunction. *PLoS ONE*, *9*(3). https://doi.org/10.1371/journal.pone.0091063

Wilson, M. S., Mentink-Kane, M. M., Pesce, J. T., Ramalingam, T. R., Thompson, R., & Wynn, T. A. (2007). Immunopathology of schistosomiasis. *Immunology and Cell Biology*, *85*(2), 148–154. https://doi.org/10.1038/sj.icb.7100014

Wilson, R. A., & Coulson, P. S. (2009). Immune effector mechanisms against schistosomiasis: looking for a chink in the parasite's armour. *Trends in Parasitology*, *25*(9), 423–431. https://doi.org/10.1016/j.pt.2009.05.011

Wilson, M. S., Madala, S. K., Ramalingam, T. R., Gochuico, B. R., Rosas, I. O., Cheever, A. W., & Wynn, T. A. (2010). Bleomycin and IL-1β-mediated pulmonary fibrosis is IL-17A dependent. *Journal of Experimental Medicine*, *207*(3), 535–552. https://doi.org/10.1084/jem.20092121

Wong, J. K., Hezareh, M., Günthard, H. F., Havlir, D. V., Ignacio, C. C., Spina, C. A., & Richman, D. D. (1997). Recovery of replication-competent HIV despite prolonged suppression of plasma viremia. *Science*, *278*(5341), 1291–1295. https://doi.org/10.1126/science.278.5341.1291

Wynn, T. A. (2011). Integrating mechanisms of pulmonary fibrosis. *Journal of Experimental Medicine*, *208*(7), 1339–1350. https://doi.org/10.1084/jem.20110551

Wynn, T. A., & Vannella, K. M. (2016). Macrophages in Tissue Repair, Regeneration, and Fibrosis. *Immunity*, *44*(3), 450–462. https://doi.org/10.1016/j.immuni.2016.02.015

Yu, Y. R. A., O'Koren, E. G., Hotten, D. F., Kan, M. J., Kopin, D., Nelson, E. R., Que, L., & Gunn, M. D. (2016). A protocol for the comprehensive flow cytometric analysis of immune cells in normal and inflamed murine non-lymphoid tissues. *PLoS ONE*, *11*(3), 1–23. https://doi.org/10.1371/journal.pone.0150606

Yun, Y. F., Asad, M., M., K. C., Mona, L., Desmond, P., & A., O. M. (2008). Virus-Specific Interleukin-17-Producing CD4+ T Cells Are Detectable in Early Human Immunodeficiency Virus Type 1 Infection . *Journal of Virology*, *82*(13), 6767–6771. https://doi.org/10.1128/JVI.02550-07

Zahara Ali, Djuro Kosanovic, Ewa Kolosionek, Ralph T. Schermuly, B. B. G., Alistair Mathie, B., & Ghazwan. (2017). Enhanced inflammatory cell profiles in schistosomiasis-induced pulmonary vascular remodeling. *Pulmonary Circulation*, *7*(1), 20–37. https://doi.org/10.1086/690553

Zugna, D., Geskus, R. B., De Stavola, B., Rosinska, M., Bartmeyer, B., Boufassa, F., Chaix, M. L., Babiker, A., & Porter, K. (2012). Time to virological failure, treatment change and interruption for individuals treated within 12 months of HIV seroconversion and in chronic infection. *Antiviral Therapy*, *17*(6), 1039–1048. https://doi.org/10.3851/IMP2312

Sandra Medrano-Garcia

samedran@ucm.es

ORCID: https://orcid.org/0000-0003-2802-2327
ResearcherID: I-2513-2017

Education

2015 – 2021 **PhD student. Doctorate Program in Biomedicine**
Immunology Department, *Complutense University of Madrid, Madrid, Spain*

- Studies on the impact of HIV and schistosome co-exposure in pulmonary vascular pathology.
- In vitro studies of human and mouse CD3-deficient T cells to understand αβ and γδ T cell development and pathophysiology.
- 6 year experience on rodent surgery.
- Mentoring of undergraduate students (BSc in Biochemistry) and Master Students (Master's Degree in Research in Immunology). Immunology Department. Medicine Faculty. UCM.
- Elected student representative at Medicine Faculty UCM. 6 consecutive years.

2014 – 2015 **International Master Thesis**
Institut für Moleculare Biophysics, *Johannes Gutenberg Universität Mainz, Germany*

- "*A. leptodactylus* hemocyanin characterization and enzymatic studies with glutamate dehydrogenase".

2009 - 2014 **BSc, Biology. Neuroscience specialty**
Complutense University of Madrid

Research Experience

2019 – Present **Research associate. Project: "**Lymphocyte integration of TCR and complement cues" (RTI2018-095673-B-I00). MICINN 2018. Principal Investigator: José R. Regueiro & Edgar Fernández-Malavé. Immunology department, School of Medicine, Complutense University of Madrid

2017 – 2018 **Research associate. Project: "**The effect of coinfection with HIV and schistosomiasis on the pulmonary vascular bed" (FIBHGM-CCA028-2017) **.** Principal Investigator: Angel L. Cogolludo Torralba. Department of Pharmacology and Toxicology, School of Medicine, Complutense University of Madrid

2018 – 2015 **Research associate. Project: "**Surface and intracellular T lymphocyte activation physiopathology". MINECO 2014. Principal Investigator: José R. Regueiro & Edgar Fernández-Malavé. Immunology department, School of Medicine, Complutense University of Madrid

2015 - 2015 **Visiting researcher. Project**: "Surgical threatment of chronic diabetic wounds and improvement of blood perfusion using auricular vagus nerve stimulation". Principal Investigator: Eugenijus Kaniusas. General Hospital of Vienna

2014 – 2015 **Research associate. Project:** "Neuroprotective and neuroregenerative effects of electrical stimulation of the vagus nerve in cerebral ischemia". Principal Investigator: Fivos Panetsos. Institute of Health Carlos III, Madrid.

Teaching Experience

2015 - Present	Theoretical-practical teaching in “Immunology”. Immunology Department. School of Medicine. Complutense University, Madrid. 85 hours
2014 - 2017	Theoretical-practical teaching in “Mathematics and statistics”. School of Biology. Complutense University, Madrid. 35 hours
2014 - 2015:	Theoretical-practical teaching collaborator. Biomedical Engineering Master Program. Vienna University of Technology. 24 hours

Publications

"Control of physiological variables by non-invasive vagus nerve stimulation aiming at ischaemic stroke therapy". **Medrano-Garcia, Sandra**; Kampusch, Stefan; Kaniusas, Eugenijus; Fivos Panetsos. *Brain Injury*, 2016.

Zheng, Kang; Hao*, **Medrano-Garcia, Sandra*** Fengjie; Nevzorova, Yulia; ; Vaquero, Javier; Gomez del Moral, Manuel; Banares, Rafael; Ramon Regueiro, Jose; Martinez-Naves, Eduardo; Fernandez-Malave, Edgar; Javier Cubero, Francisco. “N-ras protects against experimental liver fibrosis by maintaining hepatocyte homeostasis”. *Journal of Hepatology* (in revision). *equal contribution

Medrano-García S*, Morales-Cano D*, Kumar R, Graham BB, Mathie A, Butrous G, Cogolludo A*, Fernández-Malavé E*. “HIV-mediated alterations in the pulmonary immune landscape and the response to schistosome challenge”. (in preparation) *equal contribution

Awards and travel grants

Second prize on Health Sciences section in the "Three minutes Thesis Contest 2018". Complutense University of Madrid, Spain. April 2018.

Finalist Best Oral communication. "T cell antigen receptor expression regulates thymic development of effector $\gamma\delta$ T cells". 40th Congress of the Spanish Society of Immunology. Zaragoza, Spain. May 2017.

Poster Second prize. “N-Ras is a negative regulator of IL-17 expression in T lymphocytes”. V CIB Congress of Biomedical Research. Madrid, Spain. February 2017.

EFIS-EJI TRAVEL GRANT. Fifth European Congress of Immunology - ECI 2018. Amsterdam, The Netherlands.

ECOST Grant “Verification, Validation and Uncertainty Assessment in Medical EMF Applications”. Prague, Czech Republic. November 2015.

Mobility Grant of the Vienna University of Technology. Vienna, Austria, 2015.

SANTANDER CRUE CEPYME Grant for Master Science Training. Madrid, Spain. July 2015.

ECOST Grant “European network for innovative uses of EMFs in biomedical applications” (BM 1309). Split, Croatia. September 2014.

Oral communications

"HIV and schistosome co-exposure in pulmonary vascular diseases". **Sandra Medrano-Garcia**. The 1st International Symposium of Infection and Pulmonary vascular diseases. Aswan, Egypt. October 2019

"N-ras deficiency promotes inflammation and autophagy but protects against apoptosis in experimental liver fibrosis". Fundamental Biology and Pathophysiology of the Liver Congress. Scottsdale, AZ USA . June 2018 (FJ Cubero)

"Do thymic γδT cells count on the antigen receptor for effector differentiation?". **S. Medrano-Garcia**, A. V. Marin, H. De La Figuera, J. R. Regueiro, M. Muñoz-Ruiz, Fernández-Malavé. 5th European Congress of Immunology. Amsterdam, Netherlands. September 2018.

"Differential TCR Expression Requirements for Thymic Development of Effector γδ T Cells Revealed in CD3 Deficient Mice". **Sandra Medrano**; Ana V Marin; Jiménez López Pablo; Ana Peñas Pita da Veiga; Jose Ramon Regueiro; Miguel Muñoz Ruiz; Edgar Fernández Malavé. 40th Congress of the Immunology society of Spain. Zaragoza, Aragón, España. 26.05.2017.

"Clinical Applications of Auricular Vagus Nerve Stimulation: cervical dystonia, diabetic wounds, blood perfusión and stroke". **Sandra Medrano-Garcia**. Workshop on "Verification, Validation and Uncertainty Assessment in Medical EMF Applications". Prag, Czech Republic. November 2015

"EMF-based neural repair and regeneration". **Sandra Medrano-Garcia**. European network for innovative uses of EMFs in biomedical applications" (BM 1309). Split, Croatia. October 2014

"Ways to an Effective Treatment for Ischemic Stroke – Optimization of Auricular Vagus Nerve Stimulation in Rats". **Sandra Medrano-Garcia**, Stefan Kampusch, Eugenijus Kaniusas, Fivos Panetsos. Workshop on "Electromagnetic fields interaction with Excitable Tissues". Madrid, Spain. March 2015.

Posters

"How much TCR is needed for γδ T cell effector differentiation in the thymus?". E. Fernández-Malavé, **S. Medrano-García**, A. Marín-Marín, H. De La Figuera, J. Regueiro, M. Muñoz-Ruiz. γδ T-Cell Conference. Bordeaux, France. June 2018

"Do thymic γδT cells count on the antigen receptor for effector differentiation?". **S. Medrano-Garcia**, A. V. Marin, H. De La Figuera, J. R. Regueiro, M. Muñoz-Ruiz, E. Fernandez-Malavé. European Congress of Immunology 2018. Amsterdam, The Netherlands. September 2018

"Differential TCR expression requirements for thymic development of effector γδ T cell subsets revealed in CD3 deficient mice". **Sandra Medrano-García**, Ana V. Marin, J. R. Regueiro, M. Muñoz-Ruiz, E. Fernández-Malavé. Sociedad de Inmunología de la CAM (SICAM). January 2018.

"T cell antigen receptor expression regulates thymic development of effector γδ T cells". **Sandra Medrano-García**, Ana V. Marin, Pablo Jiménez-López, Edgar Fernández-Malavé. 4th Symposium on Biomedical Research IIBM-Facultad de Medicina. Universidad Autónoma de Madrid ,Spain.

"T Cell antigen receptor expression regulates thymic development of effector γδ T cells". **Sandra Medrano-Garcia**, Pablo Jiménez López, Edgar Fernández Malavé. PhDay, Universidad Complutense de Madrid. Madrid, Spain. June 2017.

"Caspase-3 provides neuroprotection by inhibitory peptide nanoparticles". **Sandra Medrano-Garcia**. VIII Jornadas Avances Moleculares en Neuropatología of UCM. Madrid, Spain. May 2017

Courses

2019	Science counts. Scientific divulgation course. UCM. 36 hours.
2018	Workshop on professional public speaking. Development of communication skills for micro-presentations. UCM. 40 hours.
2018	English for academic networking. UCM. 20 hours.
2017	English for academic writing and publishing. UCM. 20 hours.
2017	Radiation Protection Training Course. UCM. 5 hours.
2017	Histology: Using Microscopy to Study Anatomy and Identify Disease. Open University. 15 hours.
2016	Course on laboratory animals, animal experiments and alternatives. FELASA category C
2016	Course on laboratory animals, animal experiments and alternatives. FELASA category B
2015	Training School on "Clinical Trial design and Management". European Training School on "Clinical Trial design and Management. NUI Galway. Galway, Ireland. 40 hours.
2015	Biomedical Instrumentation, Technische University of Vienna. Institute of Electrodynamics, Microwave and Circuit Engineering. Vienna, Austria. 30 hours.
2013	Methods in Cellular Neuroscience. Focus Program Translational Neuroscience FTN Rhine-Main Neuroscience Network. Mainz, Germany. 25 hours.

Technical Skills

- Cell Biology: cell and tissue immunofluorescence, cell isolation, cell culture, magnetic cell sorting, *in vitro* T cell activation
- Flow cytometry (sample preparation and data analysis)
- Rodent surgery
- Molecular biology techniques (PCR, RT-PCR)
- ELISA
- Immunohistochemistry
- Breeding, handling, and microsurgery of mice and newts
- Software: FlowJo, CellQuest Pro, ImageJ, Image Studio, Endnote, GraphPad, Office, Illustrator, Photoshop.

Languages

Spanish	●●●●●
English	●●●●○
German	●●●○○

Science Awareness Activities

2017- Present	Founder: Science and Cinema. Complutense University. 1300 participants in 2020 https://www.cienciacine.com/eventos
2020- Present	Co-Founder and podcaster: Science, Cinema & Podcast. 15K downloads on 1st season https://www.podcastidae.com/podcast/ciencia-cine-podcast/
2017- Present	Spain Pint of Science Coordinator. 33000 attendants in 2019 https://pintofscience.es/ TV news: https://bit.ly/3bOGp21
2017- Present	Founder and coordinator of the activity "Immune world" for teaching Immunology in High Schools of Madrid. https://www.ucm.es/microbiologia-1/mundo-inmunologico-semana-de-la-ciencia
2020- Present	Collaborator on Podcast https://www.podcastidae.com/podcast/encierrate-con-la-ciencia/